Universidad de Málaga

Escuela Técnica Superior de Ingeniería de Telecomunicación

TESIS DOCTORAL

Performance Analysis of Non–Ideal MIMO Systems in Fading Channels

Autor:

David Morales Jiménez

Directores:

José Francisco Paris Ángel

José Tomás Entrambasaguas Muñoz

UNIVERSIDAD DE MÁLAGA

SPICUM
servicio de publicaciones

AUTOR: David Morales Jiménez

EDITA: Servicio de Publicaciones de la Universidad de Málaga

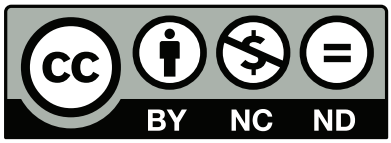

UNIVERSIDAD
DE MÁLAGA

Departamento de Ingeniería de Comunicaciones

Informe Visto Bueno del Director de la Tesis para su edición

D. José Francisco Paris Ángel y D. José Tomás Entrambasaguas Muñoz, directores de la Tesis Doctoral de título "Performance Analysis of Non-Ideal MIMO Systems in Fading Channels" realizada por David Morales Jiménez, dan el Visto Bueno para la edición de la Tesis en CD-ROM por el Servicio de Publicaciones e Intercambio Científico de la Universidad de Málaga.

Málaga, a 23 de Mayo de 2011

Fdo: José Francisco Paris Ángel

Fdo: José Tomás Entrambasaguas Muñoz

E.T.S.I. Telecomunicación, Campus de Teatinos, 29071-MÁLAGA, Tlf. 952 13 14 40 Fax 952 13 20 27

D. José Francisco Paris Ángel y D. José Tomás Entrambasaguas Muñoz, profesores doctores del Departamento de Ingeniería de Comunicaciones de la Universidad de Málaga

CERTIFICAN:

Que D. David Morales Jiménez, Ingeniero de Telecomunicación, ha realizado en el Departamento de Ingeniería de Comunicaciones de la Universidad de Málaga, bajo su dirección el trabajo de investigación correspondiente a su TESIS DOCTORAL titulada:

"**Performance Analysis of Non-Ideal MIMO Systems in Fading Channels**"

En dicho trabajo se han propuesto aportaciones originales para el problema del análisis de prestaciones en condiciones no ideales de sistemas basados en múltiples antenas (MIMO) sobre canales con desvanecimientos. Se han considerado limitaciones prácticas como son las interferencias co-canal, el canal de retorno con velocidad limitada, y la correlación espacial entre antenas. Bajo estas condiciones, se han obtenido expresiones cerradas originales para las probabilidades de error y de *outage* en sistemas MIMO que incluyen técnicas de conformación de haz en el transmisor y/o técnicas de diversidad espacial en el receptor.

Por todo ello, considera que esta Tesis es apta para su presentación al Tribunal que ha de juzgarla. Y para que conste a efectos de lo establecido en el Artículo 8º del Real Decreto 778/1998, regulador de los Estudios de Tercer Ciclo-Doctorado, AUTORIZAMOS la presentación de esta Tesis en la Universidad de Málaga.

Málaga a 23 de Mayo de 2011

Fdo: José Francisco Paris Ángel

Fdo: José Tomás Entrambasaguas Muñoz

"*Learning is a treasure that will follow its owner everywhere*"

My sincere gratitude to my colleagues, advisors, and all the people who gave me the opportunity to enjoy from learning. Special thanks to Jose Paris for all I have learnt from his motivation and devotion to research.

To my family and friends, for their unconditional support

Acknowledgment

This work has been partially supported by the Spanish Government under projects TEC2007-67289 and TEC2010-18451, and by AT4 wireless.

Table of Contents

List of Figures

List of Tables

List of Acronyms

ABEP	Average Bit Error Probability
ASEP	Average Symbol Error Probability
AWGN	Additive White Gaussian Noise
BEP	Bit Error Probability
CCI	Co-Channel Interference
CDF	Cumulative Distribution Function
CF	Characteristic Function
CSI	Channel State Information
DPSK	Differential Phase Shift Keying
DQPSK	Differencial Quadrature Phase Shift Keying
EGC	Equal Gain Combining
FSK	Frequency Shift Keying
G-MGF	Generalized Moment Generating Function
IG-MGF	Incomplete Generalized Moment Generating Function
IIMQ	Incomplete Integral of Marcum Q function
ILHI	Incomplete Lipschitz-Hankel Integral
INR	Interference-to-Noise Ratio
LOS	Line-Of-Sight
LTE	Long Term Evolution
MGF	Moment Generating Function
MIMO	Multiple-Input Multiple-Output
MRC	Maximum Ratio Combining

NLOS	Non Line-Of-Sight
OP	Outage Probability
OSTBC	Orthogonal Space-Time Block Codes
PAM	Pulse Amplitude Modulation
PDF	Probability Density Function
PSK	Phase Shift Keying
QAM	Quadrature Amplitude Modulation
RF	Radio Frequency
RV	Random Variable
SIMO	Single-Input Multiple-Output
SINR	Signal-to-Interference-plus-Noise Ratio
SIR	Signal-to-Interference Ratio
SNR	Signal-to-Noise Ratio
SC	Selection Combining
SEC	Switch-and-Examine Combining
SEP	Symbol Error Probability
SSC	Switch-and-Stay Combining
STBC	Space-Time Block Codes

Abstract

This thesis focuses on the performance analysis of multiple-input multiple-output (MIMO) systems under certain non-ideal (practical) conditions. Realistic limitations such as spatial correlation, the presence of co-channel interferences, the use of non-orthogonal signaling, and the limited-rate feedback channel, have been considered. Under these considerations, outage and bit error probabilities have been analyzed for different systems which employ beamforming techniques at the transmitter and/or different receive diversity techniques.

The main goal of this thesis is to obtain different analytic closed-form expressions for the most common performance metrics of MIMO systems in fading channels under the mentioned non-ideal conditions. The existing mathematical tools are in some cases not enough to accomplish such analysis. In other cases, the available tools and mathematical framework only allow for either a restricted analysis or intractable results, which may not give further insight on the system performance or may be numerically awkward. Therefore, the motivation of this thesis is twofold: on the one hand, to find and/or develop new mathematical tools that allow (or simplify) the analysis of such systems; on the other hand, to analyze the performance of these systems in terms of the most common measures, the outage probability (OP) and bit error probability (BEP), trying to arrive at closed-form expressions whenever possible.

The main contributions of this thesis are as follows. First, simplified expressions have been found for a type of incomplete cylindrical integrals, referred to as Lipschitz-Hankel integrals. Based on these expressions, new statistical functions for the characterization of different fading channel models have been obtained in closed-form. Second, new statistical results have been obtained for the distribution of the diagonal elements of complex Wishart matrices. These mathematical results have been applied to the OP and BEP analysis of different MIMO systems under different practical conditions, resulting in several contributions to the literature.

Resumen

Esta tesis se centra en el análisis de prestaciones de sistemas MIMO (*multiple-input multiple-output*) bajo ciertas condiciones no ideales. Se han considerado limitaciones realistas como son la correlación espacial, la presencia de interferencias co-canal, el uso de señalización no-ortogonal, y el canal de retorno de capacidad limitada. Bajo estas condiciones, se han analizado las probabilidades de error y de *outage* para sistemas MIMO que incluyen técnicas de conformación de haz en el transmisor y/o distintas técnicas de diversidad espacial en el receptor.

Se ha planteado como objetivo la obtención de diferentes expresiones cerradas y exactas para las probabilidades mencionadas. Dada la insuficiencia de las herramientas matemáticas disponibles en la bibliografía, ha sido necesario el desarrollo de nuevos métodos o herramientas de análisis. Por tanto, la motivación de la tesis es doble: por un lado, el desarrollo de estas herramientas que posibiliten o faciliten el análisis de prestaciones de los sistemas MIMO, y por otro lado, la aplicación de estas herramientas a la obtención de expresiones cerradas que permitan analizar el rendimiento de los mismos.

Las contribuciones más relevantes de esta tesis son las siguientes. En primer lugar, se han obtenido expresiones simplificadas para cierto tipo de integrales incompletas, conocidas como integrales de Lipschitz-Hankel. Estas expresiones han permitido obtener ciertas funciones estadísticas para la caracterización de diferentes modelos de canal con desvanecimientos. En segundo lugar, se han obtenido nuevos resultados estadísticos para la distribución de los elementos de la diagonal de matrices Wishart complejas. Todos estos resultados matemáticos han sido aplicados al análisis de prestaciones de distintos sistemas MIMO bajo diferentes condiciones prácticas, lo cual ha dado lugar a varias publicaciones.

Chapter 1

Introduction

In this chapter, the context and main motivations of this thesis are introduced. Besides, the results of this work have led to several contributions to the literature, which will be summarized. Finally, the structure and organization of this thesis will be stated.

1.1 Scope and Overview

Multiple antenna systems have been used for a long time to mitigate the effects of fading in wireless communications. Diversity reception techniques are applied in systems with a single transmit antenna and multiple receive antennas, also referred to as single-input multiple-output (SIMO) systems. They perform a certain combining of the individual received signals, in order to provide diversity gain. In the case of frequency-flat fading, the optimum combining strategy in terms of maximizing the output signal-to-noise power ratio (SNR) is maximum ratio combining (MRC), which requires perfect channel knowledge at the receiver. Several suboptimal combining strategies, which lead to less complex receivers, are: equal gain combining (EGC), where the received signals are added up, and selection combining (SC), where the received signal with the maximum instantaneous SNR is selected. Moreover, switched diversity strategies, such as switch-and-stay combining (SSC) or switch-and-examine combining (SEC) are simpler to implement than MRC, EGC, or SC, and thus, they are very often used in practical receivers with limited complexity. A comprehensive description of such systems can be found in [1, ch. 9] and the references therein.

However, the performance of SIMO systems is often degraded due to certain limitations or non-idealities such as the presence of co-channel interference (CCI) signals or the use of non-orthogonal signaling. Therefore, including these limitations in the performance analysis is of special interest when it comes to the design of practical (real) systems. On the one hand, it is well-known that, for a communication link without CCI, MRC is the optimal combining technique in terms of maximizing the SNR at the combiner output. However, optimal combining in the presence of CCI is much more complex than MRC and requires information about the CCI that may not be available [2]. Thus, in practice many wireless systems will use MRC even in the presence of CCI and it is of essential importance to analyze the performance of such systems under this condition. On the other hand, binary frequency-shift keying (FSK) signaling with noncoherent detection is frequently adopted in practical switched diversity systems (e.g. SEC or SSC) as a simple (low-complexity) modulation scheme. In such cases, signals can be chosen non-orthogonal at the transmitter to reduce bandwidth utilization, at the expense of certain performance degradation [3, ch. 5]. The use of non-orthogonal signaling to reduce bandwidth utilization can be seen as a practical limitation to be addressed and, therefore, the performance analysis under this condition is particularly interesting.

Applications in more recent years have become increasingly sophisticated, thereby relying on the more general multiple-input multiple-output (MIMO) systems, which have played an important role to satisfy the demand for higher capacity and coverage [4–6]. Such systems may combine the use of space-time block codes (STBC) at the transmitter [7] and receive diversity techniques such as SC, also known as receive antenna selection [8], or MRC [9]. When channel state information (CSI) is available at the transmitter, more sophisticated schemes can be employed to enhance the performance. The MIMO beamforming system, also referred to as MIMO MRC, relies on the joint MRC weights at both the transmitter and the receiver sides [10–12]. However, the performance of such systems is very often constrained by practical limitations as the antenna correlation, which reduces spatial diversity [13], or the limited-rate feedback, which has been dealt with codebook-based beamforming approaches [14–17].

The main goal of this thesis is to address the performance analysis of different SIMO and MIMO systems in fading channels under the mentioned non-ideal (practical) conditions. The existing mathematical tools are in some cases not enough to accomplish such analysis. In other cases, the available tools and mathematical framework only allow for either a restricted analysis or intractable results, which may not give further insight on the system performance or may even be numerically awkward. Therefore, the motivation of this thesis is twofold: on the one hand, to find and/or develop new mathematical tools that allow (or simplify) the analysis of such systems; on the other hand, to analyze the performance of these systems in terms of the most common measures, the outage probability (OP) and bit error probability (BEP), trying to arrive at closed-form expressions for these measures whenever possible.

Analysis of SIMO systems based on incomplete cylindrical integrals

In the context of SIMO systems, the analysis under the mentioned practical limitations leads to certain incomplete integrals involving Marcum Q and Bessel functions. These integrals, referred to as incomplete Lipschitz-Hankel integrals (ILHIs) and incomplete integrals of Marcum Q functions (IIMQs), can be studied within the theory of the incomplete cylindrical functions developed by Agrest and Maksimov [18]. ILHIs and IIMQs traditionally appear in analytical solutions within the electromagnetics context [19]. However, in general, the applications of ILHIs and IIMQs seem to have escaped the notice of most communication theorists. Besides, closed-form expressions for the solutions of these integrals have been unavailable in the literature until recent results have been provided in [20].

In particular, this type of integrals appear in the BEP analysis of switched diversity systems, such as SSC and SEC, with noncoherent or differentially coherent detection of non-orthogonal signals. However, results in the literature are not available in closed-form due to the lack of tractable solutions for these integrals. Specifically, BEP results in [21] and [22] for SSC and SEC with noncoherent detection are in the form of single finite integrals. Besides, the OP analysis of MRC systems under CCI leads to the same type of integrals when the Nakagami-q (Hoyt) fading model is assumed. Although considerable

attention has been paid to the OP analysis under Rayleigh or Nakagami-m fading [23], few published results are found for Hoyt channels, which model more severe fading conditions. Motivated on recent results in [20] concerning ILHIs and IIMQs, we have focused on the development of simplified expressions for this particular family of integrals. Also, the explicit solutions for these integrals allow obtaining new statistical functions for the characterization of some fading channels. These mathematical expressions are key results for the performance analysis of the mentioned SIMO systems.

Analysis of MIMO systems based on complex Wishart matrices

The statistical properties of Wishart matrices have been widely used to analyze the performance of MIMO systems [24–27]. Particularly, the diagonal entries of complex Wishart matrices are employed for characterizing the signal-to-noise ratio (SNR) statistics at the output of certain MIMO systems under practical limitations. The distribution of the maximum of the diagonal elements can be used to characterize the output SNR of MIMO systems with selection combining (MIMO SC) under spatially correlated fading (see, e.g., [8, 28, 29]). Also, the use of the diagonal distribution of complex Wishart matrices has been pointed out in [30] as an approach to the performance analysis of beamforming systems with limited feedback (codebook-based). The derivation of tractable analytical expressions for the SNR statistics of such systems is very important in order to evaluate performance measures such as the OP, BEP, or system capacity. The reasons above motivate us to focus on the diagonal distribution of a complex Wishart matrix, which is a particular multivariate chi-square distribution derived from complex Gaussian variables.

In the *area of multivariate analysis*, there is a rich body of works considering the joint distribution of the diagonal elements of real Wishart matrices; equivalently, multivariate chi-square distributions derived from real Gaussians [31–35]. Whereas the characteristic function (CF) is well known [33], the joint probability density function (PDF) is rather more complicated. Different approaches to the joint PDF have been proposed in the literature. An infinite series expansion for the density in terms of Laguerre polynomials was first given in [33]. Following the same approach, later work by Royen [34] provided new Laguerre expansions with improved convergence. In [35], Miller *et al.* derived expansions

for the PDF in terms of Bessel functions for the bivariate and trivariate cases. However, the case of underlying complex Gaussian random variables, i.e., complex Wishart matrices, has not been sufficiently investigated. Only very recently, Hagedorn *et al.* [36] have derived corresponding expansions for the trivariate case. To the best of the author's knowledge, the case of k-variate chi-square ($k > 3$) from a complex Wishart matrix with arbitrary correlation is not available in the literature. Moreover, the expansions in [36] for $k = 3$ are in the form of Bessel functions, which make further performance analysis (e.g., BEP) complicated.

In the *communications theory context*, the available statistical results on the multivariate chi-square distribution have been applied to the performance analysis of MIMO systems [8, 28–30]. However, the analysis is often limited due to the lack of results on the diagonal distribution of complex Wishart matrices. Moreover, analytical closed-form expressions (e.g., BEP) are rarely provided due to the intractable form of the joint PDF. In [29], the derived BEP expressions for multi-branch SC over spatially correlated fading are in the form of a multiple integral involving the joint CF. Also, BEP results in [30] for codebook-based transmit beamforming are again given in a multiple integral form. In some other works, the analysis is carried out under certain assumptions such as a real correlation matrix, equivalently considering a real Wishart matrix. In [28], closed-form BEP results are provided for dual-branch selection diversity assuming real correlation among branches. Also, the real exponential correlation model is assumed in [8] to analyze the performance of MIMO SC systems, i.e. MIMO systems where selection combining is applied at the receiver.

1.2 Contributions of this Thesis

In this thesis, we have addressed the performance analysis of different SIMO and MIMO systems in fading channels under certain practical conditions. We have aimed to obtain closed-form expressions for the two most commonly extended performance measures, outage and bit error probabilities, leading to several contributions to the literature. As stated above, in some cases the existing mathematical tools have not been enough to

accomplish such analysis and, thus, the development of new tools and statistical functions has been an essential part of this work.

The main contributions of this thesis can be split into two categories: the ones derived from the analysis of SIMO, and the ones corresponding to the analysis of MIMO systems. In both cases, the analysis has raised the need for the development of new mathematical expressions and statistical functions.

In the context of **SIMO systems**, simplified solutions have been obtained for the class of incomplete integrals ILHI based on previous results in [20]. The explicit solutions of ILHI have been used to derive new closed-form expressions for several statistical functions which help characterizing different fading channel models (see Chapter 3), specifically:

- The incomplete generalized moment generating function (IG-MGF) of the Hoyt fading distribution has been expressed by a finite number of Bessel and Marcum Q functions. Besides, an original expression for the IG-MGF of the sum of independent and identically distributed (i.i.d.) Hoyt variables have been obtained in terms of the confluent Lauricella function.

- The cumulative distribution function (CDF) of the η-μ fading distribution[1] has been obtained in terms of Bessel, Marcum Q, and elementary functions. These results for the CDF have been directly applied to the OP analysis of MRC systems over i.i.d. η-μ fading channels in [37].

The explicit solutions for the incomplete integrals ILHI and IIMQ [20], and the new derived expressions for the statistics of Hoyt fading channels have been applied to the performance analysis of SIMO systems under different conditions, leading to the following contributions:

- Exact and closed-form expressions have been derived for the average BEP of non-coherent and differentially coherent detection in multibranch switched diversity

[1] The η-μ fading distribution, introduced in Section 3.3, is a new general distribution [38] which includes, as particular cases, the classic non line-of-sight (NLOS) fading models (e.g. Nakagami-m, Hoyt, and Rayleigh).

systems under Nakagami-m fading. The derived expressions have led to easily computable results which are useful for the analysis and design of switched diversity based systems. In this kind of systems, signals may be chosen non-orthogonal (correlated) at the transmitter in order to reduce the bandwidth use. As a particular case, results for a dual-branch SSC system with noncoherent detection of non-orthogonal binary FSK under Rayleigh fading have been published in [39].

- Exact closed-form expressions have been obtained for the OP of MRC systems in Nakagami-q (Hoyt) fading channels under independent co-channel interferers with arbitrary powers. These results are obtained from the application of the new derived expressions for the IG-MGF of the Hoyt fading distribution. Besides, some simplifications and approximations for the OP in the high SNR regime have been obtained and published in [40] for the particular case of a single antenna receiver.

In the context of **MIMO systems**, it has been observed that the SNR output characterization of several well-known systems depends on the diagonal distribution of complex Wishart matrices. Therefore, the statistics of the diagonal of such matrices have been addressed resulting in the following contributions:

- Infinite series representations in terms of the Laguerre polynomials are given for the joint PDF and CDF of the diagonal elements of a complex Wishart matrix. The diagonal elements of such matrices follow a particular multivariate chi-square distribution. The expansions for the joint PDF and CDF are straightforward for numerical work and converge rapidly. Further performance analysis of MIMO systems such as exact BEP analysis is made possible due to the form of the series expansions.

- The derived expression for the joint CDF is used to obtain a new series expansion for the distribution of the maximum of k arbitrarily correlated chi-square random variables.

- Although seemingly complex, the computation of the series is mathematically tractable. An efficient MATHEMATICA™ algorithm has been developed for rapid computation of the coefficients.

The statistical results on the diagonal of complex Wishart matrices have been applied to the analysis of MIMO systems. Specifically, the distribution of the maximum of the diagonal (i.e., the maximum of k arbitrarily correlated chi-square variables) has been used to analyze the OP of two MIMO systems under different practical conditions:

- First, our statistical results have been applied to the OP analysis of MIMO SC systems in arbitrarily correlated Rayleigh fading channels. This analysis extends the results in [8] to any number of receive antennas with arbitrary correlation. Also, our results are in the form of a single series expansion in terms of the Laguerre polynomials, which facilitates the computation and makes further closed-form analysis (e.g. BEP analysis) possible.
- Then, the same analytical approach has been applied to obtain the OP of MIMO beamforming systems under limited-rate feedback, i.e., systems with codebook-based transmit beamforming and MRC at the receiver side.

The obtained expressions for the OP are given as an infinite series representation in terms of the well-known Laguerre polynomials, and have been shown to be easily computable. At the best of the author's knowledge, the derived expressions and results from both MIMO systems are novel and thus represent key contributions of this thesis.

Publications

A number of publications has been produced as a result of this work. The main publications which gather the mentioned contributions are:

- D. Morales-Jiménez, J. F. Paris, J. T. Entrambasaguas, and Kai-Kit Wong, "On the diagonal distribution of a complex Wishart matrix and its application to the analysis of MIMO systems," under review (2nd round of reviews) for possible publication in *IEEE Transactions on Communications*.
- D. Morales-Jiménez, J. F. Paris, and Kai-Kit Wong, "Closed-form analysis of multibranch switched diversity with noncoherent and differentially coherent detection,"

under review (2nd round of reviews) for possible publication in *International Journal of Communication Systems*.

- [37] D. Morales-Jiménez and J. F. Paris, "Outage probability analysis for $\eta - \mu$ fading channels," *IEEE Communications Letters*, vol. 14, no. 6, pp. 521-523, June 2010.

- [39] D. Morales-Jiménez and J. F. Paris, "Closed-form analysis of dual-branch switched diversity with binary nonorthogonal signaling," *Electronics Letters*, vol. 45, no. 23, pp. 1179-1180, November 2009.

- [40] J. F. Paris and D. Morales-Jiménez, "Outage probability analysis for Nakagami-q (Hoyt) fading channels under Rayleigh interference," *IEEE Transactions on Wireless Communications*, vol. 9, no. 4, pp. 1272-1276, April 2010.

Other publications by the author which have been produced in the context of the analysis of MIMO systems are:

- G. Gómez, D. Morales-Jiménez, J. J. Sánchez, and J. T. Entrambasaguas, "A next generation wireless simulator based on MIMO-OFDM: LTE case study," *EURASIP Journal on Wireless Communications and Networking*, vol. 2010, Article ID 161642, 14 pages, 2010.

- D. Morales-Jiménez, J. F. Paris, and J. T. Entrambasaguas, "Performance trade-offs among low-complexity detection algorithms for MIMO-LTE receivers," *International Journal of Communication Systems*, vol. 22, no. 7, Wiley, July 2009, pp. 885-897.

- D. Morales-Jiménez, G. Gómez, J. F. Paris, and J. T. Entrambasaguas, "Joint Adaptive Modulation and MIMO Transmission for Non-Ideal OFDMA Cellular Systems," in Proc. *IEEE GLOBECOM 2009 Workshops*, Hawaii (USA), pp. 1-5, Nov 2009.

1.3 Organization

The rest of this thesis is organized as follows. The mathematical derivations and tools which have been used in the performance analysis are presented in Chapter 2. Then, the statistical fading channel models assumed in the different analyses of this thesis are introduced in Chapter 3. The main body of the performance analysis is divided in chapters 4 and 5, corresponding to SIMO and MIMO systems respectively. On the one hand, Chapter 4 includes the analysis of different receive diversity systems under different practical limitations: switching combining under non-orthogonal signaling and MRC systems under the presence of co-channel interference signals. On the other hand, MIMO systems are analyzed in Chapter 5 under different conditions, specifically: MIMO systems with receive antenna selection (MIMO SC) under spatial correlation and MIMO beamforming systems under limited-rate feedback. Finally, the main conclusions of this thesis are gathered in Chapter 6.

Chapter 2

Mathematical Tools for Performance Analysis

The purpose of this chapter is to present the mathematical tools and derivations which have been used in this thesis for the performance analysis of single-input multiple-output (SIMO) and multiple-input multple-output (MIMO) systems. In this context, we have aimed to obtain closed-form expressions for the most common performance measures in the analysis of such systems.

In some cases, the existing mathematical tools are not enough to accomplish such analysis. In other cases, the available mathematical framework only allow for a restricted analysis, leading to awkward expressions which may not give further insight on the system performance and whose numerical evaluation is tough. In order to allow or simplify the analysis of such systems, new mathematical tools and statistical functions have been developed thus representing an essential part of this work.

In this chapter, we first present the notation that will be used throughout the thesis, followed by the performance metrics which will be analyzed. Then, the special functions and integrals involved in the derivations of these metrics are introduced. In particular, special attention will be paid to a certain kind of incomplete integrals, which are of particular importance in the analysis of SIMO systems under certain practical issues. Finally, the statistics of the diagonal elements of a complex Wishart matrix are addressed. This will be of particular importance when it comes to the analysis of MIMO systems.

2.1 Notation

Throughout this thesis, the following vector and matrix notations are used: bold lowercase for vectors, bold uppercase for matrices, superscripts T and H for the transpose and the Hermitian transpose, respectively. Regarding vector and matrix norms, we use $\|\cdot\|$ for the Euclidean vector norm, $|\cdot|$ for the matrix determinant, and $\|\mathbf{A}\|_s$ for the spectral norm of matrix $\mathbf{A}$, i.e., the square root of the maximum eigenvalue of $\mathbf{A}^H\mathbf{A}$. Also, we use $\mathsf{diag}(\cdot)$ for the diagonal elements of a matrix, and $\mathsf{Diag}\,(a_1,\ldots,a_k)$ for the diagonal matrix with diagonal elements $(a_1,\ldots,a_k)$.

Besides, for complex values we use $\Re\{\cdot\}$ and $|\cdot|$ for the real part and the modulus operators, respectively, and the superscript $*$ for the complex-conjugate. In general, $\mathtt{E}[\cdot]$ is used to denote the expectation operator, and $\Pr\{\cdot\}$ denotes the probability of a certain event specified in braces. Also, $\mathcal{L}[f(p);p,s]$ denotes the Laplace transform of a certain function $f(p)$.

Finally, $(a)_m = a(a+1)\ldots(a+m-1)$ is the pochhammer symbol, whereas the binomial coefficient is denoted and given by $\left(\begin{array}{c} a \\ b \end{array}\right) = \frac{a!}{b!(a-b)!}$, with ! denoting the factorial operator and $0 \leq b \leq a$.

2.2 Performance Metrics

2.2.1 Outage Probability

A standard performance criterion, characteristic of diversity systems operating over fading channels, is the so-called *outage probability* (OP) denoted by P_{out} and defined as the probability that the instantaneous error probability exceeds a specified value. Equivalently, P_{out} is the probability that the output signal-to-noise power ratio (SNR), γ, falls below a certain specified threshold, γ_o. Mathematically speaking, we have

$$P_{out} \triangleq \Pr\{\gamma \leq \gamma_o\} = F_\gamma(\gamma_o) = \int_0^{\gamma_o} f_\gamma(\gamma)d\gamma, \tag{2.2.1}$$

which is the cumulative distribution function (CDF) of γ, namely $F_\gamma(\gamma)$, evaluated at $\gamma = \gamma_o$, whereas $f_\gamma(\gamma)$ denotes the probability density function (PDF) of γ.

The main difficulties when calculating the OP lie on the fact that the output SNR statistics, specifically the PDF, is sometimes not known. In some other cases, the PDF cannot be integrated in closed-form, i.e. there are no available closed-form results for the CDF, and thus, the OP needs to be calculated via numerical integration. When this occurs, the system analysis is restricted to the numerical evaluation of the OP and thus, obtaining further insight on the performance behavior such as asymptotic approximations or bounds is either not possible or tricky.

2.2.2 Error Probabilities

Another performance criterion and undoubtedly the most difficult to compute is the average bit error probability (BEP). It is the one that is most revealing about the nature of the system behavior and the one most often illustrated in performance evaluations; thus, it is of primary interest to have a method for its evaluation that reduces the degree of difficulty as much as possible.

Given the conditional BEP $P_b(x) \triangleq \Pr\{\text{bit error} \,|\gamma = x\}$ and the PDF of the SNR f_γ, the average BEP (ABEP) is calculated by

$$\bar{P}_b = \int_0^\infty P_b(x)\, f_\gamma(x)\, dx. \tag{2.2.2}$$

The primary reason for the difficulty in evaluating the ABEP lies in the fact that the conditional (on the fading) BEP depends on the modulation/detection scheme employed by the system. As the nature of the modulation/detection schemes is nonlinear, the conditional BEP is, in general, a nonlinear function of the instantaneous SNR.

Another commonly used metric is the symbol error probability (SEP), which also depends on the modulation/detection scheme and can be directly related to the BEP. Given the conditional SEP $P_s(x) \triangleq \Pr\{\text{symbol error} \,|\gamma = x\}$, the average SEP (ASEP) is calculated as

$$\bar{P}_s = \int_0^\infty P_s(x)\, f_\gamma(x)\, dx. \tag{2.2.3}$$

The same difficulties for the evaluation of ABEP also apply to the ASEP, as the conditional SEP has also a nonlinear dependence with the fading statistics and the ASEP is calculated by averaging the conditional SEP over these statistics.

2.3 Special Functions and Integrals

2.3.1 Classical Special Functions

Legendre polynomials

Legendre polynomials are a class of orthogonal polynomials which frequently appear in the context of OP and error probabilities analysis of MIMO communication systems. The Legendre polynomials of degree n are of the form

$$P_n(z) = \frac{1}{2^n n!} \frac{d^n}{dz^n} \left(z^2 - 1\right)^n. \tag{2.3.1}$$

Several expanded forms are available for (2.3.1) in [41, (8.911)]. One of the most commonly used is given by

$$P_n(z) = \sum_{k=0}^{n} \frac{(-1)^k (n+k)!}{(n-k)! (k!)^2 2^{k+1}} \left[(1-z)^k + (-1)^n (1+z)^k\right]. \tag{2.3.2}$$

Jacobi polynomials

Jacobi polynomials are a different class of orthogonal polynomials which will appear throughout the derivations of this thesis. The Jacobi polynomial of degree n and parameters α and β is given by

$$P_n^{(\alpha,\beta)}(z) = \frac{1}{2^n} \sum_{k=0}^{n} \binom{n+\alpha}{k} \binom{n+\beta}{n-k} (z-1)^{n-k} (z+1)^k. \tag{2.3.3}$$

More detailed information on the Jacobi polynomials, as functional relations and connections with other functions can be found in [41, (8.96)].

Laguerre polynomials

Another class of orthogonal polynomials which are of interest in the context of this thesis are the so-called Laguerre polynomials. The generalized Laguerre polynomials are usually defined according to the Rodrigues' formula [41, eq. 8.970-1] as

$$L_n^{\alpha}(z) = \frac{1}{n!} e^z z^{-\alpha} \frac{d^n}{dz^n} \left(e^{-x} z^{n+\alpha} \right). \tag{2.3.4}$$

The expanded form can be directly obtained from the definition (2.3.4), thus leading to the following expression for the generalized Laguerre polynomial of degree n and parameter α,

$$L_n^{\alpha}(z) = \sum_{m=0}^{n} (-1)^m \binom{n+\alpha}{n-m} \frac{z^m}{m!}. \tag{2.3.5}$$

Further information on the Laguerre polynomials, such as alternative representations, functional relations, and asymptotic or limiting behavior, can be found in [41, (8.97)].

Gamma function

The Euler's integral of the second kind, also referred to as the gamma function, is defined as

$$\Gamma(z) = \int_0^{\infty} e^{-t} t^{z-1} dt, \tag{2.3.6}$$

with $\Re\{z\} > 0$. Alternative representations, special cases, and functional relations can be found in [41, (8.3)]. The following relation is of particular importance,

$$\Gamma(z+1) = z\Gamma(z). \tag{2.3.7}$$

Also, the gamma function is directly related to the factorial when the argument is a natural number, i.e.,

$$\Gamma(n) = (n-1)! \qquad , n \in \mathbb{N}. \tag{2.3.8}$$

Incomplete gamma function

The incomplete version of (2.3.6) is known as the incomplete gamma function, defined as

$$\gamma(\alpha, x) = \int_0^{x} e^{-t} t^{\alpha-1} dt, \tag{2.3.9}$$

with $\Re\{\alpha\} > 0$. A commonly used series representation for the incomplete gamma function is given by

$$\gamma(\alpha, x) = \sum_{n=0}^{\infty} \frac{(-1)^n x^{\alpha+n}}{n!\,(\alpha+n)}. \tag{2.3.10}$$

For alternative representations, special cases, and functional relations the reader is referred to [41, (8.3)].

Modified Bessel functions of the first kind (I_ν)

Bessel functions $Z_\nu(z)$ are solutions of the differential equation

$$\frac{d^2 Z_\nu}{dz^2} + \frac{1}{z}\frac{dZ_\nu}{dz} + \left(1 - \frac{\nu^2}{z^2}\right) Z_\nu = 0 \tag{2.3.11}$$

Special types of Bessel functions are what are called Bessel functions of the first kind $J_\nu(z)$, Bessel functions of the second kind (also called Neumann functions), and Bessel functions of the third kind (also called Hankel's functions). We will focus on a modification of $J_\nu(z)$, the so-called modified Bessel functions of the first kind $I_\nu(z)$, which will appear frequently throughout this thesis.

The Bessel functions of the first kind, which fulfill equation (2.3.11), are defined as

$$J_\nu(z) = \frac{z^\nu}{2^\nu} \sum_{k=0}^{\infty} (-1)^k \frac{z^{2k}}{2^{2k} k! \Gamma(\nu + k + 1)}, \quad |\arg z| < \pi, \tag{2.3.12}$$

and the modified Bessel functions of the first kind are given by

$$I_\nu(z) = e^{-\frac{\pi}{2}\nu i} J_\nu\left(e^{\frac{\pi}{2} i} z\right), \quad -\pi < \arg z \leq \frac{\pi}{2} \tag{2.3.13}$$

$$I_\nu(z) = e^{\frac{3}{2}\pi\nu i} J_\nu\left(e^{-\frac{3}{2}\pi i} z\right), \quad \frac{\pi}{2} < \arg z \leq \pi \tag{2.3.14}$$

Finally, the particularization of $I_\nu(z)$ for an integer order $\nu = n$ is given by

$$I_n(z) = i^{-n} J_n(iz) \tag{2.3.15}$$

Marcum Q functions

The first order Marcum Q function is defined in its more common form as

$$Q(\alpha, \beta) = \int_\beta^\infty t e^{-\frac{t^2+\alpha^2}{2}} I_0(\alpha t)\, dt, \tag{2.3.16}$$

which can be seen as the complement (with respect to unity) of the CDF corresponding to a normalized noncentral chi-square variable. It has been shown in [1, ch. 4] that the first order Marcum Q function has the following series form

$$Q(\alpha,\beta) = e^{-\frac{\alpha^2+\beta^2}{2}} \sum_{k=0}^{\infty} \left(\frac{\alpha}{\beta}\right)^k I_k(\alpha\beta) = e^{-\frac{\beta^2}{2}(1+\zeta^2)} \sum_{k=0}^{\infty} \zeta^k I_k\left(\beta^2\zeta\right), \tag{2.3.17}$$

where $\zeta \triangleq \frac{\alpha}{\beta}$. The reason for introducing the parameter ζ is to represent the ratio of the arguments of the Marcum Q function. This parameter is used to obtain more insight in the communications theory context, specifically more information about its dependence on the modulation/detection scheme can be found in [1, ch. 5].

Analogously, the generalized m-th order Marcum Q function is defined by

$$Q_m(\alpha,\beta) = \frac{1}{\alpha^{m-1}} \int_{\beta}^{\infty} t^m e^{-\frac{t^2+\alpha^2}{2}} I_{m-1}(\alpha t)\, dt. \tag{2.3.18}$$

The series form for the generalized m-th order case is given by

$$Q_m(\alpha,\beta) = e^{-\frac{\alpha^2+\beta^2}{2}} \sum_{k=1-m}^{\infty} \left(\frac{\alpha}{\beta}\right)^k I_k(\alpha\beta) = e^{-\frac{\beta^2}{2}(1+\zeta^2)} \sum_{k=1-m}^{\infty} \zeta^k I_k\left(\beta^2\zeta\right), \tag{2.3.19}$$

which holds for integer values of m. In this case, the values of the summation index k are also integer, and then $I_{-k}(z) = I_k(z)$. A valid series form for the case of a non-integer m is

$$Q_m(\alpha,\beta) = e^{-\frac{\beta^2}{2}(1+\zeta^2)} \sum_{k=1-m}^{\infty} \zeta^k I_{-k}\left(\beta^2\zeta\right). \tag{2.3.20}$$

2.3.2 Lauricella or Humbert Functions

Lauricella functions are generalizations of the Gauss hypergeometric functions to multiple variables. Among the important confluent forms of Lauricella functions, we are interested in the confluent series $\Phi_2^{(n)}$, which will appear in some derivations of this thesis, and is defined by [42, eq. 5.71.21] [43]

$$\Phi_2^{(n)}(b_1,\ldots,b_n;c;x_1,\ldots,x_n) = \sum_{m_1,\ldots,m_n=0}^{\infty} \frac{(b_1)_{m_1}\ldots(b_n)_{m_n}}{(c)_{m_1+\ldots+m_n}} \frac{x_1^{m_1}}{m_1!}\cdots\frac{x_n^{m_n}}{m_n!}, \tag{2.3.21}$$

where $(a)_m = a(a+1)\ldots(a+m-1)$ is the pochhammer symbol. The series $\Phi_2^{(n)}$ is also referred to as the Humbert's confluent hypergeometric series in n variables, and the case of two variables is often denoted by $\Phi_2 = \Phi_2^{(2)}$.

An important result on the Laplace transform of $\Phi_2^{(n)}$, which have been used in some derivations in chapters 3 and 4, is as follows [44, eq. 3.43.1.4]

$$\mathcal{L}\left[t^{c-1}\Phi_2^{(n)}\left(b_1,\ldots,b_n;c;a_1t,\ldots,a_nt\right);s\right]=\frac{\Gamma\left(c\right)}{s^c}\left(1-\frac{a_1}{s}\right)^{-b_1}\ldots\left(1-\frac{a_n}{s}\right)^{-b_n}, \quad (2.3.22)$$

with $\Re\left\{c\right\}>0$.

2.3.3 Incomplete Lipschitz-Hankel Integrals

Incomplete Lipschitz-Hankel integrals (ILHIs) are a class of incomplete cylindrical functions [18] that traditionally appear in the analytical solutions of numerous problems in electromagnetics [19]. Within the communication theory context, Pawula reported on the connection between the Rice I_e-function [45], which is a special type of ILHI, and the Marcum Q function [46–48], pointing out some advantages to be gained for performance analysis with a representation whose genesis lies in the ILHIs.

As it will be shown later in Chapter 4 within the context of performance analysis of SIMO systems, we have encountered certain ILHIs for which an explicit solution is aimed. Specifically, we are interested on exact and closed-form expressions for ILHIs of modified Bessel functions and certain type of incomplete integrals involving the generalized Marcum Q function, known as incomplete integrals of Marcum Q functions (IIMQs). Closed-form expressions for the solution of these integrals are not available in the classical references for this kind of functions, e.g. [41, 49–51]. However, Paris *et al.* have recently presented in [20] new explicit expressions for ILHIs and IIMQs which have been applied to the analysis of SIMO systems in this thesis.

In order to provide the reader with the complete mathematical framework used in the performance analysis of this thesis, this section gathers the main results on ILHIs and IIMQs obtained in [20]. First, it will be shown that the incomplete integrals IIMQs, involving the generalized Marcum Q function, are represented by a finite number of elementary functions, Marcum Q functions and ILHIs. Then, the explicit solution for ILHIs will be presented, showing that these integrals can be expressed in terms of Bessel and Marcum Q functions.

Definitions

The general family of incomplete Lipschitz-Hankel integrals of first-kind modified Bessel functions are defined as [52]

$$I_{e_{\mu,\nu}}(z;\alpha) \triangleq \int_0^z t^{\mu} e^{-\alpha\, t} I_{\nu}\left(t\right) dt, \tag{2.3.23}$$

where I_{ν} is the modified Bessel function of the first kind defined in (2.3.13)-(2.3.14), and $\alpha, z, \nu, \mu \in \mathbb{C}$, whereas, to assure convergence, $\Re\{1+\mu+\nu\} > 0$.

In particular, we are interested in the following specialization of (2.3.23).

Definition 1 (ILHI of modified Bessel functions)**.**

$$I_{e_{m,n}}(x;\alpha) \triangleq I_{e_{\mu=m,\nu=n}}(z=x;\alpha) = \int_0^x t^{m} e^{-\alpha\, t} I_{n}\left(t\right) dt, \tag{2.3.24}$$

where $\alpha \in \mathbb{R}$, $m, n \in \mathbb{N}$; $\alpha > 1$ *and* $x \in [0, \infty)$.

For simplicity, the function $I_{e_{m,n}}(x;\alpha)$ will be referred to as the ILHI of m-th degree, n-th order and parameter α.

We are also interested in the following family of incomplete integrals involving Marcum Q functions, referred to as IIMQs. This type of integrals are formally equivalent to those solved in [53, 54] whose integrands involve powers, exponentials and the Marcum Q function with two linear arguments. However, the IIMQs have finite integration limits and, thus, the solutions given in [53, 54] for the complete integrals are not valid in this case.

Definition 2 (Incomplete Integrals of Marcum Q functions (IIMQ))**.**

$$Q_{e_{m,n}}(x;\beta,a,b) \triangleq \int_0^x t^{m} e^{-\beta\, t} Q_{n}\left(a\sqrt{t}, b\sqrt{t}\right) dt, \tag{2.3.25}$$

where Q_n *is the generalized* n*-th order Marcum Q function, defined in (2.3.18),* $\beta, a, b \in \mathbb{R}$, $m, n \in \mathbb{N}$; $\beta, a, b > 0$, $n \geq 1$ *and* $x \in [0, \infty)$.

Again for simplicity, the function $Q_{e_{m,n}}(x;\beta,a,b)$ will be referred to as the IIMQ function of m-th degree, n-th order and parameters β, a, b. Note that Definition 2 includes the complete integrals solved in [53, 54] when $x \to \infty$.

Connection between the IIMQ functions and ILHIs

Recent results in [20] show that the IIMQ function can be represented by an expression involving a finite number of generalized Marcum Q functions and ILHIs. This connection between IIMQ and ILHI is stated by the following Lemma, reproduced from [20].

Lemma 1. *The IIMQ function can be represented as*

$$Q_{e_{m,n}}(x;\beta,a,b) = \frac{m!}{\beta^{m+1}}\Bigg\{1-e^{-\beta x}Q_n\left(a\sqrt{x},b\sqrt{x}\right)\sum_{r=0}^{m}\frac{\beta^r}{r!}x^r + \frac{1}{2}\sum_{r=0}^{m}\frac{\beta^r}{r!}\frac{b^{n-r-1}}{a^{n+r}}\left(a\,I_{e_{r,n}}(abx;\alpha)-b\,I_{e_{r,n-1}}(abx;\alpha)\right)\Bigg\}, \tag{2.3.26}$$

where $\alpha = \frac{a^2+b^2+2\beta}{2ab} > 1$.

Proof. See [20, Appendix I]. This proof has been included in Appendix A.1 for completeness. □

Connection between the ILHI and the Marcum Q functions

As stated above, closed-form expressions for the solution of ILHIs have been obtained in [20], showing that the ILHI can be represented in terms of Bessel and Marcum Q functions. In the subsequent, Lemma 2 and Proposition 1 gather the closed-form expressions for the ILHI, which will be applied to the analysis of SIMO systems in Chapter 4.

Lemma 2. *The ILHIs for low degrees and low orders are given by [20]*

(i) $I_{e_{0,0}}(x;\alpha) = \bar{\alpha} - 2\bar{\alpha}Q_1\left(\frac{\sqrt{x}}{\sqrt{\alpha+\sqrt{\alpha^2-1}}},\sqrt{x}\sqrt{\alpha+\sqrt{\alpha^2-1}}\right) + \bar{\alpha}e^{-\alpha x}I_0(x)$

(ii) $I_{e_{1,0}}(x;\alpha) = \alpha\bar{\alpha}^3 - 2\alpha\bar{\alpha}^3Q_1\left(\frac{\sqrt{x}}{\sqrt{\alpha+\sqrt{\alpha^2-1}}},\sqrt{x}\sqrt{\alpha+\sqrt{\alpha^2-1}}\right) + \alpha\bar{\alpha}^3e^{-\alpha x}I_0(x) - \alpha\bar{\alpha}^2e^{-\alpha x}xI_0(x) - \bar{\alpha}^2e^{-\alpha x}xI_1(x)$

(iii) $I_{e_{0,1}}(x;\alpha) = \alpha\bar{\alpha} - 1 - 2\alpha\bar{\alpha}Q_1\left(\frac{\sqrt{x}}{\sqrt{\alpha+\sqrt{\alpha^2-1}}},\sqrt{x}\sqrt{\alpha+\sqrt{\alpha^2-1}}\right) + (1+\alpha\bar{\alpha})\,e^{-\alpha x}I_0(x)$

(iv) $I_{e_{1,1}}(x;\alpha) = \bar{\alpha}^3 - 2\bar{\alpha}^3Q_1\left(\frac{\sqrt{x}}{\sqrt{\alpha+\sqrt{\alpha^2-1}}},\sqrt{x}\sqrt{\alpha+\sqrt{\alpha^2-1}}\right) + \bar{\alpha}^3e^{-\alpha x}I_0(x) - \bar{\alpha}^2e^{-\alpha x}xI_0(x) - \alpha\bar{\alpha}^2e^{-\alpha x}xI_1(x)$

where $\bar{\alpha} \triangleq \frac{1}{\sqrt{\alpha^2-1}}$.

Proof. The proof, which can be found in [20, Appendix II], is included for completeness in Appendix A.2. □

Proposition 1. *The m-th degree and n-th order ILHI is represented by an expression involving a first-order Marcum Q function and a finite number of Bessel functions, specifically [20]*

$$I_{e_{m,n}}(x;\alpha) = \mathcal{A}^0_{m,n}(\alpha) + \mathcal{A}^1_{m,n}(\alpha) Q_1\left(\frac{\sqrt{x}}{\sqrt{\alpha+\sqrt{\alpha^2-1}}}, \sqrt{x}\sqrt{\alpha+\sqrt{\alpha^2-1}}\right) + \mathrm{e}^{-\alpha x}\sum_{i=0}^{m}\sum_{j=0}^{n+1}\mathcal{B}^{i,j}_{m,n}(\alpha) x^i I_j(x), \tag{2.3.27}$$

where the set of coefficients $\mathcal{A}^l_{m,n}(\alpha), \mathcal{B}^{i,j}_{m,n}(\alpha)$ can be obtained recursively in a finite number of steps by the algorithm given in Appendix A.3.

Proof. See [20, Appendix III]. Also, for completeness sake, this proof has been included in Appendix A.3. □

Finally, the closed-form representation for the IIMQ function follows from Lemma 1 and Proposition 1.

Corollary 1. *The m-th degree and n-th order IIMQ is represented by the following expression involving a finite number of Marcum Q and Bessel functions [20]:*

$$\begin{aligned} Q_{e_{m,n}}(x;\beta,a,b) &= \frac{m!}{\beta^{m+1}} - \frac{m!}{\beta^{m+1}} e^{-\beta x} Q_n\left(a\sqrt{x}, b\sqrt{x}\right) \sum_{r=0}^{m}\frac{\beta^r}{r!}x^r + \frac{1}{2}\frac{m!}{\beta^{m+1}}\sum_{r=0}^{m}\frac{\beta^r}{r!}\frac{b^{n-r-1}}{a^{n+r}} \\ &\times \left\{ a\mathcal{A}^0_{r,n}(\alpha) - b\mathcal{A}^0_{r,n-1}(\alpha) + \left(a\mathcal{A}^1_{r,n}(\alpha) - b\mathcal{A}^1_{r,n-1}(\alpha)\right) Q_1\left(\frac{\sqrt{abx}}{\sqrt{\alpha+\sqrt{\alpha^2-1}}}, \sqrt{abx}\sqrt{\alpha+\sqrt{\alpha^2-1}}\right)\right. \\ &\left. + e^{-\alpha abx}\sum_{i=0}^{r} a\mathcal{B}^{i,n+1}_{r,n}(\alpha)(abx)^i I_{n+1}(abx) + \sum_{j=0}^{n}\left(a\mathcal{B}^{i,j}_{r,n}(\alpha) - b\mathcal{B}^{i,j}_{r,n-1}(\alpha)\right)(abx)^i I_j(abx)\right\} \end{aligned} \tag{2.3.28}$$

where $\alpha = \frac{a^2+b^2+2\beta}{2ab}$.

The finite recursive algorithm to obtain the coefficients $\mathcal{A}^l_{m,n}(\alpha), \mathcal{B}^{i,j}_{m,n}(\alpha)$ of Proposition 1 and Corollary 1 can be found in Appendix A.3. Besides, a MATHEMATICA™ program is provided in Appendix A.4 to compute the set of coefficients $\{\mathcal{A}^l_{r,k}(\alpha), \mathcal{B}^{i,j}_{r,k}(\alpha)\}$ either numerically or symbolically.

2.4 The Diagonal Distribution of Complex Wishart Matrices

The statistical properties of Wishart matrices have been extensively used to analyze the performance of MIMO systems. As it will be shown later in Chapter 5, the SNR output statistics of several MIMO systems depends on the diagonal distribution of a complex Wishart matrix. Specifically, we are interested on the distribution of the maximum of the diagonal of a complex Wishart matrix. In order to arrive at the distribution of the maximum, the joint cumulative distribution function (CDF) of the diagonal elements, which follow a particular multivariate chi-square distribution, is needed.

There is a rich body of works considering the joint distribution of the diagonal elements of real Wishart matrices; equivalently, multivariate chi-square distributions derived from real Gaussian random variables [31–35]. Whereas the characteristic function (CF) is well known [33], the joint CDF and probability density function (PDF) are rather more complicated. Different approaches to the joint CDF and PDF have been proposed in the literature for the real case. An infinite series expansion in terms of Laguerre polynomials was first given in [33]. Later work by Royen [34] provided new Laguerre expansions with improved convergence. In [35], Miller *et al.* derived expansions for the PDF in terms of Bessel functions for the bivariate and trivariate cases. However, the case of underlying complex Gaussian random variables, i.e., complex Wishart matrices, has not been sufficiently investigated. Only very recently, Hagedorn *et al.* [36] have derived corresponding expansions for the trivariate case. To the best of the author's knowledge, the case of k-variate chi-square ($k > 3$) from a complex Wishart matrix with arbitrary correlation is not available in the literature. Moreover, the expansions in [36] for $k = 3$ are in the form of Bessel functions and are not suitable for further performance analysis (e.g., closed-form ABEP analysis).

In this section, we provide novel series expansions for the joint PDF and joint CDF of the diagonal elements of complex Wishart matrices, i.e., for the general k-variate chi-square ($k > 3$) with arbitrary correlation. Then, we focus on the statistics of the maximum of the diagonal elements, presenting new series expansions for the PDF and CDF.

2.4.1 Preliminaries

Let $\mathbf{X}_j = [X_{1,j}, X_{2,j}, \ldots, X_{k,j}]^T$ be the j-th sample of a k-dimensional zero-mean complex Gaussian process ($j = 1, 2, \ldots, p$), where $\{\mathbf{X}_j\}$ are mutually independent and identically distributed (i.i.d.). The covariance (or correlation) matrix for each Gaussian random vector is $\mathbf{R} = \mathtt{E}\left[\mathbf{X}_j \mathbf{X}_j^H\right]$, i.e., $\mathbf{X}_j \sim \mathcal{CN}(\mathbf{0}, \mathbf{R})$. Then, the matrix $\mathbf{S} = \sum_{j=1}^{p} \mathbf{X}_j \mathbf{X}_j^H$ has a complex Wishart distribution denoted by $\mathcal{CW}_k(p, \mathbf{R})$, and the diagonal elements of $\mathbf{S}$, defined by

$$\mathsf{diag}(\mathbf{S}) = (Y_1, Y_2, \ldots, Y_k) = \left(\sum_{j=1}^{p} |X_{1,j}|^2, \sum_{j=1}^{p} |X_{2,j}|^2, \ldots, \sum_{j=1}^{p} |X_{k,j}|^2 \right), \tag{2.4.1}$$

are chi-square distributed with $2p$ degrees of freedom, i.e., $Y_i \sim \chi^2(0, 2p)$ having PDF

$$f_{Y_i}(y) = \frac{1}{2^p \Gamma(p)} y^{p-1} e^{-\frac{y}{2}}, \quad (i = 1, 2, \ldots, k), \tag{2.4.2}$$

where $\Gamma(\cdot)$ is the gamma function, defined in (2.3.6). Note that this is just a scaled version of the gamma distribution, $f_{Y_i}(y) = \frac{1}{2} g_p\left(y/2\right)$, with the gamma density defined as

$$g_\alpha(x) = \frac{x^{\alpha-1} e^{-x}}{\Gamma(\alpha)}, \tag{2.4.3}$$

The joint distribution of $(Y_1, Y_2, \ldots, Y_k)$, i.e., the diagonal distribution of the complex Wishart matrix $\mathbf{S}$, is a k-variate central chi-square distribution with correlation structure induced by $\mathbf{R}$. The rest of this section is devoted to the statistical analysis of this distribution. Specifically, exact infinite series expansions are provided for both the joint CDF and joint PDF denoted by $F_{Y_1,Y_2,\ldots,Y_k}(y_1, y_2, \ldots, y_k)$ and $f_{Y_1,Y_2,\ldots,Y_k}(y_1, y_2, \ldots, y_k)$, respectively.

2.4.2 Joint Cumulative Distribution Function

Our objective is to find a tractable and easily computable expansion for the CDF by following a similar approach to that in [34], where results are provided for the real case. In the complex case, the correlation structure of the underlying Gaussian random variables is different, leading to a slightly different CF with a complex correlation matrix. In the extension to the complex case, we basically apply the approach in [34] to the CF, and

then the binomial expansion and Fourier inversion are used to obtain the series. As a different CF with a complex correlation matrix is involved, the validity of the derivations in [34] has been revised and carefully checked. Then, our analysis diverges from that in [34] by using a more convenient representation and rearranging the series when it comes to the distribution of the maximum of the diagonal elements (see Section 2.4.4).

The starting point is the CF for the diagonal distribution of a real Wishart matrix, which is well known [33, 34]. After an extension to the complex case, it is possible to write the CF of the diagonal elements of a complex Wishart as

$$\Phi\left(t_1,\ldots,t_k\right) = \mathtt{E}\left[e^{i(t_1Y_1+\cdots+t_kY_k)}\right] = \left|\mathbf{I}-i\mathbf{R}\mathbf{T}\right|^{-p}, \tag{2.4.4}$$

where $\mathbf{I}$ is the k-dimensional identity matrix, $\mathbf{R} = \mathtt{E}\left[\mathbf{X}_j\mathbf{X}_j^H\right]$ is the covariance or also referred to as correlation matrix, and $\mathbf{T} = \mathsf{Diag}\left(t_1,\ldots,t_k\right)$.

Using the approach in [34] to (2.4.4), we arrive at the following representation of the CF:

$$\Phi\left(t_1,\ldots,t_k\right) = \left|\mathbf{I}-\left(\mathbf{I}-\mathbf{W}\mathbf{R}\mathbf{W}\right)\mathbf{U}\right|^{-p}\prod_{j=1}^{k}\left(1-u_j\right)^p, \tag{2.4.5}$$

where $\mathbf{W} = \mathsf{Diag}\left(w_1,\ldots,w_k\right)$, with w_j any scale factors, and $\mathbf{U} = \mathsf{Diag}\left(u_1,\ldots,u_k\right)$, with

$$u_j = 1-\left(1-i\frac{t_j}{w_j^2}\right)^{-1}. \tag{2.4.6}$$

Note that the Fourier transform of $w\cdot g_{p+n}^{(n)}\left(w\cdot y_j\right)$, where $g_{p+n}^{(n)}\left(x\right)$ denotes the n-th derivative of the gamma density $g_{p+n}\left(x\right)$, is given by

$$u_j^n\left(1-u_j\right)^p, \quad \text{for } \Re\left\{\left(1-u_j\right)^{\frac{1}{2}}\right\} > 0. \tag{2.4.7}$$

For convenience, we define $g_p^{(-1)}\left(x\right)$ as the gamma CDF, i.e.,

$$g_p^{(-1)}\left(x\right) \triangleq G_p\left(x\right) = \frac{\gamma\left(p,x\right)}{\Gamma\left(p\right)} = 1-e^{-x}\sum_{j=0}^{p-1}\frac{x^j}{j!}, \tag{2.4.8}$$

where $\gamma(\cdot,\cdot)$ is the incomplete gamma function, defined in (2.3.9).

The CF in (2.4.5) can be expressed as an infinite series by replacing $\left|\mathbf{I}-\left(\mathbf{I}-\mathbf{W}\mathbf{R}\mathbf{W}\right)\mathbf{U}\right|^{-p}$ with its binomial expansion and, then, the joint CDF is obtained by the Fourier inversion

of the series. Thus, after considering (2.4.7) as well as previous definition in (2.4.8), the following expansion for the joint CDF is obtained:

$$F_{Y_1,Y_2,\ldots,Y_k}(y_1,y_2,\ldots,y_k)=\sum_{n=0}^{\infty}\sum_{(n=n_1+\cdots+n_k)}c(n_1,\ldots,n_k)\prod_{j=1}^{k}g_{p+n_j}^{(n_j-1)}\left(w_j^2y_j\right), \tag{2.4.9}$$

where $\sum_{(n=n_1+\cdots+n_k)}$ denotes the summation over all possible integer partitions satisfying $n=n_1+\cdots+n_k$, and the coefficients $c(n_1,\ldots,n_k)$ depend on p, the scale factors w_j, and the complex correlation matrix $\mathbf{R}$. The scale factors are chosen to assure the convergence of (2.4.9), which is guaranteed under the condition [1]

$$\|\mathbf{I}-\mathbf{WRW}\|_s<1, \tag{2.4.10}$$

where $\|\mathbf{A}\|_s$ denotes the spectral norm of $\mathbf{A}$, i.e. the square root of the maximum eigenvalue of $\mathbf{A}^H\mathbf{A}$.

Now, using the Rodrigues' formula [51, eq. 22.11.6], we can write

$$g_{p+n}^{(n-1)}(x)=\frac{(n-1)!}{(p+n-1)!}e^{-x}x^pL_{n-1}^p(x), \tag{2.4.11}$$

where $L_n^a(x)$ is the n-th order generalized Laguerre polynomial, defined in (2.3.5). Thus, the joint CDF can be rewritten in terms of the Laguerre polynomials as

$$F_{Y_1,Y_2,\ldots,Y_k}(y_1,y_2,\ldots,y_k)=\sum_{n=0}^{\infty}\sum_{(n=n_1+\cdots+n_k)}c(n_1,\ldots,n_k)\prod_{j=1}^{k}\Delta_{n_j}^p\left(w_j^2y_j\right), \tag{2.4.12}$$

with

$$\Delta_n^p(x)\triangleq\begin{cases}G_p(x)=1-e^{-x}\sum_{j=0}^{p-1}\frac{x^j}{j!}, & \text{for } n=0,\\ g_{p+n}^{(n-1)}(x)=\frac{(n-1)!}{(p+n-1)!}e^{-x}x^pL_{n-1}^p(x) & \text{for } n>0.\end{cases} \tag{2.4.13}$$

What remains to complete the expansion of the joint CDF in (2.4.12) is to find an easily computable expression for the coefficients $c(n_1,\ldots,n_k)$, which is addressed by the following proposition.

Proposition 2. *The coefficients $c(n_1,\ldots,n_k)$ for the series expansion in (2.4.12) can be obtained as the coefficients of the n-order homogeneous polynomial θ_n as*

$$\begin{aligned}\theta_n(u_1,u_2,\ldots,u_k)&=\sum_{(n=n_1+\cdots+n_k)}c(n_1,\ldots,n_k)\prod_{j=1}^{k}u_j^{n_j}\\&=\sum_{(n=\ell_1+2\ell_2+\cdots+k\ell_k)}\frac{\Gamma(p+\ell_1+\cdots+\ell_k)}{\Gamma(p)}\prod_{j=1}^{k}\frac{(-D_j)^{\ell_j}}{\ell_j!},\end{aligned} \tag{2.4.14}$$

[1] The sufficient condition for convergence of the series follows from the binomial expansion of (2.4.5), and a proof can be obtained from [34, Theorem 2.1].

where D_j denotes the polynomial generated from the determinants of the submatrices of $\mathbf{A} = \mathbf{I} - \mathbf{WRW}$ *as*

$$D_j = (-1)^j \sum_{\mathsf{size}(\mathcal{S})=j} |\mathbf{A}_{\mathcal{S}}| \prod_{m \in \mathcal{S}} u_m, \tag{2.4.15}$$

with $\mathbf{A}_{\mathcal{S}}$ representing the submatrix of $\mathbf{A}$ with the rows and columns specified by the non-empty subset $\mathcal{S} \subseteq \{1, 2, \ldots, k\}$, and $\sum_{\mathsf{size}(\mathcal{S})=j}$ denoting the summation computed over all possible subsets $\mathcal{S}$ whose size is j.

Proof. See Appendix B.1. □

It should be noted that all the coefficients in the series for a given value of n are obtained from the polynomial θ_n, which makes the computation very efficient. Also, it is likely to find a great number of null coefficients, especially for a large number of variables (k). As a consequence, the terms in the series to be computed are reduced to those appearing in the polynomial θ_n, which significantly decreases the computation cost. Appendix B.2 includes a MATHEMATICA™ program with an efficient algorithm to compute the polynomial θ_n, where the coefficients $c(n_1, \ldots, n_k)$ can be easily extracted from.

2.4.3 Joint Density Function

The joint PDF of the diagonal elements of a complex Wishart matrix $f_{Y_1,Y_2,\ldots,Y_k}(y_1, y_2, \ldots, y_k)$ can be obtained by differentiation of the CDF in (2.4.12), which allows us to write

$$f_{Y_1,Y_2,\ldots,Y_k}(y_1, y_2, \ldots, y_k) = \sum_{n=0}^{\infty} \sum_{(n=n_1+\cdots+n_k)} c(n_1, \ldots, n_k) \prod_{j=1}^{k} \frac{d\left[\Delta_{n_j}^{p}\left(w_j^2 y_j\right)\right]}{dy_j}. \tag{2.4.16}$$

The derivative of the delta function, defined in (2.4.13), is given by

$$\frac{d\Delta_n^p(x)}{dx} = g_{p+n}^{(n)}(x) = \frac{n!}{(p+n-1)!} e^{-x} x^{p-1} L_n^{p-1}(x). \tag{2.4.17}$$

Then, by substituting (2.4.17) into (2.4.16), the expansion for the joint PDF is expressed as

$$f_{Y_1,Y_2,\ldots,Y_k}(y_1, y_2, \ldots, y_k) = \sum_{n=0}^{\infty} \sum_{(n=n_1+\cdots+n_k)} c(n_1, \ldots, n_k) \prod_{j=1}^{k} w_j^2 g_{p+n_j}^{(n_j)}\left(w_j^2 y_j\right). \tag{2.4.18}$$

Note that the joint PDF is given in terms of the n-th derivative of the gamma density, which in turn is directly related to the generalized Laguerre polynomials, as shown in (2.4.17).

2.4.4 Statistics for the Maximum of the Diagonal Elements

The diagonal of a complex Wishart matrix is a type of multivariate central chi-square distribution with a certain underlying complex correlation matrix. The distribution of the maximum of these correlated variables is of special interest within the performance analysis of many communication systems [8, 28–30, 55]. This section presents expressions for the CDF and PDF of this distribution. In particular, the CDF of the maximum will be applied to the OP analysis of MIMO systems in Chapter 5. For a better representation and an efficient computation of the CDF, an important series rearrangement is also provided in this section. Besides, expressions for the special bivariate case and an approximation for small values of the argument of the CDF are addressed. This approximation finds applicability in the OP analysis when the high SNR regime is considered.

CDF and PDF

Let us consider Z to be the maximum of the k correlated central chi-square random variables, i.e., $Z = \max\{Y_1, Y_2, \ldots, Y_k\}$. On the one hand, the CDF of Z is given by

$$\begin{aligned} F_Z(z) &= \Pr\{Z \leq z\} \\ &= \Pr\{Y_1 \leq z, Y_2 \leq z, \ldots, Y_k \leq z\} \\ &= F_{Y_1,Y_2,\ldots,Y_k}(z, z, \ldots, z). \end{aligned} \tag{2.4.19}$$

That is, the CDF of the maximum is obtained by setting the argument of the joint CDF in (2.4.12) to $(z, z, \ldots, z)$, which yields

$$F_Z(z) = \sum_{n=0}^{\infty} \sum_{(n=n_1+\cdots+n_k)} c(n_1, \ldots, n_k) \prod_{j=1}^{k} \Delta_{n_j}^{p}\left(w_j^2 z\right), \tag{2.4.20}$$

where $\Delta_n^p(x)$ are as previously defined in (2.4.13), and $c(n_1, \ldots, n_k)$ are obtained as in Proposition 2. On the other hand, the PDF of Z can be obtained by differentiation of (2.4.20), thus yielding

$$f_Z(z) = \sum_{n=0}^{\infty} \sum_{(n=n_1+\cdots+n_k)} c(n_1, \ldots, n_k) \sum_{j=1}^{k} w_j^2 g_{p+n_j}^{(n_j)}\left(w_j^2 z\right) \prod_{\substack{i\in\{1,\ldots,k\} \\ i\neq j}} \Delta_{n_i}^{p}\left(w_i^2 z\right), \tag{2.4.21}$$

with $g_{p+n}^{(n)}(x)$ as previously defined in (2.4.17).

Series rearrangement

The derived series expansions for both the CDF and PDF of Z can be rearranged under the assumption of having a single scale factor $w = w_1 = w_2 = \cdots = w_k$. Let $P^{(n)} = \left\{P_i^{(n)}\right\}$, for $i = 1, \ldots, s_n$, be the set of all integer partitions of n into k elements and s_n its size. Note that the sequence $(n_1, \ldots, n_k)$ is just some permutation of $P_i^{(n)} = \left\{p_{i,1}^{(n)}, \ldots, p_{i,k}^{(n)}\right\}$. Also, note that there is one term (coefficient) in the series for each ordered sequence $(n_1, \ldots, n_k)$ that satisfies $n = n_1 + \cdots + n_k$, i.e., one term for each permutation of $P_i^{(n)}$. Under the single scale factor assumption, the CDF series becomes

$$F_Z(z) = \sum_{n=0}^{\infty} \sum_{(n=n_1+\cdots+n_k)} c(n_1, \ldots, n_k) \prod_{j=1}^{k} \Delta_{n_j}^{p}\left(w^2 z\right), \tag{2.4.22}$$

where the dependence of the product with the ordered sequence $(n_1, \ldots, n_k)$ vanishes since all the delta functions have the same argument. Now, the product in (2.4.22) depends only on the scale factor w and on the integer partition $P_i^{(n)}$. Then, all the terms corresponding to permutations of the same integer partition can be grouped under a new term with coefficient $\hat{c}\left(P_i^{(n)}\right)$, thus yielding the rearranged series

$$F_Z(z) = \sum_{n=0}^{\infty} \sum_{i=1}^{s_n} \hat{c}\left(p_{i,1}^{(n)}, \ldots, p_{i,k}^{(n)}\right) \prod_{j=1}^{k} \Delta_{p_{i,j}^{(n)}}^{p}\left(w^2 z\right), \tag{2.4.23}$$

where $\hat{c}\left(p_{i,1}^{(n)}, \ldots, p_{i,k}^{(n)}\right) = \sum_{(n_1,\ldots,n_k)\in P_i^{(n)*}} c(n_1, \ldots, n_k)$ with $P_i^{(n)*}$ being the set of all possible permutations of $P_i^{(n)}$. It is emphasized that, with this rearrangement, the number of terms in the series for a given n is reduced by the total number of permutations of the integer partitions of n, which allows for an easy and rapid computation. In Appendix B.2, a MATHEMATICA™ program is provided to efficiently compute $\hat{c}\left(p_{i,1}^{(n)}, \ldots, p_{i,k}^{(n)}\right)$ for $i = 1, \ldots, s_n$ and $n = 0, \ldots, N_{max}$, where N_{max} is the truncation limit. The distribution of the maximum, given by the rearranged series in (2.4.23), has been applied to the OP analysis of MIMO systems in Chapter 5. As it will be shown later in Chapter 5, the time to compute all the coefficients for a typical truncation limit $N_{max} = 8$, which gives an accurate CDF representation (4-figure accuracy), is less than one second.

The bivariate case ($k = 2$)

The joint CDF in this case is given by

$$F_{Y_1,Y_2}(y_1, y_2) = \sum_{n=0}^{\infty} \sum_{(n=n_1+n_2)} c(n_1, n_2) \Delta_{n_1}^p \left(w_1^2 y_1\right) \Delta_{n_2}^p \left(w_2^2 y_2\right), \tag{2.4.24}$$

with $\Delta_n^p(x)$ as previously defined.

Under the single scale factor assumption $w_1 = w_2 = 1$, the polynomial in (2.4.14) to obtain the coefficients $c(n_1, n_2)$ reduces to

$$\theta_n(u_1, u_2) = \begin{cases} 0, & n \quad \text{odd}, \\ \frac{(p-1+n/2)!}{(p-1)!(n/2)!} |r|^n (u_1 u_2)^{n/2}, & n \quad \text{even}, \end{cases} \tag{2.4.25}$$

where r is the complex value from the correlation matrix $\mathbf{R} = \begin{pmatrix} 1 & r \\ r^* & 1 \end{pmatrix}$. Thus, there is only one non-null coefficient for each even value of n given by

$$c(n/2, n/2) = \frac{(p-1+n/2)!}{(p-1)!\,(n/2)!} |r|^n, \tag{2.4.26}$$

and the series for the joint CDF in the bivariate case can be rewritten as

$$F_{Y_1,Y_2}(y_1, y_2) = G_p(y_1)\, G_p(y_2) + \frac{e^{-y_1} e^{-y_2} y_1^p y_2^p}{(p-1)!} \sum_{n=1}^{\infty} \frac{(n-1)!}{n\,(p+n-1)!} |r|^{2n} L_{n-1}^p(y_1)\, L_{n-1}^p(y_2), \tag{2.4.27}$$

where $G_p(x)$ is the gamma CDF, defined in (2.4.8). Finally, the distribution of the maximum is obtained by setting $y_1 = y_2 = z$ in (2.4.27), which yields

$$F_Z(z) = G_p(z)^2 + \frac{e^{-2z} z^{2p}}{(p-1)!} \sum_{n=1}^{\infty} \frac{(n-1)!}{n\,(p+n-1)!} |r|^{2n} L_{n-1}^p(z)^2. \tag{2.4.28}$$

Approximation for $z \to 0$

In order to obtain an approximation of $F_Z(z)$ for small values of z, we first study the behavior of the delta functions $\Delta_n^p(x)$ in the limit $x \to 0$. After substituting the exponential function by its Taylor expansion in (2.4.13) and some straightforward algebra, we arrive at

$$\lim_{x \to 0} \Delta_n^p(x) = \frac{x^p}{p!}. \tag{2.4.29}$$

Then, (2.4.29) is used in (2.4.20) to obtain the following approximation which holds for $z \to 0$

$$F_Z(z) \approx \alpha \left(\frac{1}{p!}\right)^k z^{pk} \prod_{j=1}^{k} w_j^{2p}, \tag{2.4.30}$$

where α is the sum of all the coefficients, namely

$$\alpha = \sum_{n=0}^{\infty} \sum_{(n=n_1+\ldots+n_k)} c(n_1, \ldots, n_k). \tag{2.4.31}$$

Also, it is possible to see from (B.1.1) in Appendix B that the sum of coefficients can be obtained as

$$\alpha = |\mathbf{I} - (\mathbf{I} - \mathbf{WRW})|^{-p} = |\mathbf{WRW}|^{-p}. \tag{2.4.32}$$

Then, the approximation for the CDF of the maximum is rewritten as

$$F_Z(z) \approx |\mathbf{WRW}|^{-p} \left(\frac{1}{p!}\right)^k z^{pk} \prod_{j=1}^{k} w_j^{2p}, \tag{2.4.33}$$

which, under the single scale factor assumption, simplifies to

$$F_Z(z) \approx |\mathbf{R}|^{-p} \left(\frac{1}{p!}\right)^k z^{pk}. \tag{2.4.34}$$

2.5 Summary

In this chapter, we have presented the mathematical tools used in the performance analysis of SIMO and MIMO systems. First, the notation and main performance metrics which are aimed to be analyzed have been introduced. Then, some special functions and statistical distributions which will appear throughout this thesis have been addressed, by paying special attention to some special incomplete integrals, specifically ILHI and IIMQ, and the diagonal distribution of complex wishart matrices. Both these special integrals and the diagonal distribution of Wishart matrices are key tools to the performance analyses in this thesis. Of special importance are the derivations and expressions provided in the context of the diagonal distribution of complex Wishart matrices, which represent a significant contribution to the literature.

Regarding the incomplete integrals ILHI and IIMQ, important results for their solutions recently given in [20] have been presented for a better comprehension and completeness of the derivations in Chapter 4. Basically, these results show that the IIMQs are represented by a finite number of elementary functions, Marcum Q functions and ILHIs. Then, the ILHI is reduced to a closed-form expression involving a finite number of modified Bessel and Marcum Q functions.

In the context of complex Wishart matrices, we have derived the joint PDF and CDF of the diagonal elements, which follow a particular multivariate chi-square distribution. The CDF expression is in the form of an infinite series representation in terms of the well-known Laguerre polynomials, which has been shown to be easily computable. This expression has been used to obtain the distribution of the maximum of the diagonal elements, which allows analyzing the performance of two different MIMO systems under practical conditions as it will be shown in Chapter 5.

Chapter 3

Fading Channel Models

Radiowave propagation through wireless channels is a complicated phenomenon characterized by various effects such as multipath and shadowing. A precise mathematical description of this phenomenon is either unknown or too complex for tractable communication systems analyses. However, considerable efforts have been made for the statistical characterization of these effects. As a result, there is a big body of statistical models for fading channels that depend on the particular propagation environment and the underlying communication scenario. In particular, we are interested on the non line-of-sight (NLOS) propagation scenario, where there is no visual line between the transmitter and receiver antennas and, thus, the communication relies on the multiple reflections of the radio signal.

The primary purpose of this chapter is to briefly review the principal characteristics and models for fading channels. A more detailed explanation of this subject can be found in standard textbooks [56–58]. This chapter also introduces the terminology and notation regarding the NLOS fading models that will be used throughout the thesis.

This chapter is organized as follows. A brief description of the main characteristics of fading channels is presented in the next section. The classical NLOS fading distributions, usually adopted as models for frequency-flat fading channels, i.e. corresponding to narrowband transmission, without line-of-sight are described in Section 3.2. Finally, the $\eta - \mu$ fading distribution, which has been recently proposed in [38] is analyzed in detail in Section 3.3.

3.1 General Overview

When fading affects narrowband systems, the received carrier amplitude is modulated by the fading amplitude α, where α is a random variable (RV) with mean-square value $\Omega = \mathtt{E}[\alpha^2]$ and probability density function (PDF) $f_\alpha(\alpha)$, which is dependent on the nature of the radio propagation environment. After passing through the fading channel, the signal is perturbed at the receiver by additive white Gaussian noise (AWGN), which is typically assumed to be statistically independent of the fading amplitude α, and which is characterized by a Gaussian RV with zero mean and variance σ^2. Equivalently, the received instantaneous signal power is modulated by α^2. Thus, we define the instantaneous signal-to-noise power ratio (SNR) per symbol by $\gamma = \alpha^2 E_s/\sigma^2$ and the average SNR per symbol by $\bar{\gamma} = \Omega E_s/\sigma^2$, where E_s is the energy per symbol. In addition, the PDF of γ is obtained by introducing a change of variables in the expression for the fading PDF $f_\alpha(\alpha)$, yielding

$$f_\gamma(\gamma) = \frac{f_\alpha\left(\sqrt{\frac{\Omega\gamma}{\bar{\gamma}}}\right)}{2\sqrt{\frac{\gamma\bar{\gamma}}{\Omega}}}. \tag{3.1.1}$$

Another statistical function to characterize fading channels is the cumulative distribution function (CDF) of γ, $F_\gamma(x)$, which gives the probability of γ being less than or equal to a certain value x. The CDF of γ can be related to the outage probability of certain communication systems over fading channels, and is defined as

$$F_\gamma(x) \triangleq \int_0^x f_\gamma(\gamma)\, d\gamma. \tag{3.1.2}$$

Besides, the moment generating function (MGF) $M_\gamma(s)$ associated with the fading PDF $f_\gamma(\gamma)$, and defined by

$$M_\gamma(s) = \int_0^\infty f_\gamma(\gamma)\, e^{s\gamma} d\gamma, \tag{3.1.3}$$

provides an alternative route to analytical results compared with working directly with the PDF or CDF. The i-th moment of γ can be obtained as $\mathtt{E}[\gamma^i] = M_\gamma^{(i)}(0)$, i.e., by evaluating the i-th derivative of $M_\gamma(s)$ at $s = 0$. A generalization of the MGF of the instantaneous SNR, namely the generalized MGF (G-MGF) of γ, is found to be useful in

the analysis of communication systems subject to fading. The G-MGF of γ is defined by

$$M_{\gamma}(n,s) = \int_0^{\infty} \gamma^n f_{\gamma}(\gamma)\, e^{s\gamma} d\gamma. \tag{3.1.4}$$

Finally, the incomplete G-MGF (IG-MGF), which includes (3.1.4) as a particular case is defined by

$$\mathcal{G}_{\gamma}(n,s;\zeta) = \int_{\zeta}^{\infty} x^n \, \mathrm{e}^{sx} \, f_{\gamma}(\gamma)\, dx, \tag{3.1.5}$$

where[1] $s \in \mathbb{C}$, n is a nonnegative integer and $\zeta \in \mathbb{R}$ with $\zeta \geq 0$. Note that (3.1.5) includes, as particular cases, several important statistical functions associated to γ: $\mathcal{G}_{\gamma}(0,0;\zeta)$ is the complementary CDF; $\mathcal{G}_{\gamma}(0,s;0)$ is the MGF; $\mathcal{G}_{\gamma}(0,s;\zeta)$ is the marginal MGF and $\mathcal{G}_{\gamma}(n,s;0)$ is the generalized MGF. The IG-MGF of γ has been found of special importance in the context of the outage probability analysis of certain communication systems under co-channel interference, and will appear throughout the derivations of Chapter 4.

3.2 Classical Fading Distributions

Multipath fading is due to the constructive and destructive combination of randomly delayed, reflected, scattered, and diffracted signal components. This type of fading is relatively fast and is therefore responsible for the short-term signal variations. Depending on the nature of the radio propagation environment, there are different models describing the statistical behavior of the multipath fading envelope. In particular, the analyses carried out in this thesis correspond to the non line-of-sight (NLOS) propagation condition, where there is no visual line between the transmitter and receiver antennas. We now present the different fading distributions that have been used in this thesis to model the multipath envelope in NLOS fading channels, their corresponding PDF, CDF, and MGF, and their relation to physical channels.

[1] The variable s is only evaluated along the real line, however the complex domain is assumed here, in accordance with the usual definition of the MGF in the context of communications theory [1].

3.2.1 Rayleigh Distribution

The Rayleigh distribution is one of the most frequently used to model multipath fading when no line-of-sight (LOS) path exists between the transmitter and receiver antennas, i.e. under a NLOS propagation scenario. The Rayleigh fading model typically agrees very well with experimental data for mobile systems in a general NLOS scenario [58]. It also applies to the propagation of reflected and refracted paths through the troposphere and ionosphere, and to ship-to-ship radio links [59–61].

In this case, the channel fading amplitude α is distributed according to

$$f_{\alpha}(\alpha) = \frac{2\alpha}{\Omega} e^{\frac{-\alpha^2}{\Omega}}, \qquad \alpha \geq 0, \tag{3.2.1}$$

and hence, following (3.1.1), the instantaneous SNR per symbol of the channel γ is distributed according to an exponential distribution with PDF

$$f_{\gamma}(\gamma) = \frac{1}{\bar{\gamma}} e^{\frac{-\gamma}{\bar{\gamma}}}, \tag{3.2.2}$$

and corresponding CDF given by

$$F_{\gamma}(x) = 1 - e^{-\frac{x}{\bar{\gamma}}}. \tag{3.2.3}$$

Finally, the MGF of γ for the Rayleigh fading model is given by

$$M_{\gamma}(s) = (1 - s\bar{\gamma})^{-1}. \tag{3.2.4}$$

3.2.2 Nakagami-q (Hoyt) Distribution

The Nakagami-q distribution, also referred to as the Hoyt distribution [62], is commonly used to describe the short-term signal variation of certain wireless communication systems subject to fading [1, 62, 63]. It is typically observed on satellite links subject to strong ionospheric scintillation [64, 65] and, thus, the Hoyt fading distribution has been used in satellite-based communications to characterize more severe fading conditions than those modeled by Rayleigh [63, 66].

The PDF of the Nakagami-q distribution is given by [62]

$$f_{\alpha}(\alpha) = \frac{(1+q^2)\,\alpha}{q\Omega} e^{-\frac{\left(1+q^2\right)^2 \alpha^2}{4q^2\Omega}} I_0\left(\frac{(1-q^4)\,\alpha^2}{4q^2\Omega}\right) \quad , \alpha \geq 0, \tag{3.2.5}$$

where I_0 is the zero-th order modified Bessel function of the first kind and q is the Nakagami-q fading parameter, which ranges from 0 to 1. With different values of the fading parameter, the Hoyt distribution spans the range from one-sided Gaussian fading ($q = 0$) to Rayleigh fading ($q = 1$).

Using (3.1.1) and (3.2.5), it is shown that the SNR per symbol of the channel (γ) is distributed according to [1, eq. 2.11]

$$f_\gamma(\gamma) = \frac{(1+q^2)}{2q\bar{\gamma}} e^{-\frac{\left(1+q^2\right)^2 \gamma}{4q^2\bar{\gamma}}} I_0\left(\frac{(1-q^4)\,\gamma}{4q^2\bar{\gamma}}\right), \gamma \geq 0. \tag{3.2.6}$$

The CDF of γ for the Nakagami-q fading model has been recently obtained in closed-form in [67] and is given by

$$F_\gamma(x) = Q\left(u\sqrt{\frac{x}{\bar{\gamma}}}, v\sqrt{\frac{x}{\bar{\gamma}}}\right) - Q\left(v\sqrt{\frac{x}{\bar{\gamma}}}, u\sqrt{\frac{x}{\bar{\gamma}}}\right), \tag{3.2.7}$$

where $u \triangleq \frac{\sqrt{1-q^4}}{2q}\sqrt{\frac{1+q}{1-q}}$, $v \triangleq \frac{\sqrt{1-q^4}}{2q}\sqrt{\frac{1-q}{1+q}}$, and $Q(\cdot,\cdot)$ is the first order Marcum Q function, defined in (2.3.16).

Finally, the corresponding MGF of γ is in this case given by

$$M_\gamma(s) = \left(1 - 2s\bar{\gamma} + \frac{(2s\bar{\gamma})^2 q^2}{(1+q^2)^2}\right)^{-1/2}. \tag{3.2.8}$$

The generalized MGF of γ is of special importance in the context of the outage probability analysis of certain communication systems under Hoyt fading channels. Specifically, its incomplete version, the IG-MGF of γ $\mathcal{G}_\gamma(n, s; \zeta)$, has been applied to the analysis of maximum ratio combining (MRC) systems under Hoyt fading and co-channel interference in Chapter 4. A closed-form expression for $\mathcal{G}_\gamma(n, s; \zeta)$, which includes as a particular case the G-MGF, has been recently provided in [40] and can be found in Appendix D.

3.2.3 Nakagami-m Distribution

The Nakagami-m distribution [68] is used to model the multipath scattering with relatively large delay-time spreads. Its PDF is in essence a central chi-square distribution given by

$$f_\alpha(\alpha) = \frac{2m^m \alpha^{2m-1}}{\Omega^m \Gamma(m)} e^{\frac{-m\alpha^2}{\Omega}}, \alpha \geq 0, \tag{3.2.9}$$

where $\Gamma(\cdot)$ is the Gamma function, defined in (2.3.6), and m is the Nakagami-m fading parameter, which ranges from 1/2 to ∞.

The Nakagami-m distribution spans via the m parameter a wide range of multipath distributions. For instance, it includes the one-sided Gaussian distribution ($m = 1/2$) and the Rayleigh distribution ($m = 1$) as special cases. In the limit as $m \to \infty$, the Nakagami-m fading channel converges to a nonfading AWGN channel. Furthermore, when $m < 1$, it is possible to obtain a one-to-one mapping between the m parameter and the q parameter allowing the Nakagami-m distribution to closely approximate the Nakagami-q (Hoyt) distribution, and this mapping is given by

$$m = \frac{\left(1+q^2\right)^2}{2\left(1+2q^4\right)}, m \leq 1. \tag{3.2.10}$$

Applying (3.1.1) to (3.2.9) shows that the SNR per symbol γ is distributed according to a gamma distribution with PDF given by

$$f_\gamma(\gamma) = \frac{m^m \gamma^{m-1}}{\bar{\gamma}^m \Gamma(m)} e^{\frac{-m\gamma}{\bar{\gamma}}}, \gamma \geq 0, \tag{3.2.11}$$

and corresponding CDF given by

$$F_\gamma(x) = \frac{\gamma\left(m, \frac{m}{\bar{\gamma}}x\right)}{\Gamma(m)}, \tag{3.2.12}$$

where $\gamma(\cdot,\cdot)$ is the incomplete gamma function, defined in (2.3.9). Finally, the MGF of γ for the Nakagami-m fading model is given by

$$M_\gamma(s) = \left(1 - \frac{s\bar{\gamma}}{m}\right)^{-m}. \tag{3.2.13}$$

3.3 The η-μ Fading Distribution

The η-μ distribution is a general fading distribution recently proposed in [38] to better represent the small-scale variation of the fading signal in a NLOS condition. By setting two shape parameters η and μ, this model includes as particular cases all the classical NLOS fading distributions presented in the previous section, i.e., Rayleigh, Nakagami-q (Hoyt), and Nakagami-m. It has been shown that the fit of the η-μ distribution to experimental data is better than the classical NLOS distributions previously mentioned. A detailed description of the η-μ fading model can be found in [38] and references therein.

3.3.1 Physical Channel Model for the η-μ Distribution

The general fading model for the η-μ distribution considers a signal composed of clusters of multipath waves propagating in a non-homogeneous environment. Within any cluster, the phases of the scattered waves are random, and they have similar delay times with the delay-time spreads of different clusters being relatively large.

The η-μ distribution may appear in two different formats, for which two corresponding physical models have been defined [38]. In Format 1, the in-phase and quadrature components of the fading signal within each cluster are assumed to be independent from each other and to have different powers. In Format 2, the in-phase and quadrature components of the fading signal within each cluster are assumed to have identical powers and to be correlated with each other.

The two shape parameters of the distribution, η and μ, have a physical meaning within the defined physical models. On the one hand, $\mu > 0$ represents the real extension of $N/2$, where N is the number of clusters of multipath. Note that the physical parameter μ is of a continuous nature, while the number of clusters N is defined as an integer for the physical model. Values of μ may be obtained from physical field measurements and, thus, may be different from multiples of $1/2$, corresponding to non-integer values of the number of clusters [2]. On the other hand, η has different meanings and ranges for the two different formats. In Format 1, $0 < \eta < \infty$ is the scattered-wave power ratio between the in-phase and quadrature components of each cluster of multipath. In Format 2, $-1 < \eta < 1$ is the correlation coefficient between the scattered-wave in-phase and quadrature components of each cluster of multipath.

3.3.2 Statistical Functions for the η-μ Distribution

As for the classical fading distributions, we next present the main statistical functions for the distribution of the SNR per symbol γ in the η-μ fading model.

[2] Non-integer values of clusters have been found in practice, and are extensively reported in the literature (See [69] and references therein).

As stated above, there are two different formats for the η-μ distribution with different meanings and values of η. We will use the same notation as in [38], where two other parameters, h and H which are functions of η, are defined. The convenience of using these two parameters is to have a unified representation for both formats.

The PDF of γ for the η-μ fading model is given by [38]

$$f_{\gamma}\left(\gamma\right)=\frac{2\sqrt{\pi}\mu^{\mu+\frac{1}{2}}h^{\mu}}{\Gamma\left(\mu\right)H^{\mu-\frac{1}{2}}\bar{\gamma}}\left(\frac{\gamma}{\bar{\gamma}}\right)^{\mu-\frac{1}{2}}\exp\left(-2\mu h\tfrac{\gamma}{\bar{\gamma}}\right)I_{\mu-\frac{1}{2}}\left(2\mu H\tfrac{\gamma}{\bar{\gamma}}\right), \tag{3.3.1}$$

where $\Gamma(\cdot)$ is the gamma function, I_{ν} is the ν-th order modified Bessel function, $\mu>0$ is the parameter representing half of the number of clusters of multipath, and h and H are defined for the two different formats as

$$\begin{cases} h=\frac{2+\eta^{-1}+\eta}{4}, & H=\frac{\eta^{-1}-\eta}{4}; \quad 0<\eta<\infty \quad \text{for Format 1,} \\ h=\frac{1}{1-\eta^{2}}, & H=\frac{\eta}{1-\eta^{2}}; \quad -1<\eta<1 \quad \text{for Format 2.} \end{cases} \tag{3.3.2}$$

One format can be obtained from the other by the relation

$$\eta_{\text{format 2}}=\frac{1-\eta_{\text{format 1}}}{1+\eta_{\text{format 1}}}. \tag{3.3.3}$$

The CDF of the instantaneous SNR per symbol for the η-μ fading model can be written as [38]

$$F_{\gamma}\left(\gamma\right)=1-Y_{\mu}\left(\frac{H}{h},\sqrt{\frac{2h\mu\gamma}{\bar{\gamma}}}\right), \tag{3.3.4}$$

where $Y_{\mu}(x,y)$ is the Yacoub's integral, defined in [38] and given by

$$Y_{\mu}(x,y)\triangleq\frac{\sqrt{\pi}2^{\frac{3}{2}-\mu}\left(1-x^{2}\right)^{\mu}}{\Gamma(\mu)x^{\mu-\frac{1}{2}}}\int_{y}^{\infty}e^{-t^{2}}t^{2\mu}I_{\mu-\frac{1}{2}}\left(t^{2}x\right)\,dt, \tag{3.3.5}$$

with $-1<x<1$ and $y\geq 0$.

As introduced earlier in Section 2.2.1, the outage probability (OP) can be directly obtained from the CDF. Given the recent relevancy of η-μ fading channels, obtaining analytical expressions for the OP is particularly interesting. Therefore, we have aimed to obtain a closed-form expression for the CDF of the η-μ fading distribution. Section 3.3.3 presents the derived expressions for the Yacoub's integral $Y_{\mu}(x,y)$, which in turn allows to express the CDF in terms of Bessel, Marcum Q, and elementary functions. These results for the CDF and its application to the OP analysis of MRC systems over independent

and identically distributed (i.i.d.) η-μ fading channels have been recently presented in [37].

Finally, the MGF of γ for the η-μ fading model is given by [70]

$$M_{\gamma}(s) = \left(\frac{4\mu^2 h}{(2(h-H)\mu + s\bar{\gamma})(2(h+H)\mu + s\bar{\gamma})} \right)^{\mu}. \tag{3.3.6}$$

Relations with other NLOS fading models

As mentioned above, the η-μ fading distribution includes, as particular cases, the classical NLOS fading models which have been presented in Section 3.2.

The Rayleigh distribution is obtained from the η-μ distribution by setting $\mu = 0.5$ and $\eta = 1$ for Format 1. In the subsequent, we will only specify the values of η for Format 1, since the corresponding ones for Format 2 can be readily obtained from the relation (3.3.3). The Nakagami-q (Hoyt) distribution is exactly obtained from the η-μ distribution by setting $\mu = 0.5$ and, then, the Hoyt parameter is given by the relation $q^2 = \eta$. Finally, the Nakagami-m distribution is obtained in an exact manner with $\mu = m$ and $\eta = 0$, or equivalently, with $\mu = m/2$ and $\eta = 1$.

Besides, the distribution of a squared η-μ variable (e.g. the SNR per symbol γ for the η-μ fading model) has the reproductive property. That is, the sum of L i.i.d. squared η-μ variates is also η-μ distributed, but with parameters η and $L\mu$. Therefore, the statistical functions (e.g, PDF or CDF) for the sum of L i.i.d. variates following any of the classical NLOS fading models (Rayleigh, Hoyt, or Nakagami-m) can be readily obtained from the given expressions for the η-μ distribution by first setting $\mu = L\mu$ and then setting η and μ according to the desired fading model.

3.3.3 Closed-form Expressions for Yacoub's Integral

In this section, we derive closed-form expressions for Yacoub's integral $Y_{\mu}(x, y)$ which allow us to obtain new closed-form expressions for the CDF of the η-μ fading distribution. Two types of analytical results are obtained for either arbitrary fading or physical fading

models. First, we obtain a general expression in terms of the confluent Lauricella function $\Phi_2^{(2)}$ [42, eq. 5.71.21][43] for arbitrary η-μ fading channels. Next we consider physical fading models, i.e. those with an integer number of multipath clusters $N = 2\mu$, and show that Y_μ can be integrated in terms of the classical Marcum Q and Bessel functions.

Arbitrary η-μ distribution

The η-μ fading distribution is fully characterized in terms of measurable physical parameters. Therefore, it is possible to fit experimental data by adequately setting the two shape parameters η and μ. In the following proposition we derive a general expression for (3.3.5), which is valid for an arbitrary value of the μ parameter, i.e. for a real positive μ.

Proposition 3. *Yacoub's integral Y_μ defined in (3.3.5) can be expressed as*

$$\begin{aligned} Y_\mu(x,y) = 1 - &\frac{(1-x^2)^\mu\, y^{4\mu}}{\Gamma(1+2\mu)} \\ &\times \Phi_2\left(\mu, \mu; 1+2\mu; -(1+x)y^2, -(1-x)y^2\right), \end{aligned} \tag{3.3.7}$$

where $\Phi_2 \equiv \Phi_2^{(2)}$ is the confluent Lauricella function, defined by (2.3.21).

Proof. See Appendix C.1. □

Physical η-μ distribution

Now we restrict the analysis to the case of physical channel models, which assume an integer number of multipath clusters. In this case, only a multiple of 1/2 is allowed for the μ parameter, being $N = 2\mu$ the number of clusters. In the subsequent, it is shown that Y_μ with an integer value of 2μ can be expressed in terms of classical functions within the communications theory context.

For convenience in the derivation of this expression, we consider two different cases for either an odd or an even number of multipath clusters N, i.e. for either half-integer or integer values of μ. On the one hand, if μ is a half-integer, the integral Y_μ can be rewritten in terms of the ILHI, introduced in Definition 1 of Section 2.3.3. The explicit solution for the ILHI, given in Proposition 1 of Section 2.3.3, may be applied to obtain Y_μ

in closed-form. On the other hand, for integer values of μ the final Y_μ expression is given by a linear combination of elementary functions involving polynomials and exponentials. These exact and closed-form results for the Yacoub's integral are gathered in the next Proposition.

Proposition 4. *For integer values of 2μ, the Yacoub's integral Y_μ defined in (3.3.5) can be expressed by one of the two following formulas. If 2μ is odd, i.e. μ is a half-integer, Y_μ is expressed as*

$$Y_\mu(x,y) = 1 - \frac{2^{\frac{1}{2}-\mu}\sqrt{\pi}\,(1-x^2)^\mu}{|x|^{2\mu}\,\Gamma(\mu)} I_{e_{\mu-\frac{1}{2},\mu-\frac{1}{2}}}\left(|x|\,y^2; \frac{1}{|x|}\right), \tag{3.3.8}$$

where $I_{e_{m,n}}$ is the ILHI, given in closed-form by (2.3.27).

Otherwise, when 2μ is even, the Yacoub's integral is calculated as

$$\begin{aligned} Y_\mu(x,y) = 1 - \left(1-x^2\right)^\mu \Bigg\{ & \frac{1}{(1+x)^\mu (1-x)^\mu} + \\ & \sum_{k=0}^{\mu-1} \frac{(-1)^{\mu-1}(1-x)^k 2^{-\mu-k}}{\Gamma(\mu-k)(1+x)^{k+1}} x^{-\mu-k} y^{2\mu-2-2k} \\ & \times e^{-y^2(1+x)} P_k^{(-1-k,-\mu-k)}\left(\frac{3x+1}{x-1}\right) + \\ & \sum_{k=0}^{\mu-1} \frac{(-1)^{k+1}(1+x)^k 2^{-\mu-k}}{\Gamma(\mu-k)(1-x)^{k+1}} x^{-\mu-k} y^{2\mu-2-2k} \\ & \times e^{-y^2(1-x)} P_k^{(-1-k,-\mu-k)}\left(\frac{3x-1}{x+1}\right) \Bigg\} \end{aligned}, \tag{3.3.9}$$

where $P_n^{(a,b)}$ are the Jacobi polynomials, defined in (2.3.3).

Proof. See Appendix C.2. □

The closed-form expressions for the CDF of the η-μ fading distribution, given in (3.3.4), are obtained by replacing Y_μ with the derived expressions (3.3.7), (3.3.8), or (3.3.9), respectively for an arbitrary, half-integer, or integer values of μ.

3.4 Summary

In this chapter, a brief overview of the fading channel models employed throughout this thesis has been provided. We have presented the classical NLOS fading distributions, commonly used to characterize the small-scale variation of the signal when a direct line-of-sight link is not available. Also, the terminology and notation regarding the statistical functions for the characterization of these fading models have been introduced.

Besides, the η-μ fading distribution [38], a new and more general NLOS fading distribution which includes the classical NLOS distributions as particular cases, has been introduced. Moreover, new exact closed-form expressions for the CDF of the η-μ fading distribution have been derived. These expressions are of particular interest given the recent relevancy of the η-μ fading distribution. First, a general expression in terms of the confluent Lauricella function has been provided for arbitrary values of μ. Next, we have addressed physical η-μ channel models, i.e. those with integer values of 2μ, and exact closed-form expressions have been obtained for the CDF in terms of Marcum Q, Bessel and elementary functions. These results have been applied to the OP analysis of MRC over i.i.d. η-μ fading channels in [37].

Chapter 4

Performance Analysis of Non-Ideal SIMO Systems

As mentioned before, we have aimed to analyze the performance of systems with multiple antennas only at the receiver side, also referred to as single-input multiple-output (SIMO) systems, under certain practical limitations. Specifically, we have focused on the derivation of new closed-form expressions for the bit error and outage probabilities of switched diversity systems under non-orthogonal signaling and maximum ratio combining (MRC) systems under the presence of co-channel interferences. In such analyses, a certain family of incomplete integrals involving the classical Marcum Q and modified Bessel functions have been encountered. These types of integrals, namely ILHI and IIMQ, have been introduced in Chapter 2, where explicit expressions for their solutions can be found (see Section 2.3.3).

In this chapter, the closed-form expressions for the family of incomplete integrals ILHI and IIMQ [20] have been applied to the performance analysis of two different SIMO systems under practical conditions. First, we present a closed-form analysis for the bit error probability (BEP) of switched diversity systems under non-orthogonal signaling when noncoherent or differentially coherent detection is employed in Nakagami-m fading channels. Then, MRC systems under the presence of co-channel interferences are analyzed in terms of the outage probability (OP) in Nakagami-q (Hoyt) fading channels.

4.1 Switched Diversity Systems under Non-Orthogonal Signaling

Switched diversity has been thoroughly studied by communication theorists and engineers as an attempt for exploiting space diversity by simple practical systems. From the signal processing point of view, switched diversity is simpler to implement than MRC, equal gain combining (EGC) or selection combining (SC). The simplest and best studied switched diversity systems are switch-and-stay combining (SSC) and switch-and-examine combining (SEC) over independent and identically distributed (i.i.d.) channels. A comprehensive description of such systems can be found in [1, ch. 9] and the references therein.

Besides, binary frequency-shift keying (FSK) signaling with noncoherent symbol detection is often adopted in practical SSC and SEC systems as a simple (low-complexity) modulation scheme. In such cases, signals can be chosen non-orthogonal at the transmitter to reduce bandwidth utilization, at the expense of certain performance degradation [3, ch. 5]. Moreover, the performance of these systems can be improved with slightly higher complexity modulation schemes such as phase shift keying (PSK) with differentially coherent detection. As simple modulation schemes, noncoherent and differentially coherent detection are of particular interest in low-complexity SEC receivers, which could be part of a multi-hop or relay network.

This section focuses on the performance analysis of SSC and SEC over i.i.d. Nakagami-m fading channels. In [21] and [22] an analytical framework was presented for the performance of coherent, noncoherent and differentially coherent detection. Adopting the moment generating function (MGF) approach, results in [21] and [22] for the average BEP (ABEP) were in the form of single finite integrals. In [71], a new analysis was performed to calculate these integrals in exact closed-form for *coherent detection* (PSK, PAM and QAM) in Nakagami-m fading channels with integer parameter m. However, exact closed-form expressions for *noncoherent* and *differentially coherent* detection have not been found in the literature. Only very recently, new results have appeared in [39] for the particular case of a dual-branch SSC system with noncoherent detection of non-orthogonal binary FSK under Rayleigh fading.

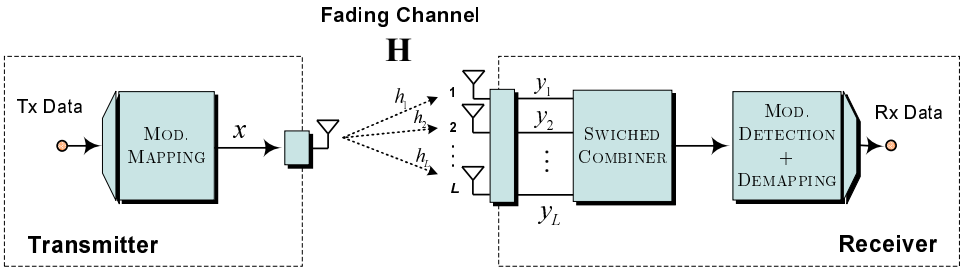

Figure 4.1: Switched diversity system model.

In this section, a unifying closed-form BEP analysis is presented for *noncoherent* and *differentially coherent* detection in multibranch switched diversity systems over i.i.d. Nakagami-m fading channels. The analysis in this section extends previous results obtained in [39], providing a three-fold generalization: first, the number of branches is extended to an L-branch diversity system; second, the analysis is extended to the more general Nakagami-m fading model; and third, the BEP analysis includes other modulation schemes such as the differential quadrature PSK (DQPSK)[1]. Recent results obtained in [20] for the class of incomplete integrals ILHI and IIMQ are applied to the unified analysis in this section. The general BEP expression derived here is in the form of a finite combination of Marcum Q, Bessel, and elementary functions, thus avoiding the need for numerical integration.

The remainder of this section is structured as follows. Section 4.1.1 is devoted to characterize the statistics of the analyzed switched diversity systems. Then, exact and approximated closed-form expressions for the average BEP are derived in Section 4.1.2 and some numerical results are provided in Section 4.1.3.

4.1.1 System Model

Let us assume a switched diversity system with L i.i.d. Nakagami-m branches as the one depicted in Figure 4.1. It is known that the output statistics of SSC does not depend on the number of diversity branches and SEC has the same output statistics as SSC when $L = 2$ [22]. As noted in [71], the average BEP in SSC is obtained by setting $L = 2$ in SEC. Therefore, we restrict the analysis to the general L-branch SEC.

[1] Our analytical results are applicable to any modulation format whose conditional BEP fits into the general expression (4.1.5).

An L-branch SEC receiver will switch to a different path (branch) if the current path is not of acceptable quality, i.e. if the instantaneous signal-to-noise ratio (SNR) falls below a certain predefined switching threshold. If this occurs, the combiner switches and examines the quality of the next available path. This switching-examining process is repeated until either an acceptable path is found or all available diversity paths have been examined.

For SEC, the probability density function (PDF) of the SNR per symbol γ_S at the output of the combiner is [1, eq. 9.341]

$$f_{\gamma_S}(x) = \begin{cases} [F_\gamma(\gamma_T)]^{L-1} f_\gamma(x), & 0 \leqslant x < \gamma_T \\ \sum_{\ell=0}^{L-1} [F_\gamma(\gamma_T)]^\ell f_\gamma(x), & x \geqslant \gamma_T \end{cases}, \tag{4.1.1}$$

where f_γ and F_γ are the PDF and the cumulative distribution function (CDF) of the instantaneous SNR per symbol γ on each diversity branch, whereas γ_T denotes the switching threshold. The Nakagami-m distribution with integer m is considered for γ, which covers many cases of interest in practice, in particular, Rayleigh fading when $m = 1$. For an integer Nakagami m parameter, it is well known that $F_\gamma(\gamma_T)$ and $f_\gamma(x)$ in (4.1.1) are given by [1, table 9.5] [41, eq. 8.352-2]

$$F_\gamma(\gamma_T) = 1 - e^{-\frac{m}{\bar{\gamma}}\gamma_T} \sum_{\ell=0}^{m-1} \frac{\gamma_T^\ell}{(\ell)!} \left(\frac{m}{\bar{\gamma}}\right)^\ell \tag{4.1.2}$$

and

$$f_\gamma(x) = \left(\frac{m}{\bar{\gamma}}\right)^m \frac{x^{m-1}}{(m-1)!} e^{-m\frac{x}{\bar{\gamma}}}, \tag{4.1.3}$$

where $\bar{\gamma}$ is the average SNR per symbol on each diversity branch.

4.1.2 Error Probabilities Analysis

General and exact ABEP analysis

Given the conditional BEP $P_b(x) \triangleq \Pr\{\text{bit error} \,|\gamma_S = x\}$ and the PDF at the output of the combiner f_{γ_S}, the average BEP for multibranch SEC is calculated by

$$\bar{P}_b = \int_0^\infty P_b(x) f_{\gamma_S}(x) \, dx. \tag{4.1.4}$$

Table 4.1: Parameters for several noncoherent and differentially coherent modulation formats.

	Orthogonal Binary Signals	Non-orthogonal Binary Signals*	DPSK	DQPSK
a	0	$\left(\frac{1-\sqrt{1-\rho^2}}{2}\right)^{1/2}$	0	$\left(1-\frac{1}{\sqrt{2}}\right)^{1/2}$
b	1	$\left(\frac{1+\sqrt{1-\rho^2}}{2}\right)^{1/2}$	$\sqrt{2}$	$\left(1+\frac{1}{\sqrt{2}}\right)^{1/2}$
η	1	1	1	1

* where $0 \leq \rho \leq 1$ is the magnitude of the cross-correlation coefficient between the two signals.

A generic expression for the conditional BEP of noncoherent and differentially coherent modulations is given by [56, eq. 4B.21], [1, ch. 8]

$$P_b(x) = Q_1\left(a\sqrt{x}, b\sqrt{x}\right) - \frac{\eta}{1+\eta} e^{-\frac{a^2+b^2}{2}x} I_0(abx), \tag{4.1.5}$$

where Q_1 is the first-order Marcum Q function, defined in (2.3.16), I_0 is the zero-th order modified Bessel function, and a, b and η are modulation-dependent parameters. A number of special cases are of particular importance and their parameters[2] are specified in Table 4.1.

In some special cases, the conditional BEP takes a simple form. When $a = 0$, e.g. see orthogonal binary signaling and differential PSK (DPSK) in Table 4.1, expression (4.1.5) reduces to [1, eq. 4.45]

$$P_b(x) = \frac{1}{1+\eta} e^{-\frac{b^2}{2}x}. \tag{4.1.6}$$

Thus, the general approach what follows can be easily circumvented and the average BEP calculations are relatively simple. A similar simplification occurs when $b = 0$. This fact justifies the assumption $ab \neq 0$ adopted in the subsequent analysis[3].

[2] Note that (4.1.5) is defined in terms of the instantaneous SNR per symbol γ_S; thus, DQPSK parameters slightly differ from those given in [56] or [1].

[3] Nevertheless our expressions are also valid for $a = 0$ or $b = 0$ if these cases are properly interpreted as limits.

One approach to compute the average BEP in (4.1.4) is to express (4.1.5) by its alternative form as a single finite integral, and then the integration over γ_S can be obtained from its MGF which leads to a single finite integral expression [21, eq. (39)]. Here the average BEP is derived by following a different approach in order to arrive at an exact closed-form expression.

Substituting (4.1.5) and (4.1.1) into (4.1.4) and after some simple algebraic manipulations the following generic expression for the average BEP is obtained

$$\begin{aligned}\bar{P}_b = {} & \alpha_{L,m}\left(\gamma_T;\bar{\gamma}\right)\left[\mathcal{I}_1\left(a,b,\bar{\gamma},m\right)-\frac{\eta}{1+\eta}\mathcal{I}_2\left(a,b,\bar{\gamma},m\right)\right] \\ & -\alpha_{L-1,m}\left(\gamma_T;\bar{\gamma}\right)\left[\mathcal{J}_1\left(\gamma_T;a,b,\bar{\gamma},m\right)-\frac{\eta}{1+\eta}\mathcal{J}_2\left(\gamma_T;a,b,\bar{\gamma},m\right)\right],\end{aligned} \tag{4.1.7}$$

where $\alpha_{L,m}\left(\gamma_T;\bar{\gamma}\right)$ are known coefficients defined as

$$\alpha_{L,m}\left(\gamma_T;\bar{\gamma}\right) \triangleq \frac{\left(\frac{m}{\bar{\gamma}}\right)^m}{(m-1)!}\left[\frac{1-\left[F_\gamma\left(\gamma_T\right)\right]^L}{1-F_\gamma\left(\gamma_T\right)}\right], \tag{4.1.8}$$

with $F_\gamma\left(\gamma_T\right)$ given in (4.1.2) and where $\mathcal{I}_1$, $\mathcal{I}_2$, $\mathcal{J}_1$, $\mathcal{J}_2$ are integrals defined as

$$\begin{cases}\mathcal{I}_1\left(a,b,\bar{\gamma},m\right) \triangleq \displaystyle\int_0^\infty x^{m-1}e^{-\frac{m}{\bar{\gamma}}x}Q_1\left(a\sqrt{x},b\sqrt{x}\right)dx \\ \mathcal{I}_2\left(a,b,\bar{\gamma},m\right) \triangleq \displaystyle\int_0^\infty x^{m-1}e^{-\left[\frac{m}{\bar{\gamma}}+\frac{a^2+b^2}{2}\right]x}I_0\left(abx\right)dx \\ \mathcal{J}_1\left(\gamma_T;a,b,\bar{\gamma},m\right) \triangleq \displaystyle\int_0^{\gamma_T} x^{m-1}e^{-\frac{m}{\bar{\gamma}}x}Q_1\left(a\sqrt{x},b\sqrt{x}\right)dx \\ \mathcal{J}_2\left(\gamma_T;a,b,\bar{\gamma},m\right) \triangleq \displaystyle\int_0^{\gamma_T} x^{m-1}e^{-\left[\frac{m}{\bar{\gamma}}+\frac{a^2+b^2}{2}\right]x}I_0\left(abx\right)dx\end{cases} \tag{4.1.9}$$

What remains to achieve the goal of this analysis is to show that $\mathcal{I}_1$, $\mathcal{I}_2$, $\mathcal{J}_1$ and $\mathcal{J}_2$ can be given in exact closed-form by a finite combination of Marcum Q, Bessel and elementary functions.

The complete integrals $\mathcal{I}_1$ and $\mathcal{I}_2$ are crucial for performance analysis of differentially coherent and noncoherent modulations in fading channels and were studied in [53, 54]. In [53], an exact closed-form expression for $\mathcal{I}_1$ was derived in terms of the Gauss hypergeometric function

$$\begin{aligned}\mathcal{I}_1\left(a,b,\bar{\gamma},m\right) = {} & \frac{(m-1)!}{(m/\bar{\gamma})^m}\left\{1+\frac{b^2}{c_1}\sum_{\ell=0}^{m-1}\left(\ell+1\right)\left(\frac{2m}{\bar{\gamma}c_1}\right)^\ell\right. \\ & \left.\times\left[\frac{a^2}{c_1}{}_2F_1\left(\frac{\ell+2}{2},\frac{\ell+2}{2}+\frac{1}{2};2;\frac{4a^2b^2}{c_1^2}\right)-\frac{1}{1+\ell}{}_2F_1\left(\frac{\ell+1}{2},\frac{\ell+1}{2}+\frac{1}{2};1;\frac{4a^2b^2}{c_1^2}\right)\right]\right\},\end{aligned} \tag{4.1.10}$$

where $c_1 \triangleq a^2+b^2+2\frac{m}{\bar{\gamma}}$. Applying [51, eq. 15.4.10] and the recurrence relations [41, eq. 8.731-4] and [41, eq. 8.914-1] the following identities are obtained

$$ {}_2F_1\left(\frac{\ell+2}{2},\frac{\ell+2}{2}+\frac{1}{2};2;c_2\right)=\frac{2c_2^{-1}\left(1-c_2\right)^{-\frac{\ell}{2}}}{2\ell+1}\left\{P_{\ell+1}\left(\tfrac{1}{\sqrt{1-c_2}}\right)-P_{\ell-1}\left(\tfrac{1}{\sqrt{1-c_2}}\right)\right\}, \tag{4.1.11} $$

$$ {}_2F_1\left(\frac{\ell+1}{2},\frac{\ell+1}{2}+\frac{1}{2};1;c_2\right)=\frac{\left(1-c_2\right)^{-\frac{\ell}{2}}}{2\ell+1}\left\{(\ell+1)P_{\ell+1}\left(\tfrac{1}{\sqrt{1-c_2}}\right)+\ell P_{\ell-1}\left(\tfrac{1}{\sqrt{1-c_2}}\right)\right\}, \tag{4.1.12} $$

where $c_2 \triangleq \frac{4a^2b^2}{c_1^2}$ and $P_n(\cdot)$ are the Legendre polynomials, given by (2.3.2). Substituting (4.1.11) and (4.1.12) into (4.1.10) and after some algebra, we obtain the following expression for $\mathcal{I}_1$ in terms of elementary functions

$$ \begin{aligned} &\mathcal{I}_1\left(a,b,\bar{\gamma},m\right)=(m-1)!\left(\frac{\bar{\gamma}}{m}\right)^m \\ &\times\left\{1+\frac{b^2}{c_1}\sum_{\ell=0}^{m-1}\frac{\left(\frac{\ell+1}{2\ell+1}\right)\left(\frac{2m}{\bar{\gamma}c_1\sqrt{1-c_2}}\right)^{\ell}}{\left(\frac{c_1}{2b^2}-1\right)^{-1}}\left[P_{\ell+1}\left(\tfrac{1}{\sqrt{1-c_2}}\right)-\left(1+\frac{\left(\frac{c_1}{2b^2}-1\right)^{-1}}{\left(\frac{\ell+1}{2\ell+1}\right)}\right)P_{\ell-1}\left(\tfrac{1}{\sqrt{1-c_2}}\right)\right]\right\}. \end{aligned} \tag{4.1.13} $$

After a simple rescaling, a generalization of $\mathcal{I}_2$ is directly found in the table of integrals [41, eq. 6.624-5] in terms of the associate Legendre function. As in the case of $\mathcal{I}_1$, $\mathcal{I}_2$ reduces to a simple expression in terms of Legendre polynomials:

$$ \mathcal{I}_2\left(a,b,\bar{\gamma},m\right)=\frac{(m-1)!}{(ab)^m}\left(\frac{c_2}{1-c_2}\right)^{\frac{m}{2}}P_{m-1}\left(\frac{1}{\sqrt{1-c_2}}\right). \tag{4.1.14} $$

Integrals $\mathcal{J}_1$ and $\mathcal{J}_2$ belong, respectively, to the family of incomplete integrals IIMQ and ILHI, which have been addressed in Chapter 2. Recent work in [20] has provided explicit solutions for these types of integrals, which have been included in Section 2.3.3. In the subsequent, we exploit these results to obtain closed-form expressions for $\mathcal{J}_1$ and $\mathcal{J}_2$. On the one hand, after a simple rescaling and further simplifications, Lemma 1 in Section 2.3.3 is exploited to obtain the following expression for $\mathcal{J}_1$

$$ \begin{aligned} \mathcal{J}_1\left(\gamma_T;a,b,\bar{\gamma},m\right)=(m-1)!\left(\frac{\bar{\gamma}}{m}\right)^m&\left\{1-e^{-\frac{m}{\bar{\gamma}}\gamma_T}Q_1\left(a\sqrt{\gamma_T},b\sqrt{\gamma_T}\right)\sum_{\ell=0}^{m-1}\frac{\left(\frac{m}{\bar{\gamma}}\right)^{\ell}}{\ell!}\gamma_T^{\ell}\right. \\ &\left.+\frac{1}{2}\sum_{\ell=0}^{m-1}\frac{\left(\frac{m}{\bar{\gamma}}\right)^{\ell}}{\ell!}\frac{1}{(ab)^{\ell}}\left(I_{e_{\ell,1}}\left(ab\gamma_T;\frac{1}{\sqrt{c_2}}\right)-\frac{b}{a}I_{e_{\ell,0}}\left(ab\gamma_T;\frac{1}{\sqrt{c_2}}\right)\right)\right\}, \end{aligned} \tag{4.1.15} $$

where $I_{e_{r,k}}$ is the ILHI, as defined in Definition 1 of Section 2.3.3. On the other hand, a simple rescaling allows us to express $\mathcal{J}_2$ as

$$\mathcal{J}_2\left(\gamma_T; a, b, \bar{\gamma}, m\right) = \frac{1}{(ab)^m} I_{e_{m-1,0}}\left(ab\gamma_T; \frac{1}{\sqrt{c_2}}\right). \tag{4.1.16}$$

Note that both $\mathcal{J}_1$ and $\mathcal{J}_2$ are now expressed in terms of the ILHI $I_{e_{r,k}}$, which is given in closed-form by (2.3.27).

The final average BEP is obtained by substituting the derived expressions (4.1.13), (4.1.14), (4.1.15), and (4.1.16) for $\mathcal{I}_1$, $\mathcal{I}_2$, $\mathcal{J}_1$, and $\mathcal{J}_2$, respectively, into (4.1.7), which yields

$$\begin{aligned}
\bar{P}_b = \alpha_{L,m}\left(\gamma_T; \bar{\gamma}\right) \Bigg[(m-1)! \left(\frac{\bar{\gamma}}{m}\right)^m \Bigg\{ 1 + \left(\frac{1}{2} - \frac{b^2}{c_1}\right) \sum_{\ell=0}^{m-1} \left(\frac{\ell+1}{2\ell+1}\right) \left(\frac{2m}{\bar{\gamma} c_1 \sqrt{1-c_2}}\right)^{\ell} \\
\times \left[P_{\ell+1}\left(\frac{1}{\sqrt{1-c_2}}\right) - \left(1 + \frac{1}{\left(\frac{\ell+1}{2\ell+1}\right)\left(\frac{c_1}{2b^2}-1\right)}\right) P_{\ell-1}\left(\frac{1}{\sqrt{1-c_2}}\right) \right] \Bigg\} \\
- \frac{\eta}{1+\eta} \frac{(m-1)!}{(ab)^m} \left(\frac{c_2}{1-c_2}\right)^{\frac{m}{2}} P_{m-1}\left(\frac{1}{\sqrt{1-c_2}}\right) \Bigg] \\
- \alpha_{L-1,m}\left(\gamma_T; \bar{\gamma}\right) \Bigg[(m-1)! \left(\frac{\bar{\gamma}}{m}\right)^m \Bigg\{ 1 - e^{-\frac{m}{\bar{\gamma}}\gamma_T} Q_1\left(a\sqrt{\gamma_T}, b\sqrt{\gamma_T}\right) \sum_{\ell=0}^{m-1} \frac{m^\ell}{\ell!} \left(\frac{\gamma_T}{\bar{\gamma}}\right)^{\ell} \\
+ \frac{1}{2} \sum_{\ell=0}^{m-1} \frac{m^\ell}{\ell!} \frac{1}{(ab\bar{\gamma})^\ell} \left(I_{e_{\ell,1}}\left(ab\gamma_T; \frac{1}{\sqrt{c_2}}\right) - \frac{b}{a} I_{e_{\ell,0}}\left(ab\gamma_T; \frac{1}{\sqrt{c_2}}\right) \right) \Bigg\} \\
- \frac{\eta}{1+\eta} \frac{1}{(ab)^m} I_{e_{m-1,0}}\left(ab\gamma_T; \frac{1}{\sqrt{c_2}}\right) \Bigg],
\end{aligned} \tag{4.1.17}$$

where the ILHI $I_{e_{r,k}}$ is represented in closed-form by (2.3.27) and the coefficients $\alpha_{L,m}$, c_1 and c_2 are as previously defined. Note that (4.1.17) is an exact closed-form expression for the average BEP in terms of Bessel, Marcum Q, and elementary functions, which is general and valid for any modulation format whose conditional BEP can be expressed by (4.1.5).

Modulation schemes with $\eta = 1$

An interesting special case occurs when $\eta = 1$ which includes noncoherent detection of correlated binary signaling and DQPSK (see Table 4.1). As noted in [1, ch. 9], comparing

equations (40) and (42) of [72], the following compact expression for the conditional BEP is obtained in this case ($\eta = 1$)

$$P_b(x) = \frac{1}{2}\left[1 - Q_1\left(b\sqrt{x}, a\sqrt{x}\right) + Q_1\left(a\sqrt{x}, b\sqrt{x}\right)\right]. \tag{4.1.18}$$

Then, after considering (4.1.18) and $\eta = 1$, the average BEP in (4.1.7) can be rewritten in terms of $\mathcal{I}_1$ and $\mathcal{J}_1$ as

$$\begin{aligned}\bar{P}_b = &\frac{1}{2}\alpha_{L,m}(\gamma_T;\bar{\gamma})\left[1 - \mathcal{I}_1(b,a,\bar{\gamma},m) + \mathcal{I}_1(a,b,\bar{\gamma},m)\right] \\ &-\frac{1}{2}\alpha_{L-1,m}(\gamma_T;\bar{\gamma})\left[1 - \mathcal{J}_1(b,a,\bar{\gamma},m) + \mathcal{J}_1(a,b,\bar{\gamma},m)\right],\end{aligned} \tag{4.1.19}$$

where $\mathcal{I}_1$ and $\mathcal{J}_1$ are given in (4.1.13) and (4.1.15), respectively. In this case, the average BEP is given in terms of two differences of $\mathcal{I}_1$ and $\mathcal{J}_1$ with symmetric arguments.

Asymptotic analysis in the high SNR regime

The derived average BEP expressions are given in terms of Bessel, Marcum Q, and elementary functions. Given that the analytical properties of these special functions are well-studied, obtaining further insight from these expressions is straightforward, e.g. upper and lower bounds or asymptotic approximations [1, ch. 4].

Moreover, the derived closed-form expressions for integrals $\mathcal{I}_1$ and $\mathcal{I}_2$ allow us to obtain an approximation of the average BEP in the high SNR regime. Let us consider $\bar{\gamma} \to \infty$ and, as a consequence, $\gamma_T \to \infty$. Thus, as the switching threshold increases, the involved incomplete integrals tend to their corresponding complete version, i.e. $\mathcal{J}_1 \to \mathcal{I}_1$ and $\mathcal{J}_2 \to \mathcal{I}_2$. Taking this into account, the generic average BEP in (4.1.7) can be approximated by

$$\bar{P}_b \approx \left(\frac{m}{\bar{\gamma}}\right)^m \frac{\left[F_\gamma(\gamma_T)\right]^{L-1}}{(m-1)!}\left[\mathcal{I}_1(a,b,\bar{\gamma},m) - \frac{\eta}{1+\eta}\mathcal{I}_2(a,b,\bar{\gamma},m)\right], \tag{4.1.20}$$

where F_γ is the CDF of the instantaneous SNR per diversity branch, as previously defined. Then, $\mathcal{I}_1$ and $\mathcal{I}_2$ are replaced with (4.1.13) and (4.1.14) into (4.1.20) and further algebraic manipulations are performed to obtain the following approximation:

$$\begin{aligned}\bar{P}_b \approx \left[F_\gamma(\gamma_T)\right]^{L-1}&\left[\left\{1 + \left(\frac{1}{2} - \frac{b^2}{c_1}\right)\sum_{\ell=0}^{m-1}\left(\frac{\ell+1}{2\ell+1}\right)\left(\frac{2mc_3}{c_1\bar{\gamma}}\right)^\ell\right.\right. \\ &\left.\left.\times\left[P_{\ell+1}(c_3) - \left(\frac{c_1(\ell+1) + \ell 2b^2}{(\ell+1)(c_1 - 2b^2)}\right)P_{\ell-1}(c_3)\right]\right\} - \frac{\eta}{1+\eta}\left(\frac{2mc_3}{c_1\bar{\gamma}}\right)^m P_{m-1}(c_3)\right],\end{aligned} \tag{4.1.21}$$

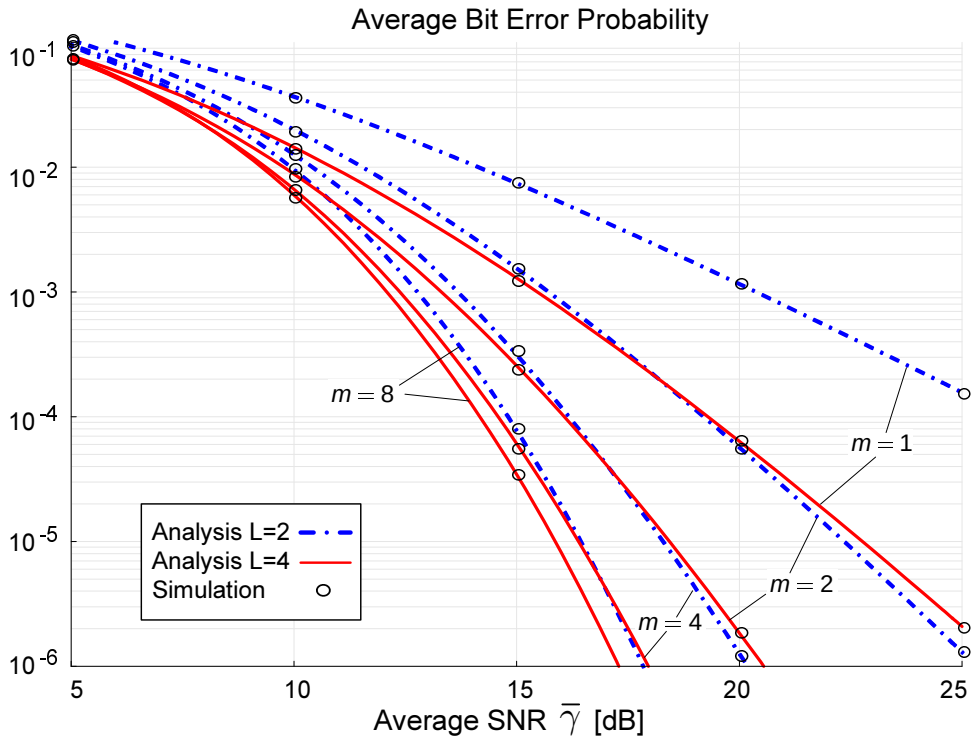

Figure 4.2: Average BEP versus average SNR per branch for DQPSK using optimum thresholds.

where, for convenience, we define $c_3 \triangleq \frac{1}{\sqrt{1-c_2}}$, and c_2 is as previously defined. Note that the previous expression, which is given in terms of elementary functions, provides a good approximation of the average BEP in the high SNR regime, being asymptotically exact as $\bar{\gamma} \to \infty$.

4.1.3 Numerical Results

In this section, we show the usefulness of the obtained results in the analysis and design of multibranch switched diversity systems with differentially coherent detection over Nakagami-m fading channels. Some numerical results are provided from the evaluation of the derived average BEP expressions. Besides, Monte-Carlo simulations are presented in order to validate our analytical derivations.

Figure 4.2 depicts the average BEP as a function of the average SNR per branch $\bar{\gamma}$ for DQPSK (see Table 4.1) considering different values of the Nakagami parameter m and

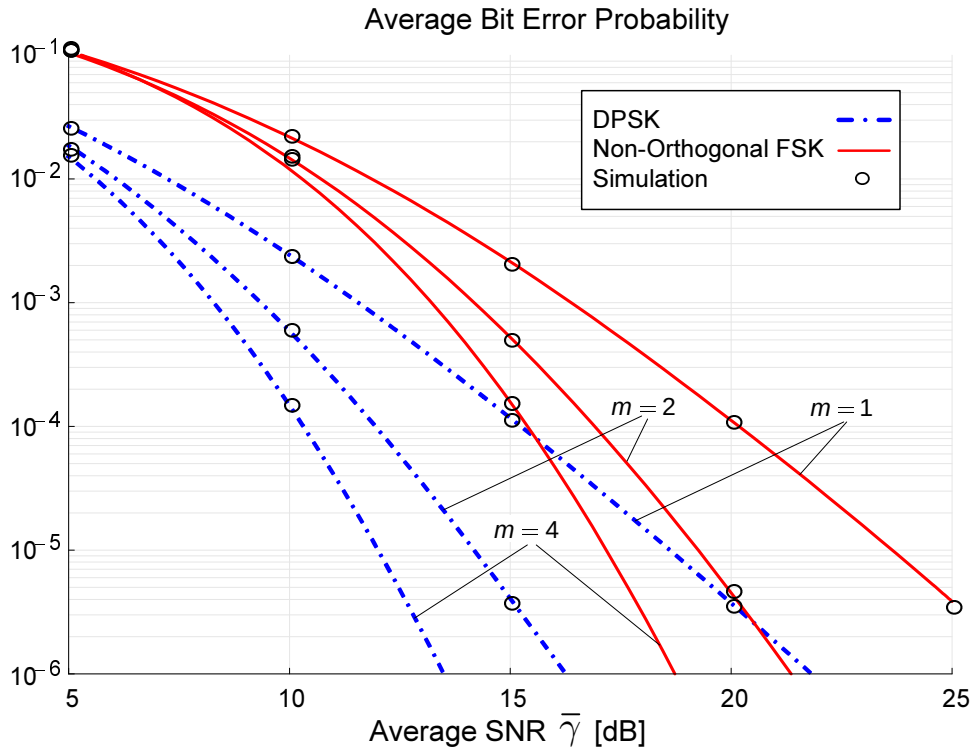

Figure 4.3: Average BEP for DPSK and non-orthogonal FSK ($\rho = 0.5$) modulation schemes with $L = 4$ diversity branches.

number of branches L. The optimum switching threshold $\gamma_T^\star$ which minimizes the average BEP is adopted for every $\bar{\gamma}$. The optimum value $\gamma_T^\star$ has been obtained by applying standard numerical minimization methods to the expression (4.1.17). The plotted curves show that the system performance within the $10^{-6} - 10^{-3}$ range is essentially determined by the product of m and L, which can be interpreted as a global diversity order measure. Simulation results are also superimposed to the analytical curves, confirming the validity of the derived expressions.

To illustrate the generality of the derived analytical results for different signaling formats (see Table 4.1), Figure 4.3 shows the average BEP for non-orthogonal FSK ($\rho = 0.5$), compared with the corresponding results for DPSK. As in Figure 4.2, optimum switching threshold are assumed. Figure 4.4 shows the trade off between the correlation (frequency separation) in non-orthogonal FSK and the number of diversity branches for different values of the Nakagami-m parameter. It is observed that the performance loss associated to a larger cross-correlation is higher as m increases.

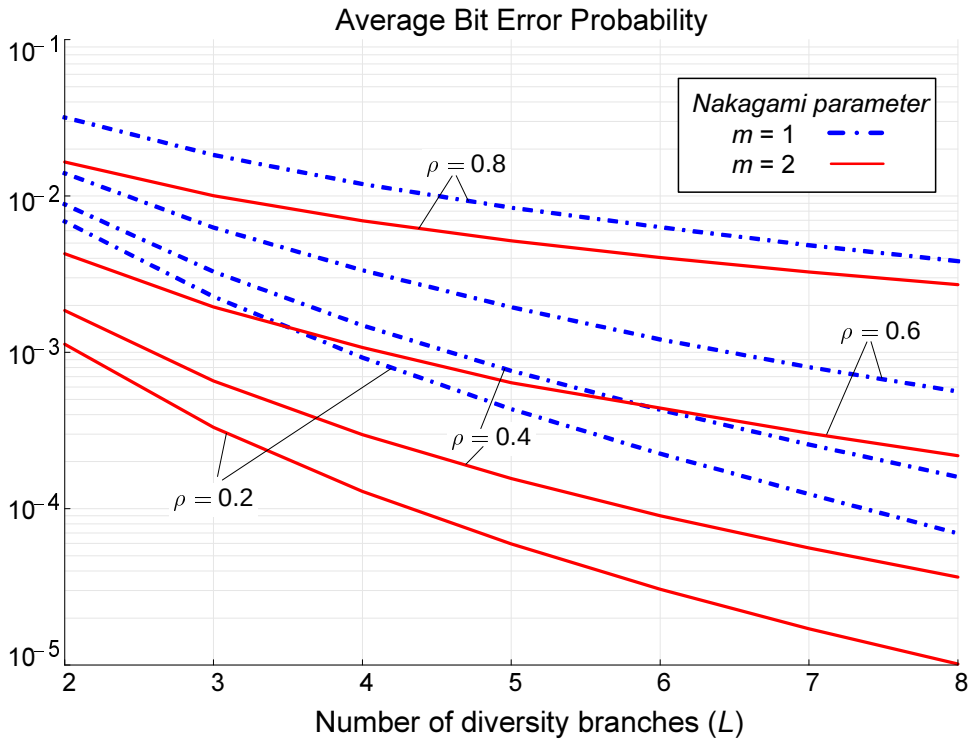

Figure 4.4: Average BEP versus number of diversity branches (L) with non-orthogonal binary FSK signaling for different values of the cross-correlation (ρ) and the Nakagami-m parameter.

Figure 4.5 shows the sensitivity of the average BEP to the selection of the switching threshold γ_T. Let us define the relative error $\epsilon \triangleq \gamma_T/\gamma_T^\star$. When $\epsilon = 1$ the optimum threshold is always chosen, while $\epsilon \neq 1$ represents a certain relative deviation from the optimum value. The plotted curves show that multibranch switched diversity exhibits high sensitivity to a wrong switching threshold when the channel presents high values of m, e.g. when the radio channel has a strong line-of-sight (LOS) component. Also, it is shown that the average BEP degradation due to the threshold deviation is greater as the average SNR increases. For an average SNR of 15 dB and $m = 4$ the average BEP is degraded by one order of magnitude when $\epsilon = 2$ (3 dB).

In Figure 4.6 the asymptotic approximation of the average BEP in (4.1.21) is compared with the exact closed-form expression in (4.1.17). Both expressions have been numerically evaluated in the high SNR regime for several values of the number of branches L and the Nakagami parameter. It is shown that (4.1.21) fits reasonably well with the exact average BEP in (4.1.17) for average SNR values higher than 20 dB. Also, it can be seen that the approximation is asymptotically tighter as the average SNR increases.

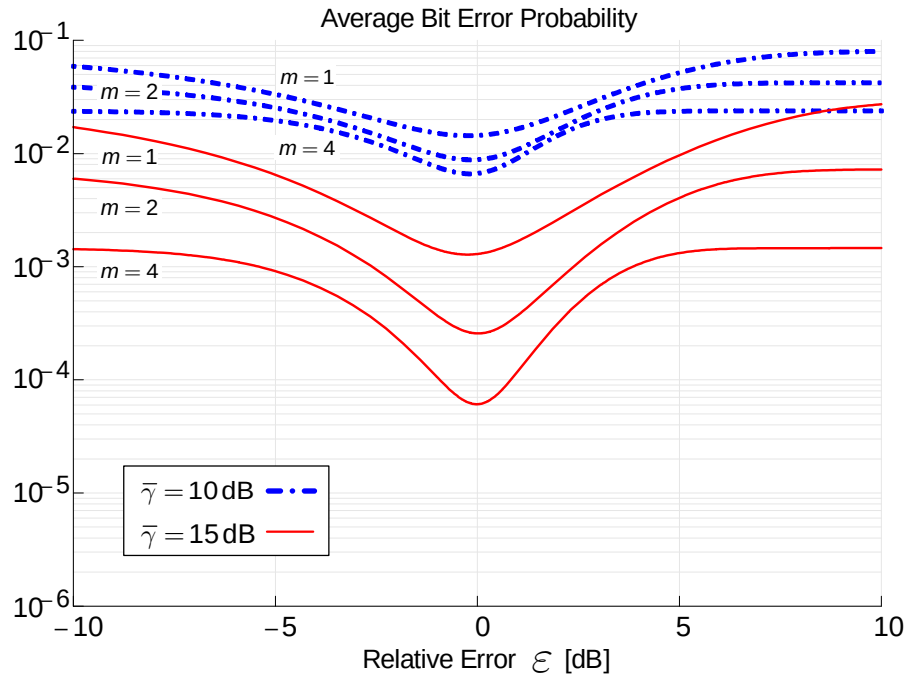

Figure 4.5: Average BEP versus the optimum threshold deviation for DQPSK with $L = 4$.

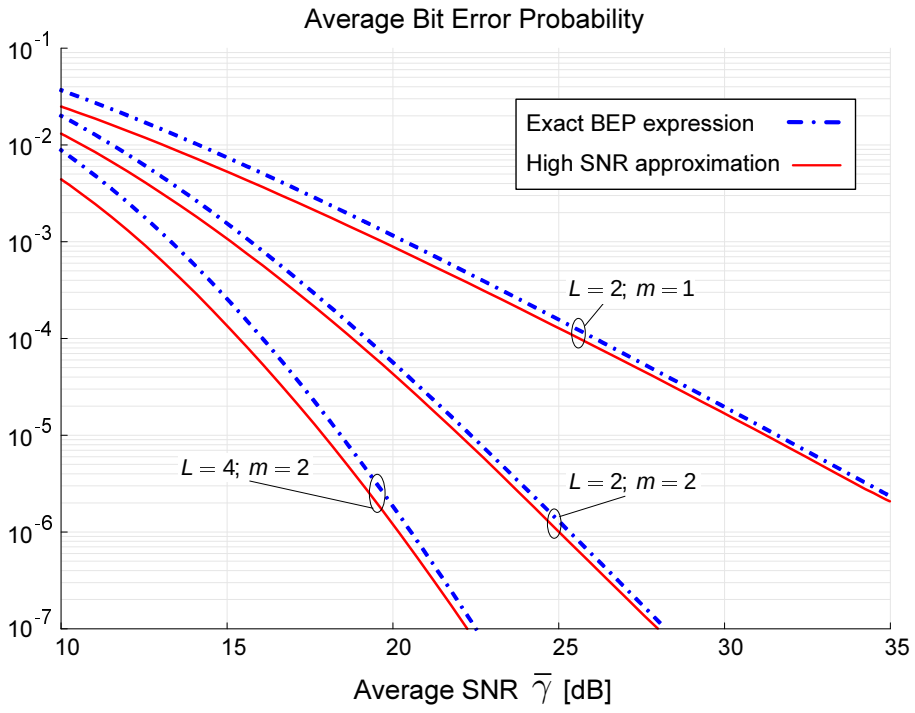

Figure 4.6: Exact average BEP and high SNR approximation for DQPSK with optimum switching thresholds and several values of the number of branches L and Nakagami parameter m.

4.2 Maximal Ratio Combining under Co-channel Interference

Diversity combining is a well-known strategy to mitigate the performance degradation of multipath fading and co-channel interference (CCI) in wireless systems. During the last decades, extensive efforts have been given to the analysis of transmitter or receiver diversity to characterize the performance of different combining methods for different numbers of antennas and fading distributions [73, 74]. For a communication link without CCI, it is well-known that maximal ratio combining (MRC) is the optimal combining technique in terms of maximizing the SNR at the output of the combiner. However, optimal combining in the presence of CCI is much more complex than MRC and typically requires information about the CCI that may not be available. Therefore, in practice many wireless systems will use MRC even in the presence of CCI.

Outage probability (OP) is a key performance metric of wireless communication systems under CCI. An excellent explanation of this topic can be found in [1, ch. 10] and references therein. Although considerable attention has been paid to the OP analysis in general, few published results are found in the literature for Hoyt fading channels, which have been considered in satellite-based cellular communications to characterize more severe fading conditions than those modeled by Rayleigh [63, 66]. The main reason for the lack of results for Hoyt fading is the mathematical tractability of the OP analysis. In particular, the general approach adopted in [1, ch. 10] is not applicable since the Gaussian characterization of the Hoyt distribution is not circularly symmetric. Only recently, exact closed-form results for the OP of a single antenna receiver in *interference-free* Hoyt fading channels have been published in [67]. Moreover, only a few works in the literature include background noise in the OP analysis. The analysis in [23] includes background noise and assumes Nakagami-n (Rician) or Nakagami-m fading for the desired signal and Rayleigh faded interferers. Recently, closed-form expressions were provided in [66] for the outage probability of Rayleigh fading under mixed Rayleigh and Hoyt interference.

In this section, closed-form expressions are derived for the outage probability of MRC systems in Hoyt fading channels under co-channel interference. This analysis extends the

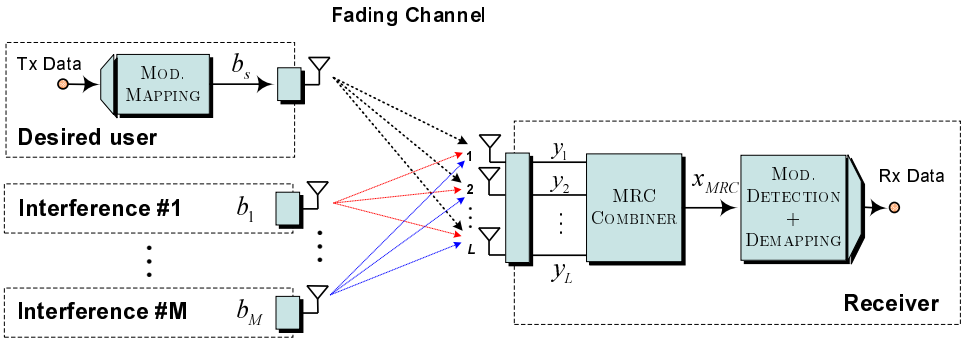

Figure 4.7: Maximal ratio combining under co-channel interference system model.

results in [67] to MRC systems and generalizes the OP analysis for Hoyt fading channels by assuming the joint presence of background noise and independent Rayleigh interferers with arbitrary powers. These results are obtained through an appropriate generalization of the moment-generating function (MGF) of the Hoyt fading distribution.

The remainder of this section is organized as follows. The system model is presented in Section 4.2.1. The outage probability analysis is presented in Section 4.2.2, while the generalization of the MGF employed in such analysis is provided in Appendix D. Finally, some numerical results are given in Section 4.2.3.

4.2.1 System Model

Let us consider a wireless communication system with L uncorrelated receive antennas where MRC is applied at the receiver. The received signal from the desired user at every antenna is assumed to be corrupted by M interference signals, as shown in Figure 4.7. In addition, the desired signal at each antenna is corrupted by additive white Gaussian noise (AWGN) with zero mean and σ^2 variance. The desired and interference signals, with arbitrary powers, experience flat fading and a coherent receiver is employed which is assumed to have perfect knowledge of the instantaneous channel state. The signals at every receive antenna from the desired user are affected by Hoyt fading, while co-channel interference signals are assumed to experience independent Rayleigh fading.

Let $\mathbf{h}_s = [h_{s1}, \ldots, h_{sL}]^T$ and $\mathbf{h}_i = [h_{i1}, \ldots, h_{iL}]^T$ denote, respectively, the channel gain vectors of the desired and the i-th interfering user at the antenna array. Then, the

received baseband signal vector $\mathbf{y}$ can be written as

$$\mathbf{y} = \mathbf{h}_s b_s + \sum_{i=1}^{M} \sqrt{W_i}\mathbf{h}_i b_i + \mathbf{n}, \tag{4.2.1}$$

where W_i is the mean power of the i-th interferer at each antenna, $\mathbf{n}$ is the L-dimensional received noise vector, and b_s and b_i are, respectively the transmitted symbols from the desired and i-th interfering user, which are assumed to be normalized such that $|b_s| = |b_i| = 1$.

In an MRC receiver, the antenna array elements are weighted by the channel gains associated with the desired user, yielding the output signal

$$x_{MRC} = \mathbf{h}_s^H \mathbf{y} = \|\mathbf{h}_s\|^2 b_s + \sum_{i=1}^{M} \sqrt{W_i}\mathbf{h}_s^H \mathbf{h}_i b_i + \mathbf{h}_s^H \mathbf{n}. \tag{4.2.2}$$

It is shown in [23] that, under the considered model, the instantaneous signal-to-interference-plus-noise ratio (SINR) can be written as

$$\gamma = \frac{X}{Z + \sigma^2}, \tag{4.2.3}$$

where $X = \|\mathbf{h}_s\|^2 = \sum_{n=1}^{L} |h_{sn}|^2$ is the effective power of the desired signal at the output of the combiner, with $|h_{sn}|$ being the Hoyt distributed envelope of the channel gain for the n-th branch, and Z is the total instantaneous power of the interfering signals. It follows that X is distributed as the sum of L i.i.d. squared Hoyt variables and the mean of X, denoted by W_s is given by $W_s = \mathtt{E}[X] = L\Omega$, where Ω is the mean of the squared envelope of the channel gain at each receiver branch, i.e., $\Omega = \mathtt{E}\left[|h_{sn}|^2\right]$, $n = 1, ..., L$.

As stated above, the effective power of the desired signal after combining is distributed as the sum of L i.i.d. Hoyt random variables. Therefore, its PDF, f_X, can be readily obtained from the PDF of the $\eta - \mu$ distribution (see Section 3.3). Recall that the $\eta - \mu$ distribution includes as a particular case the Hoyt (Nakagami-q) distribution by setting the parameters $\mu = \frac{1}{2}$ and $\eta = q^2$. After taking into account the reproductive property of the $\eta - \mu$ distribution[4] and some straightforward algebraic manipulations, the PDF of X is obtained from (3.3.1) as

$$f_X(x) = \frac{\sqrt{\pi}}{\Gamma\left(\frac{L}{2}\right) q \left(1-q^2\right)^{\frac{L-1}{2}} \Omega L} \left(\frac{L\left(1+q^2\right)}{2}\right)^{\frac{L+1}{2}} \left(\frac{x}{\Omega L}\right)^{\frac{L-1}{2}} \exp\left(-\frac{(1+q^2)^2}{4q^2}\frac{x}{\Omega}\right) I_{\frac{L-1}{2}}\left(\frac{(1-q^4)}{4q^2}\frac{x}{\Omega}\right), \tag{4.2.4}$$

where I_ν is the ν-th order modified Bessel function of the first kind.

Under all the assumptions and considerations mentioned above, we next present the outage probability analysis for a general L-branch system with co-channel interference signals.

4.2.2 Outage Probability Analysis

Let us divide the total number of interferers M into J groups, where every interferer in a group has the same mean power W_i. Consider n_i interferers in a given group with mean power W_i. It is shown in [23] that the outage probability in this scenario can be computed as

$$\begin{aligned} P_{out} \doteq \Pr\left\{\tfrac{X}{Z+\sigma^2} \leq \gamma_o\right\} = \underbrace{\int_0^{\gamma_o\sigma^2} f_X(x)\,dx}_{P^\star_{out}} + \\ \sum_{i=1}^{J}\sum_{j=1}^{n_i}\sum_{k=0}^{n_i-j}\sum_{l=0}^{k} E_{i,j}\frac{e^{\sigma^2/W_i}(-\sigma^2)^{k-l}}{l!(k-l)!W_i^k\gamma_o^l}\int_{\gamma_o\sigma^2}^{\infty} x^l \mathrm{e}^{-\frac{x}{\gamma_o W_i}} f_X(x)\,dx, \end{aligned} \tag{4.2.5}$$

where Z is the total power of the interfering signals, γ_o is a predefined threshold, σ^2 is the background noise power, $E_{i,j}$ are certain constants defined in [23, eq. 6], and f_X is the PDF of the power of the desired signal at the output of the combiner.

The OP in (4.2.5) is expressed in terms of two incomplete integrals. Thus, in order to obtain a closed-form expression for the OP, we proceed by working these integrals out. The first one represents the OP in the interference-free case and is given by the CDF of X. Recently, a closed-form expression for this CDF has been provided in [37]. By making use of [37, eq. 7], the first term in (4.2.5) can be expressed as

$$\underbrace{\int_0^{\gamma_o\sigma^2} f_X(x)\,dx}_{P^\star_{out}} = 1 - Y_{\frac{L}{2}}\left(\frac{1-q^2}{1+q^2}, \frac{(1+q^2)}{2q}\sqrt{\frac{L\gamma_o\sigma^2}{\Omega L}}\right), \tag{4.2.6}$$

where Y_μ represents the Yacoub's integral, which has been defined by (3.3.5) in Section 3.3. Closed-form expressions for Y_μ were provided in [37] and can also be found in (3.3.8) and

[4] As shown in Section 3.3.2, the PDF of the sum of L i.i.d. squared Hoyt variables can be obtained from the PDF of the $\eta-\mu$ distribution by setting $\mu = \frac{L}{2}$ and $\eta = q^2$.

(3.3.9) for an odd and an even value of L, respectively. It is highlighted that, for an even number of diversity branches L, which is very likely in practical receivers with pairs of orthogonally polarized antennas, Y_μ is expressed in terms of the Jacobi polynomials defined in (2.3.3).

The second term in (4.2.5) represents the impact of the interference on the outage probability. This term consists of a linear combination of the incomplete generalized MGF (IG-MGF) of X, $\mathcal{G}_X(\cdot,\cdot;\cdot)$, defined in (3.1.5). Specifically, the integrals in the second term of (4.2.5) can be easily identified with the IG-MGF as

$$\int_{\gamma_o\sigma^2}^{\infty} x^l \mathrm{e}^{-\frac{x}{\gamma_o W_i}} f_X(x)\, dx = \mathcal{G}_X\left(l, -\frac{1}{\gamma_o W_i}; \gamma_o\sigma^2\right). \tag{4.2.7}$$

Several derivations have been done in order to arrive at a closed-form expression for $\mathcal{G}_X(\cdot,\cdot;\cdot)$, i.e., the IG-MGF of X. Appendix D includes the derivations and closed-form expressions for some statistical functions related to the Hoyt fading distribution, including the IG-MGF of the sum of L i.i.d. squared Hoyt variates in Section D.3. Recall that, in the considered MRC system, the effective power of the desired signal at the combiner output X is distributed as the sum of L i.i.d. squared Hoyt variates.

Then, the final outage probability expression for MRC systems in Hoyt fading channels under the presence of Rayleigh-faded interference signals is obtained by substituting (4.2.6) and (4.2.7) into (4.2.5), which yields

$$\begin{aligned} P_{out} = 1 - Y_{\frac{L}{2}}&\left(\frac{1-q^2}{1+q^2}, \frac{(1+q^2)}{2q}\sqrt{\frac{L\gamma_o\sigma^2}{\Omega L}}\right) \\ &+ \sum_{i=1}^{J}\sum_{j=1}^{n_i}\sum_{k=0}^{n_i-j}\sum_{l=0}^{k} E_{i,j}\frac{e^{\sigma^2/W_i}(-\sigma^2)^{k-l}}{l!(k-l)!W_i^k\gamma_o^l}\mathcal{G}_X\left(l, \frac{-1}{\gamma_o W_i}; \gamma_o\sigma^2\right), \end{aligned} \tag{4.2.8}$$

where the coefficients $E_{i,j}$ are given in [23, eq. 6], Y_μ is given by (3.3.8) and (3.3.9) for an odd and an even value of L, respectively, and $\mathcal{G}_X(\cdot,\cdot,\cdot)$ is the IG-MGF of the sum of L i.i.d. squared Hoyt variates, which is directly obtained from Corollary 3 in Appendix D.3. It can be seen that the outage probability in (4.2.8) is, in essence, expressed in terms of the confluent Lauricella function, defined in (2.3.21), and the Jacobi polynomials.

Although the obtained expression is given in closed-form and is easy to compute, the confluent Lauricella function may not be considered as a classical function within the

communication theory context. As an attempt to give an OP expression in terms of classical functions, some derivations for the particular case of a single antenna receiver have been done. In the subsequent, the analysis for this particular case is presented.

Single antenna receiver ($L = 1$)

In this case, the power of the desired signal X is a squared Hoyt variable with mean W_s and parameter q. The PDF of X is given by (3.2.6) as

$$f_X(x) = \frac{(1+q^2)}{2q\Omega} \exp\left(-\tfrac{(1+q^2)^2}{4q^2}\tfrac{x}{\Omega}\right) I_0\left(\tfrac{(1-q^4)}{4q^2}\tfrac{x}{\Omega}\right), \tag{4.2.9}$$

where I_0 is the zeroth order modified Bessel function of the first kind, the parameter $\Omega = W_s$ is the mean of X, and q is the Hoyt fading parameter.

As stated above, the general expression for the OP in (4.2.5) is expressed in terms of two incomplete integrals. Following the same approach as in the MRC case, we proceed by working these integrals out in order to arrive at a closed form expression for the OP of a single antenna receiver. Recently, an elegant and compact expression has been obtained in [67] for the OP in the interference-free case in the particular case of having a single receive antenna ($L = 1$), i.e., when X is a squared Hoyt variable. In this case, this term is expressed as[5]

$$P^{\star}_{out} = Q\left(u\sqrt{\tfrac{\gamma_o\sigma^2}{W_s}}, v\sqrt{\tfrac{\gamma_o\sigma^2}{W_s}}\right) - Q\left(v\sqrt{\tfrac{\gamma_o\sigma^2}{W_s}}, u\sqrt{\tfrac{\gamma_o\sigma^2}{W_s}}\right), \tag{4.2.10}$$

where $u \doteq \frac{\sqrt{1-q^4}}{2q}\sqrt{\frac{1+q}{1-q}}$, $v \doteq \frac{\sqrt{1-q^4}}{2q}\sqrt{\frac{1-q}{1+q}}$ and Q is the Marcum Q function.

As in the MRC general case, the second term of (4.2.5) is a linear combination of the IG-MGF of X, $\mathcal{G}_X(\cdot,\cdot;\cdot)$, noting that X is, in this case, a single squared Hoyt variable. Therefore, the identification in (4.2.7) holds after considering that $\mathcal{G}_X(\cdot,\cdot;\cdot)$ is the IG-MGF of a single Hoyt variable. Appendix D.2 provides the derivations and expressions for $\mathcal{G}_X(\cdot,\cdot;\cdot)$, which allow us to obtain the OP in closed-form.

Then, the final outage probability expression for a single antenna receiver in Hoyt fading channels under the presence of Rayleigh-faded interference signals is obtained by

[5] A minor error in [67, eq. 9] is corrected here.

substituting (4.2.10) and (4.2.7) into (4.2.5), which yields

$$P_{out} = Q\left(u\sqrt{\tfrac{\gamma_o\sigma^2}{W_s}}, v\sqrt{\tfrac{\gamma_o\sigma^2}{W_s}}\right) - Q\left(v\sqrt{\tfrac{\gamma_o\sigma^2}{W_s}}, u\sqrt{\tfrac{\gamma_o\sigma^2}{W_s}}\right) + \sum_{i=1}^{J}\sum_{j=1}^{n_i}\sum_{k=0}^{n_i-j}\sum_{l=0}^{k} E_{i,j}\frac{e^{\sigma^2/W_i}(-\sigma^2)^{k-l}}{l!(k-l)!W_i^k\gamma_o^l}\mathcal{G}_X\left(l, \frac{-1}{\gamma_o W_i}; \gamma_o\sigma^2\right), \tag{4.2.11}$$

where the coefficients $E_{i,j}$ are given in [23, eq. 6], and $\mathcal{G}_X(\cdot,\cdot,\cdot)$ is the IG-MGF of a squared Hoyt variable, which is directly obtained from Corollary 2 in Appendix D.2. Note that the outage probability in this case is expressed in terms of a finite combination of first order Marcum Q, Bessel, and elementary functions.

Single antenna receiver and one dominant interferer

This particular scenario assumes a single antenna receiver under the presence of one dominant interferer with mean power W_1, either neglecting the remainder $M-1$ of the interferers or including them in the analysis as background Gaussian noise. In this case, the outage probability expression can be significantly simplified. By setting $J = n_1 = 1$ in (4.2.5) and considering the expression for $\mathcal{G}_X\left(0, -\frac{1}{\gamma_o W_1}; \gamma_o\sigma^2\right)$, which follows from Corollary 2 (see Appendix D), the outage probability is obtained as

$$P_{out} = P_{out}^{\star} + \frac{2qe^{\sigma^2/W_1}}{1-q^2}\left\{-\bar{\alpha}(s_1)\,\mathrm{e}^{-\alpha(s_1)\zeta_0} I_0(\zeta_0) + 2\bar{\alpha}(s_1)\, Q\left(\frac{\sqrt{\zeta_0}}{\sqrt{\alpha(s_1)+\bar{\alpha}(s_1)^{-1}}}, \sqrt{\zeta_0}\sqrt{\alpha(s_1)+\bar{\alpha}(s_1)^{-1}}\right)\right\}, \tag{4.2.12}$$

where $P_{out}^{\star}$ is given by (4.2.10), $s_1 \doteq -\frac{W_s}{\gamma_o W_1}\frac{4q^2}{1-q^4}$, $\zeta_0 \doteq \frac{1-q^4}{4q^2}\frac{\gamma_o\sigma^2}{W_s}$, and $\alpha(s) \doteq \frac{1+q^2}{1-q^2} - s$, $\bar{\alpha}(s) \doteq \frac{1}{\sqrt{\alpha(s)^2-1}}$.

In order to obtain further insight from the OP expression in (4.2.12), the following well-known metrics are defined:

$$\begin{cases} \mathrm{SNR} \doteq \dfrac{W_s}{\gamma_o\sigma^2} \\ \mathrm{SIR} \doteq \dfrac{W_s}{\gamma_o W_1} \end{cases} \qquad \begin{cases} \mathrm{SINR} \doteq \dfrac{W_s}{\gamma_o W_1 + \gamma_o\sigma^2} \\ \mathrm{INR} \doteq \dfrac{\gamma_o W_1}{\gamma_o\sigma^2} \end{cases}, \tag{4.2.13}$$

where SNR and SIR are the signal-to-noise and signal-to-interference ratios, while SINR

and INR are the signal-to-interference-plus-noise and interference-to-noise ratios, respectively. Note that these metrics are defined as normalized and averaged magnitudes. The first pair of metrics can be expressed as a function of the second pair as

$$\begin{cases} \mathrm{SNR} = (1+\mathrm{INR})\,\mathrm{SINR} \\ \mathrm{SIR} = \left(1+\mathrm{INR}^{-1}\right)\mathrm{SINR} \end{cases} . \tag{4.2.14}$$

Then, after substituting (4.2.10) into (4.2.12) and considering [1, eq. 9.107] as well as previous definitions, the OP for a single antenna receiver ($L=1$) with one dominant interferer can be written in closed-form as

$$\begin{aligned} P_{out} = {} & Q\left(\frac{u}{\sqrt{\mathrm{SNR}}}, \frac{v}{\sqrt{\mathrm{SNR}}}\right) - Q\left(\frac{v}{\sqrt{\mathrm{SNR}}}, \frac{u}{\sqrt{\mathrm{SNR}}}\right) \\ & + \exp\left(\frac{\mathrm{SIR}}{\mathrm{SNR}}\right)\left(\frac{u^2-v^2}{2uv}\right)\bar{\alpha}\left(\frac{-\mathrm{SIR}}{uv}\right) \\ & \left[1 - Q\left(\frac{h(\mathrm{SIR})}{\sqrt{\mathrm{SNR}}}, \frac{f(\mathrm{SIR})}{\sqrt{\mathrm{SNR}}}\right) + Q\left(\frac{f(\mathrm{SIR})}{\sqrt{\mathrm{SNR}}}, \frac{h(\mathrm{SIR})}{\sqrt{\mathrm{SNR}}}\right)\right], \end{aligned} \tag{4.2.15}$$

where

$$\begin{cases} h(\mathrm{SIR}) \doteq \sqrt{uv}\sqrt{\alpha\left(\dfrac{-\mathrm{SIR}}{uv}\right) + \bar{\alpha}\left(\dfrac{-\mathrm{SIR}}{uv}\right)^{-1}} \\ f(\mathrm{SIR}) \doteq \dfrac{uv}{h(\mathrm{SIR})} \end{cases},$$

and $\alpha(\cdot)$, $\bar{\alpha}(\cdot)$, u and v are as previously defined. Note that (4.2.15) is expressed in terms of the well-known SIR and SNR metrics. Besides, this expression involves only elementary and Marcum Q functions. Given that the analytical properties of the Marcum Q function are well-studied, obtaining further insight from (4.2.15) is straightforward, e.g. upper bounds or asymptotic approximations [1, ch. 4]. As an example, the derivative of the Marcum Q function in [53, eq. 2] is exploited here to obtain a second order Taylor approximation of Q as follows

$$Q\left(a\sqrt{t}, b\sqrt{t}\right) \approx 1 - t\cdot\frac{b^2}{2} + t^2\cdot\frac{1}{2}\left(\frac{a^2b^2}{2} + \frac{b^4}{4}\right). \tag{4.2.16}$$

Hence, after considering (4.2.16) with $t \doteq 1/\mathrm{SNR}$ and $t \to 0$, the following approximation can be found

$$\begin{aligned} P_{out} \approx {} & \frac{u^2-v^2}{2\cdot\mathrm{SNR}} + \frac{v^4-u^4}{8\cdot\mathrm{SNR}^2} + \exp\left(\frac{1}{\mathrm{INR}}\right)\left(\frac{u^2-v^2}{2uv}\right) \\ & \bar{\alpha}\left(\frac{-\mathrm{SIR}}{uv}\right)\left[1 + \frac{f^2-h^2}{2\cdot\mathrm{SNR}} + \frac{h^4-f^4}{8\cdot\mathrm{SNR}^2}\right]. \end{aligned} \tag{4.2.17}$$

Note that the previous expression provides a good approximation of the outage probability in the high SNR regime, being asymptotically tight as SNR $\to \infty$. For a given value of SINR, the tradeoff between interference and noise is represented by INR. When interference dominates over noise, i.e. INR $\to \infty$, then SNR $\to \infty$. Therefore, for a given SINR, the approximation in (4.2.17) fits well with the exact outage probability in the high INR regime.

On the other hand, when noise dominates over interference, i.e., INR $\to 0$, then SNR $\to$ SINR and SIR $\to \infty$. In this case the outage probability can be approximated by (4.2.10), which corresponds to the interference-free case.

4.2.3 Numerical Results

As a result of the OP analysis, a closed-form expression have been derived for a general L-branch MRC receiver in a Hoyt-faded channel under the presence of co-channel interference signals. Besides, some simplified expressions have been obtained for the particular case of a single antenna receiver ($L = 1$). This section presents some results from the numerical evaluation of these expressions. Moreover, several Monte-Carlo simulations have been carried out in order to validate our results.

Figure 4.8 and Figure 4.9 show some results for the OP of an L-branch MRC receiver from the numerical evaluation of the general expression (4.2.8). On the one hand, Figure 4.8 represents the OP related to the normalized average SINR expressed in decibels as

$$10 \log_{10} \left(\frac{W_s}{\gamma_o \sum W_i + \gamma_o \sigma^2} \right),$$

for several values of the number of diversity branches L and Hoyt parameter $q = 1/16$. In this particular example, three interferers are considered with mean powers $W_1 = 1/4$ and $W_2 = W_3 = 1/8$, while the background noise power is $\sigma^2 = 1/10$. Simulation results have been superimposed onto the analytical results from (4.2.8) showing that they are in perfect agreement.

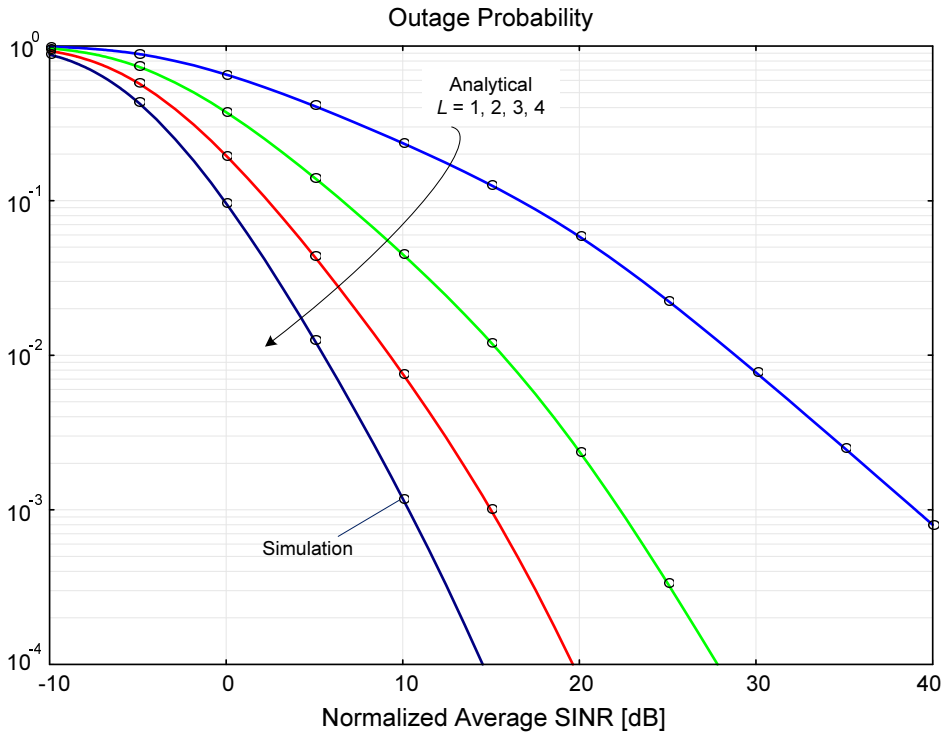

Figure 4.8: Outage probability versus normalized average SINR for an MRC receiver with L diversity branches, Hoyt fading parameter $q = 1/16$, background noise power $\sigma^2 = 1/10$, and 3 interferers with $W_1 = 1/4$, $W_2 = W_3 = 1/8$.

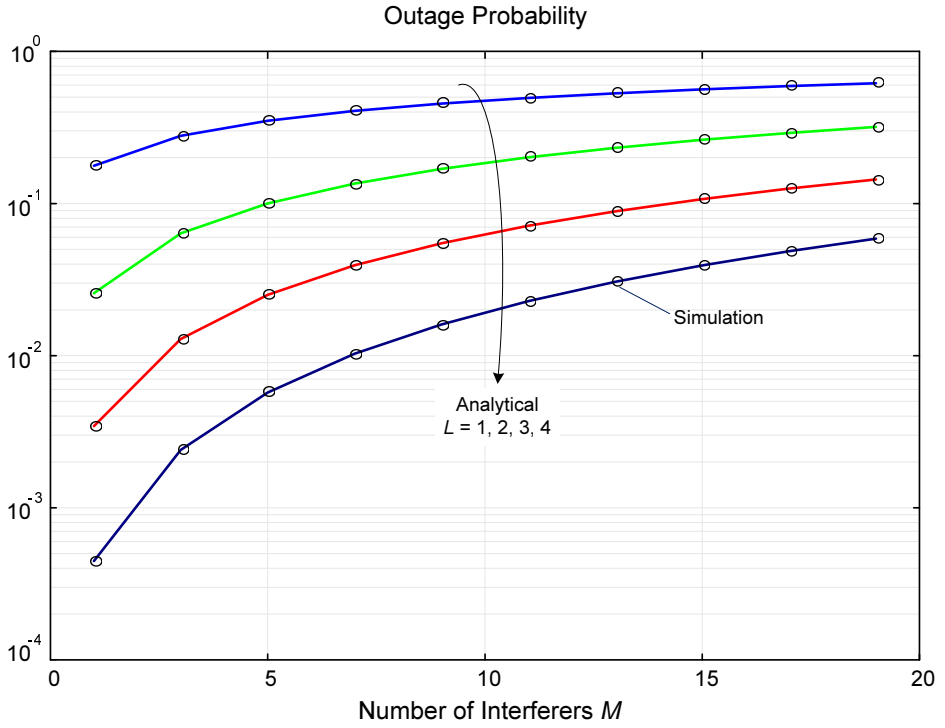

Figure 4.9: Outage probability versus number of interferers for an L-branch MRC receiver with Hoyt parameter $q = 1/16$, normalized power of the desired signal $W_s/\gamma_o = 1/4$, background noise power $\sigma^2 = 1/200$, and same power $W_1 = 1/100$ for all the interferers.

On the other hand, Figure 4.9 depicts the outage probability versus the number of interferers for the considered MRC receiver with different values of L and Hoyt parameter $q = 1/16$. In this case, the considered CCI scenario is as follows: normalized mean power of the desired signal $W_s/\gamma_o = 100$, background noise mean power $\sigma^2 = 1/200$, and the same mean power $W_1 = 1/100$ for all the interferers. First, it can be seen that the performance in terms of OP degrades significantly as the number of interferers increases. Also, it is observed from Figure 4.9 that the performance degradation associated to the presence of interference signals is significantly higher for greater values of L. Besides, the validity of the derived OP expression (4.2.8) is checked once more against the Monte-Carlo simulation results.

Figures 4.10 and 4.11 show some OP results for the single antenna receiver from the numerical evaluation of (4.2.11). On the one hand, Figure 4.10 represents the outage probability related to the normalized average SINR for several values of the Hoyt parameter q. The 3-interferers CCI scenario previously described is considered, i.e., background noise mean power $\sigma^2 = 1/10$ and 3 interferers with mean powers $W_1 = 1/4$ and $W_2 = W_3 = 1/8$. As expected, it can be seen that the OP degrades as the Hoyt parameter increases.

On the other hand, Figure 4.11 depicts the outage probability versus the number of interferers for the same CCI scenario considered in Figure 4.9, i.e., $W_s/\gamma_o = 100$, $\sigma^2 = 1/200$, and same power $W_1 = 1/100$ for all the interferers. Simulation results have been superimposed in both Figure 4.10 and Figure 4.11 onto the analytical results from (4.2.11), confirming the validity of this expression.

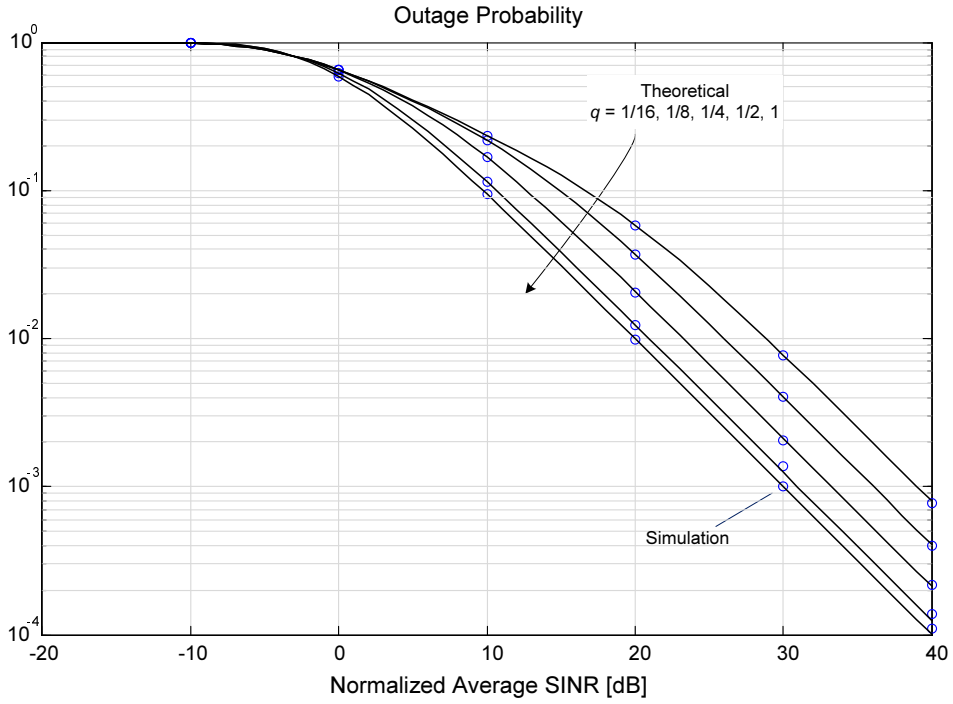

Figure 4.10: Outage probability vs average SINR for a single antenna receiver ($L = 1$) with background noise power $\sigma^2 = 1/10$, and 3 interferers with $W_1 = 1/4$, $W_2 = W_3 = 1/8$.

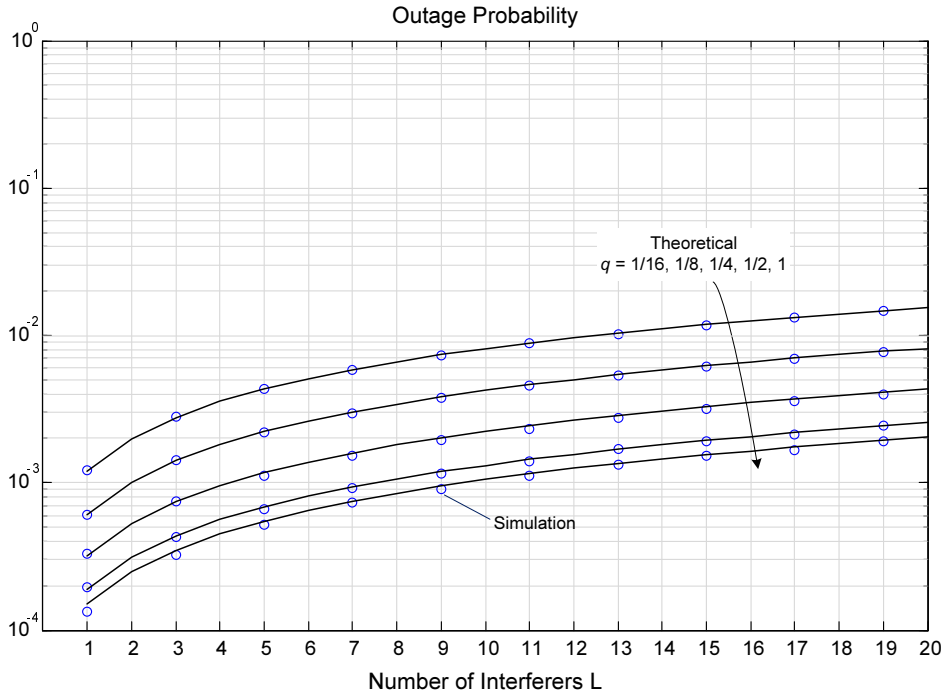

Figure 4.11: Outage probability versus number of interferers for a single antenna receiver with $W_s/\gamma_o = 100$, $\sigma^2 = 1/200$, and same power $W_1 = 1/100$ for all the interferers.

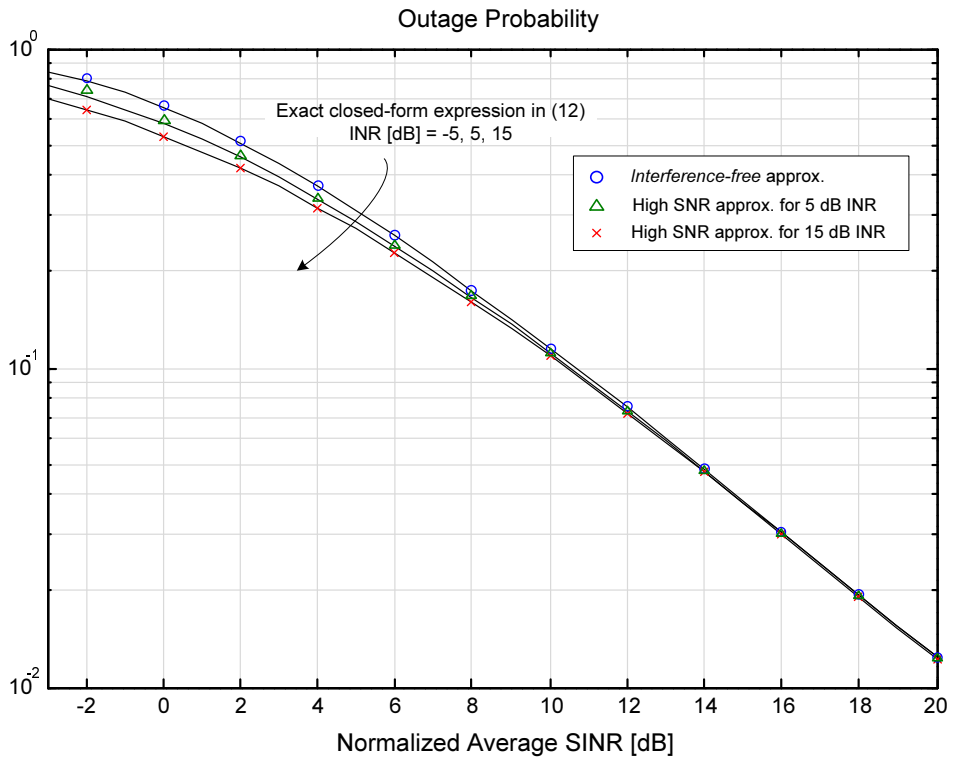

Figure 4.12: Outage probability versus normalized average SINR for a single antenna receiver and one dominant interferer with $q = 1/2$.

Finally, Figure 4.12 shows some numerical results for the single antenna receiver when one dominant interferer is considered. The outage probability in (4.2.15) is represented as a function of SINR for different values of INR and Hoyt parameter $q = 1/2$. Also, the approximated values from expression (4.2.17) are superimposed in the same figure for the medium and high INR values (i.e. 5 and 15 dB), whereas the interference-free expression in (4.2.10) is represented as an approximation for the low INR regime (i.e., -5 dB). On the one hand, this figure shows that (4.2.17) fits well with the exact expression (4.2.15) in the medium-high INR regime. Besides, it is observed that the approximation is tighter as the INR increases. On the other hand, it is shown that the interference-free approximation is reasonably tight for low INR values. Hence, the exact OP expression for the single antenna receiver with one dominant interferer can be approximated by (4.2.10) and (4.2.17) for the low and medium-high INR regime, respectively. Finally, Figure 4.12 shows that noise has a slightly greater impact on outage probability than interference for the low SINR regime.

4.3 Summary

In this chapter, we have analyzed the performance of two different SIMO systems under the presence of practical limitations such as non-orthogonal signaling at the transmitter or co-channel interferences. Specifically, SIMO systems employing switching combining have been analyzed in terms of bit error probabilities when correlated signals are intentionally employed at the transmitter side. Then, systems employing MRC at the multiple-antenna receiver have been analyzed in terms of the OP under the presence of co-channel interference signals.

On the one hand, we have derived exact closed-form expressions for the average BEP of multibranch switched diversity systems over i.i.d. Nakagami-m fading channels. Practical schemes which use noncoherent or differentially coherent symbol detection have been considered. In this kind of systems, signals may be chosen non-orthogonal (correlated) at the transmitter in order to reduce the bandwidth use. The general BEP expression includes as particular cases the following signaling formats: correlated binary signaling, DPSK, and DQPSK. The derived expressions have led to easily computable results which are useful for the analysis and design of switched diversity based systems. In particular, our analytical results have been applied to study the impact of the switching threshold selection on the system performance.

On the other hand, exact closed-form expressions have been obtained for the OP of MRC systems in Nakagami-q (Hoyt) fading channels under independent co-channel interferers with arbitrary powers. The considered scenario assumes the joint presence of background white Gaussian noise and independent Rayleigh interferers with arbitrary powers. These results are obtained through an appropriate generalization of the MGF of the Hoyt fading distribution. Specifically, the incomplete generalized MGF (IG-MGF) has been obtained in closed-form for the sum of squared Hoyt variables and applied to the OP analysis of MRC systems.

Chapter 5

Performance Analysis of Non-Ideal MIMO Systems

As stated before, the statistical properties of Wishart matrices have been extensively used to analyze the performance of multiple-input multiple-output (MIMO) systems. In particular, the signal-to-noise ratio (SNR) output statistics of several MIMO systems depends on the diagonal distribution of a complex Wishart matrix. Concretely, this distribution appears when the analysis is carried out under practical conditions such as the spatial correlation or the limited-rate feedback. Therefore, we have focused on the diagonal distribution of complex Wishart matrices, whose statistics have been addressed in Section 2.4.

In this chapter, the derived expressions for the cumulative distribution function (CDF) of the maximum of the diagonal elements of a complex Wishart matrix are applied to the performance analysis of two different MIMO systems under practical conditions. First, the outage probability (OP) is analyzed for MIMO selection combining (MIMO SC) systems under arbitrarily correlated Rayleigh fading. Then, the same analytical approach is applied to MIMO beamforming systems under limited-rate feedback, i.e., systems which employ codebook-based transmit beamforming and maximum ratio combining (MRC) at the receiver side.

5.1 MIMO SC Systems under Spatial Correlation

It is well known that the MIMO channel capacity increases with the minimum number of transmit and receive antennas when fading channels are independent and identically distributed (i.i.d.) [5]. However, in a real environment, signals received by the different antennas are found to be spatially correlated. The main reasons behind are related to the insufficient physical separation between the antennas and/or the geometry of the propagation environment. An important performance degradation of MIMO systems due to the presence of such correlation has been accordingly shown in [13].

To provide capacity gains, MIMO systems rely on the use of as many radio-frequency (RF) chains as antennas, thus increasing the cost and complexity. Receive antenna selection systems, also referred to as selection combining (SC), were proposed as a tradeoff between system performance and complexity (cost) by keeping the same number of antennas and reducing the number of RF chains. With this scheme, only the signal on the antenna which is experiencing the maximum SNR is processed and, thus, only one RF chain is needed at the receiver. Further discussion about antenna selection systems can be found in [75].

Several works in the literature have already addressed the performance analysis of MIMO systems with SC, referred to as MIMO SC, under spatially correlated fading channels [8, 28, 29]. However, these analyses are often limited due to the lack of results on the diagonal distribution of complex Wishart matrices. Moreover, analytical closed-form expressions are rarely provided due to the intractable form of the joint probability density function (PDF). In [29], the derived bit error probability (BEP) and OP expressions for multi-branch SC over spatially correlated fading are in the form of a multiple integral involving the joint characteristic function (CF). In some other works, the analysis is carried out under certain assumptions such as a real correlation matrix, equivalently considering a real Wishart matrix. In [28], closed-form BER results are provided for dual-branch selection diversity assuming real correlation among branches. Also, the real exponential correlation model is assumed in [8] to analyze the performance of MIMO SC systems.

In this section, we address the outage probability analysis of MIMO SC systems in arbitrarily correlated Rayleigh fading channels. This analysis relies on our previous results on the diagonal distribution of complex Wishart matrices (see Section 2.4). The analysis presented in this section extends the results in [8] to any number of receive antennas with arbitrary correlation. Also, our results are in the form of a single series expansion in terms of the Laguerre polynomials, which facilitates the computation and makes further closed-form analysis (e.g. BEP analysis) possible.

5.1.1 System Model

Consider a MIMO communication system with N_T transmit and N_R receive antennas, where all the antennas are used for transmission and only a single receive antenna, which maximizes the instantaneous SNR, is selected. The MIMO fading channel is modeled by the $N_R \times N_T$ random matrix $\mathbf{H}$, defined according to the well-known Kronecker spatial correlation model [76]

$$\mathbf{H} = [\mathbf{h}_1, \mathbf{h}_2, \ldots, \mathbf{h}_{N_T}] = \mathbf{R}_R^{\frac{1}{2}} \mathbf{G} \mathbf{R}_T^{\frac{1}{2}}, \tag{5.1.1}$$

where $\mathbf{R}_T$ and $\mathbf{R}_R$ are the transmit and receive correlation matrices, respectively, whereas the entries of $\mathbf{G}$ are i.i.d. complex Gaussian random variables with zero mean and unit variance. Transmit antennas are assumed to be spaced far enough so that the transmitter side correlation is negligible, or $\mathbf{R}_T = \mathbf{I}$, and thus, spatial correlation only appears at the receiver side. In this case, the column vectors of the channel matrix $\mathbf{h}_j = [h_{1j}, h_{2j}, \ldots, h_{N_R j}]^T$, for $j = 1, \ldots, N_T$, are zero-mean i.i.d. complex Gaussian processes with covariance matrix $\mathbf{R}_R$, i.e., $\mathbf{h}_j \sim \mathcal{CN}(\mathbf{0}, \mathbf{R}_R)$. Also, note that the matrix $\mathbf{S}_h = \sum_{j=1}^{N_T} \mathbf{h}_j \mathbf{h}_j^H$ has the complex Wishart distribution $\mathcal{CW}_{N_R}(N_T, \mathbf{R}_R)$ and its N_R diagonal elements are the square norms of the row vectors of $\mathbf{H}$.

The baseband complex envelope of the received signal after the matched filter is expressed as $\mathbf{y} = \mathbf{H}\mathbf{x} + \mathbf{n}$, where $\mathbf{n}$ is the N_R-dimensional white noise vector whose elements are complex Gaussian random variables with zero mean and variance σ_n^2. The transmitted signal is denoted by the column vector $\mathbf{x}$ and the total average transmit power is normalized to one, i.e., $\mathtt{E}\left[\mathbf{x}^H \mathbf{x}\right] = 1$, and evenly distributed among all the antennas. Under these assumptions, the average SNR at each receiver branch is given by $\bar{\gamma} = \frac{1}{\sigma_n^2}$.

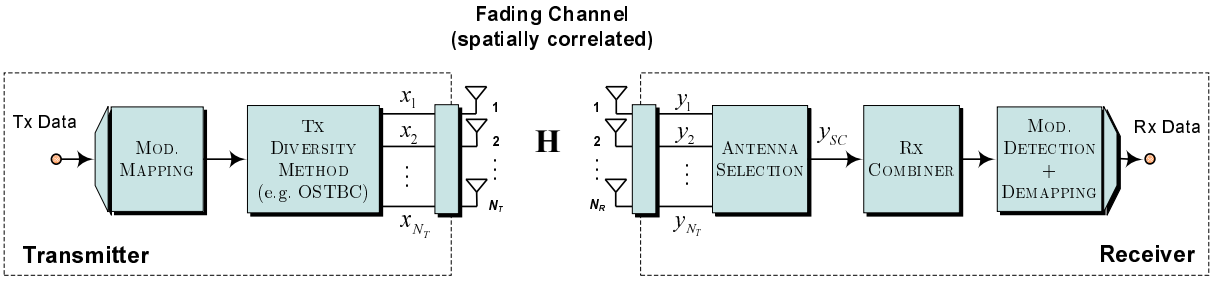

Figure 5.1: MIMO SC system model.

The receive antenna selection technique, also referred to as SC, selects the antenna which maximizes the instantaneous SNR [8]. In the considered MIMO system with SC, we also assume that channel state information (CSI) is perfectly known at the receiver but not available at the transmitter, where some diversity technique is applied (e.g., orthogonal space-time block codes).

5.1.2 Outage Probability Analysis

Under the considerations above, the instantaneous SNR at the output of the combiner is given by

$$\gamma = \frac{\bar{\gamma}}{N_T} Z, \tag{5.1.2}$$

where

$$Z = \max_{1 \le i \le N_R} \sum_{j=1}^{N_T} |h_{ij}|^2 \tag{5.1.3}$$

is the maximum of the squared norms of the row vectors of the channel matrix, which are the diagonal elements of the complex Wishart matrix $\mathbf{S}_h$. The statistics of complex Wishart matrices has been addressed before in Chapter 2, including a series expansion for the distribution of the maximum of the diagonal elements. Therefore, the CDF of Z can be obtained from the derived series expansion in (2.4.23) as

$$F_Z(z) = \sum_{n=0}^{\infty} \sum_{i=1}^{s_n} \hat{c}\left(p_{i,1}^{(n)}, \ldots, p_{i,N_R}^{(n)}\right) \prod_{j=1}^{N_R} \Delta_{p_{i,j}^{(n)}}^{N_T}\left(w^2 z\right), \tag{5.1.4}$$

where $\Delta_n^{\alpha}(\cdot)$ are the so-called delta functions, defined in (2.4.13), s_n is the number of possible integer partitions of n into N_R elements, $P_i^{(n)} = \left\{p_{i,1}^{(n)}, \ldots, p_{i,N_R}^{(n)}\right\}$ is the i-th integer partition of n, $i = 1, ..., s_n$, and the coefficients $\hat{c}\left(p_{i,1}^{(n)}, \ldots, p_{i,N_R}^{(n)}\right)$ are the ones

defined below (2.4.23). These coefficients depend on N_T and on the correlation matrix $\mathbf{R}_R$, and can be easily computed with the algorithm provided in Appendix B.2. Recall that the delta functions, as defined in (2.4.13), are basically a scaled version of the generalized Laguerre polynomials multiplied by the exponential function.

As a result, the outage probability for the MIMO system with SC under spatially correlated fading is given by

$$\begin{aligned} P_{out}(x) &\triangleq \Pr\{\gamma \leq \gamma_0\} = \Pr\left\{Z \leq N_T \frac{\gamma_0}{\bar{\gamma}}\right\} \\ &= F_Z\left(N_T \frac{1}{x}\right) = \sum_{n=0}^{\infty} \sum_{i=1}^{s_n} \hat{c}\left(p_{i,1}^{(n)}, \ldots, p_{i,N_R}^{(n)}\right) \prod_{j=1}^{N_R} \Delta_{p_{i,j}^{(n)}}^{N_T}\left(\frac{w^2 N_T}{x}\right), \end{aligned} \tag{5.1.5}$$

where γ_0 is the outage threshold and $x \triangleq \frac{\bar{\gamma}}{\gamma_0}$ is the normalized average SNR. To the best of the author's knowledge, this expression for the outage probability is original. Also, it is emphasized that (5.1.5) is a general expression valid for an *arbitrary* correlation matrix and *any* number of receive antennas. Recently in [8], the same system was analyzed but only under the assumption of a real exponential correlation matrix for $N_R > 3$ due to the lack of results for the diagonal distribution of a complex Wishart matrix. This was however a valid correlation model only when the antennas are placed in a uniform linear array [77] and therefore, our analysis extends the results in [8] to the general arbitrary correlation case.

The statistical results in Section 2.4.4 for the maximum of the diagonal elements of a complex Wishart matrix have been used to obtain a general OP expression. Also, some particular cases and approximations for the distribution of the maximum were provided in Section 2.4.4. In the subsequent, these simplified expressions are applied to the asymptotic analysis of the OP in the high SNR regime. Besides, a simplified formula for the OP in the particular case of a dual-branch receiver ($N_R = 2$) is provided.

Diversity order

After taking (2.4.34) into account, the outage probability in the high SNR regime can be approximated by

$$P_{out}(x) \approx |\mathbf{R}_R|^{-p} \left(\frac{1}{N_T!}\right)^{N_R} \frac{N_T^{N_T N_R}}{x^{N_T N_R}}, \tag{5.1.6}$$

which suggests that a diversity order of $N_T N_R$ is achieved. The same result has been obtained in [8], thus confirming the validity of our derivations.

Dual branch case ($N_R = 2$)

For a dual branch receiver, the simplified expression for the bivariate case in (2.4.28) can be used to arrive at the outage probability, which is given by

$$P_{out}(x) = G_{N_T}\left(\frac{N_T}{x}\right)^2 + \frac{e^{\frac{-2N_T}{x}}}{x^{2N_T}} \frac{N_T^{2N_T}}{(N_T-1)!} \sum_{n=1}^{\infty} \frac{(n-1)!}{n\,(N_T+n-1)!} |r|^{2n} L_{n-1}^{N_T}\left(\frac{N_T}{x}\right)^2, \tag{5.1.7}$$

where r is the out-diagonal element of the correlation matrix $\mathbf{R}_R$. As shown by the simplified expression, the outage probability increases with $|r|$, which can be dealt by increasing the number of transmit antennas N_T.

5.1.3 Numerical Results

The derived expressions have been numerically evaluated in order to analyze the performance of MIMO SC systems under spatially correlated fading. To check the validity of the derived expressions, we also provide some Monte-Carlo simulation results for the CDF of the SNR at the output of the combiner.

On the one hand, Figure 5.2 shows the CDF of Z, which is a scaled version of the SNR at the output of the combiner. The analytical expression in (5.1.4) has been evaluated for two different arbitrary correlation matrices, $\mathbf{R}_1$ and $\mathbf{R}_2$ (see Table 5.1), corresponding to $N_R = 4$ and $N_R = 6$ receive antennas respectively, $w = 1$, and several values of N_T. The truncation limit of the series in (5.1.4) has been set to $N_{max} = 8$, which yields a total of 25 terms for $N_R = 4$ and 36 terms for $N_R = 6$. It is emphasized that the computation of the corresponding coefficients by the algorithm provided in Appendix B.2 takes less than one second in a common PC. The simulation values of the CDF are also superimposed to the analytical curves in Figure 5.2 showing that, with just a few terms of the series, they are nearly in perfect agreement. The rapid convergence of the series is illustrated in Table 5.2, which presents the truncation limit and number of terms needed to achieve 2, 3, and 4 significant figure accuracy.

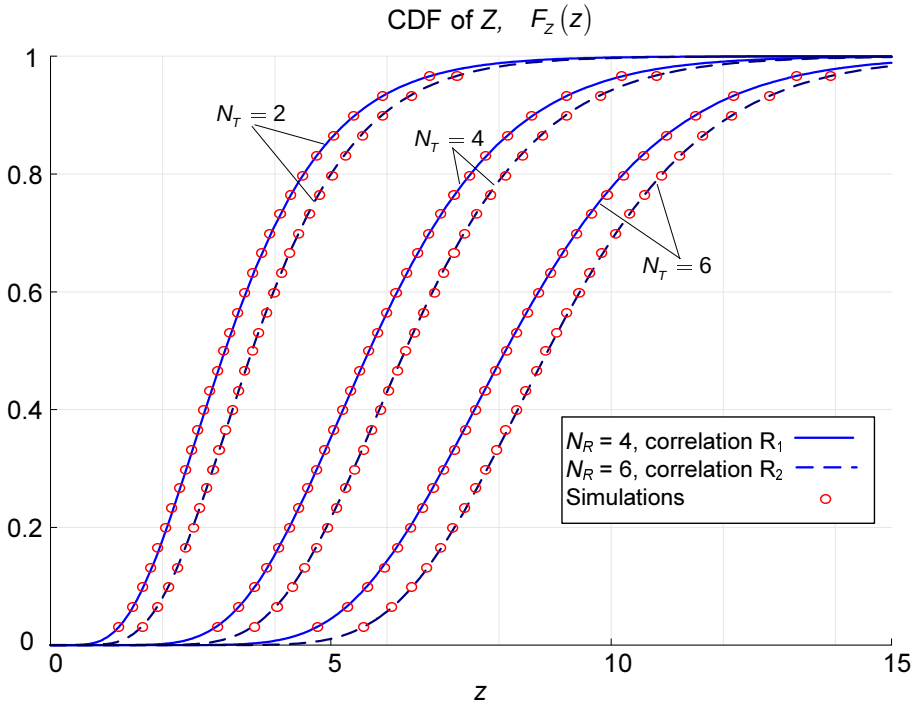

Figure 5.2: CDF of Z, the maximum of the square norms of the row vectors of the channel matrix $\mathbf{H}$.

Table 5.1: Correlation matrices considered in the performance analysis of the SC system.

$\mathbf{R}_1$	$\begin{pmatrix} 1 & 0.50 & 0.25+0.33j & -0.10+0.33j \\ 0.50 & 1 & 0.17-0.33j & -0.17 \\ 0.25-0.33j & 0.17+0.33j & 1 & 0.33-0.25j \\ -0.10-0.33j & -0.17 & 0.33+0.25j & 1 \end{pmatrix}$
$\mathbf{R}_2$	$\begin{pmatrix} 1 & 0.50 & 0.25+0.33j & -0.10+0.33j & 0.12j & 0.11+0.17j \\ 0.50 & 1 & 0.17-0.33j & -0.17 & 0.17-0.17j & -0.17 \\ 0.25-0.33j & 0.17+0.33j & 1 & 0.33-0.25j & -0.33 & 0.33-0.17j \\ -0.10-0.33j & -0.17 & 0.33+0.25j & 1 & 0.33-0.11j & 0.12 \\ -0.12j & 0.17+0.17j & -0.33 & 0.33+0.11j & 1 & -0.20 \\ 0.11-0.17j & -0.17 & 0.33+0.17j & 0.12 & -0.20 & 1 \end{pmatrix}$
$\mathbf{R}_3$	$\begin{pmatrix} 1 & 0.77j & 0.67-0.22j & 0.17+0.52j \\ -0.77j & 1 & -0.17-0.52j & 0.67-0.22j \\ 0.67+0.22j & -0.17+0.52j & 1 & 0.77j \\ 0.17-0.52j & 0.67+0.22j & -0.77j & 1 \end{pmatrix}$

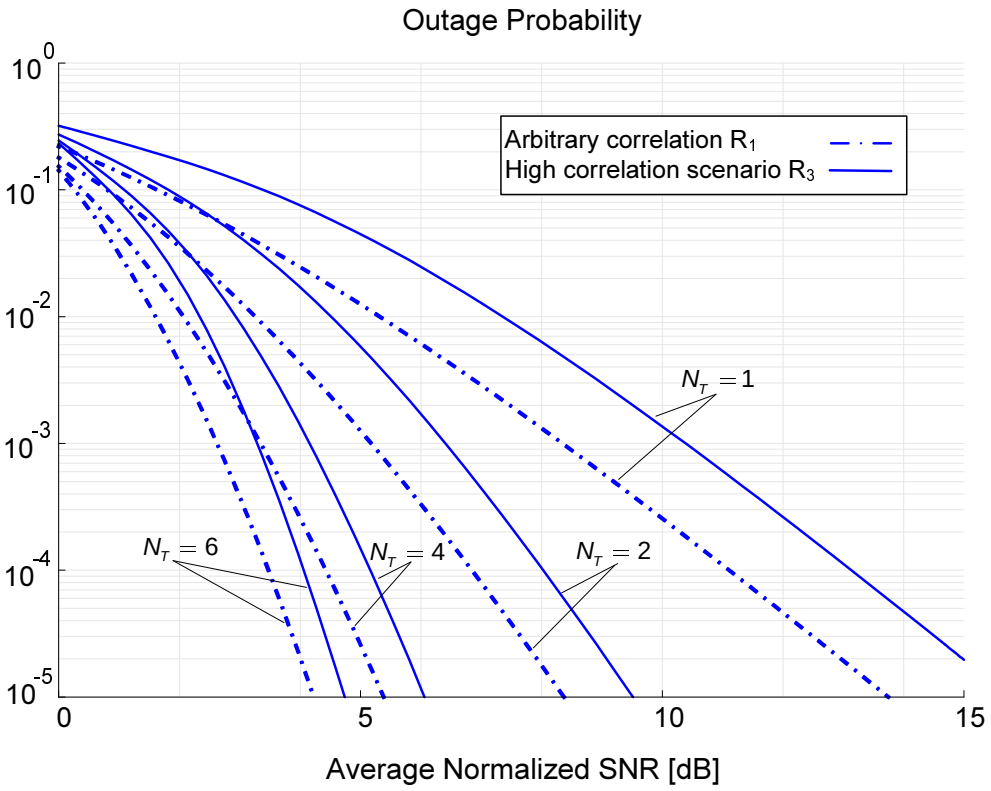

Figure 5.3: Outage probability versus average normalized SNR for a SC system with different antenna configurations and arbitrary correlation matrices.

On the other hand, the outage probability of the SC system with $N_R = 4$ is plotted in Figure 5.3 for different values of N_T and two correlation matrices. In this case, the high-correlation matrix proposed in [78] for a typical microcell scenario ($\mathbf{R}_3$), is compared to the low-medium correlation scenario defined by the arbitrary matrix $\mathbf{R}_1$. The scale factor has been set to $w = 0.93$ for $\mathbf{R}_3$ to assure the convergence of the series. It is observed that the high-correlation scenario determined by $\mathbf{R}_3$ degrades significantly the performance with respect to the arbitrary $\mathbf{R}_1$. However, it is shown that the performance loss associated to the high-correlation scenario can be reduced by increasing the number of transmit antennas.

Table 5.2: Truncation limit (N_{max}) and number of terms needed in (5.1.4) ($N_T = 4$) to achieve 2, 3, and 4 significant figure accuracy.

		$N_R = 4$ ($\mathbf{R}_1$)			$N_R = 6$ ($\mathbf{R}_2$)		
		$Z = 5$	$Z = 7.5$	$Z = 10$	$Z = 5$	$Z = 7.5$	$Z = 10$
2-Figure	N_{max}	2	2	2	2	2	2
	Terms	2	2	2	2	2	2
3-Figure	N_{max}	4	4	2	4	2	2
	Terms	6	6	2	6	2	2
4-Figure	N_{max}	8	6	4	8	6	4
	Terms	25	13	6	36	16	6

5.2 MIMO Beamforming under Limited Feedback

The capacity of MIMO systems can be significantly enhanced when CSI is available at the transmitter side [5]. The MIMO beamforming system, also referred to as MIMO MRC, relies on the joint MRC weights at both the transmitter and the receiver sides [10–12]. However, full CSI knowledge at the transmitter is often unrealistic, especially in systems where the forward and reverse links fade independently (e.g., frequency division duplexing systems). In practical systems, a limited-rate feedback channel is considered to report partial channel information from the receiver back to the transmitter. One way to deal with the limited-rate feedback limitation is to design a beamforming vector codebook and make this codebook available to both the transmitter and the receiver. During operation, the receiver reports back the index of the optimal beamforming vector to be used in subsequent transmissions.

Limited feedback beamforming systems have been extensively investigated [14–17]. However, exact performance analysis for an arbitrary beamformer codebook does not exist in the current literature.

In this section, the performance of MIMO beamforming systems under limited-rate feedback is analyzed in terms of the outage probability. An exact expression for the OP is provided based on our previous results on the diagonal distribution of complex Wishart matrices (see Section 2.4)

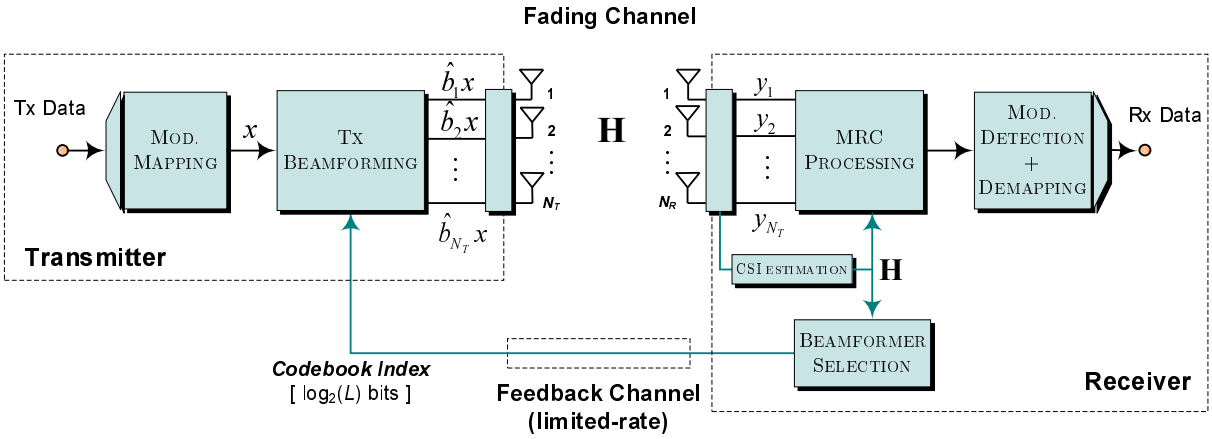

Figure 5.4: MIMO beamforming system model.

5.2.1 System Model

Here, we consider a MIMO beamforming system with N_T transmit and N_R receive antennas, where codebook-based transmit beamforming is applied together with MRC at the receiver (see Figure 5.4). The MIMO channel is modeled by the $N_R \times N_T$ random matrix $\mathbf{H}$, whose entries are i.i.d. complex Gaussian random variables with zero mean and unit variance. The beamformer codebook matrix $\mathbf{B} = [\mathbf{b}_1, \mathbf{b}_2, \ldots, \mathbf{b}_L]$ consists of L different $N_T \times 1$ column vectors $\mathbf{b}_i$, for $i = 1, \ldots, L$. For each channel realization, the receiver selects a beamformer vector which maximizes the instantaneous SNR and reports it back to the transmitter over a finite-rate feedback channel using $\log_2(L)$ bits. In this case, the complex envelope of the received signal after the matched filter (before the MRC processing) is expressed as $\mathbf{y} = \mathbf{H}\hat{\mathbf{b}}x + \mathbf{n}$, where x is the transmitted symbol, $\hat{\mathbf{b}}$ is the selected beamformer vector that satisfies

$$\hat{\mathbf{b}} = \arg \max_{\mathbf{b} \in \mathbf{B}} \|\mathbf{H}\mathbf{b}\|^2 , \tag{5.2.1}$$

and $\mathbf{n}$ is the N_R-dimensional white noise vector whose elements are complex Gaussian random variables with zero mean and variance σ_n^2. The total average transmit power is normalized to one, and consequently, $\mathtt{E}\left[|x|^2\right] = 1$ and $\|\mathbf{b}_i\|^2 = 1$, for $i = 1, \ldots, L$. Thus, the average SNR at each receive antenna is given by $\bar{\gamma} = \frac{1}{\sigma_n^2}$.

5.2.2 Outage Probability Analysis

Assuming the channel matrix $\mathbf{H}$ perfectly known at the receiver, the instantaneous SNR after the MRC processing is expressed as $\gamma = \bar{\gamma} Z$ with

$$Z = \max_{1 \le i \le L} \|\mathbf{H}\mathbf{b}_i\|^2 = \max_{1 \le i \le L} \sum_{j=1}^{N_R} |\mathbf{h}_j \mathbf{b}_i|^2, \tag{5.2.2}$$

where $\{\mathbf{h}_j\}$ are the row vectors of $\mathbf{H}$. It is observed that Z is the maximum of the squared norms $v_i = \|\mathbf{H}\mathbf{b}_i\|^2$, for $i = 1, \ldots, L$, which can be identified as the diagonal elements of a certain complex Wishart matrix. Specifically, v_i are the diagonal elements of the matrix $\mathbf{S}_{bf} = \sum_{j=1}^{N_R} \mathbf{k}_j \mathbf{k}_j^H$, with $\mathbf{k}_j = \mathbf{B}^H \mathbf{h}_j^H$, which follows the complex Wishart distribution $\mathcal{CW}_L(N_R, \mathbf{B}^H\mathbf{B})$. Equivalently, Z is the maximum of L correlated central chi-square variables with $2N_R$ degrees of freedom and underlying correlation matrix $\mathbf{R}_{bf} = \mathbf{B}^H\mathbf{B}$, i.e., with correlation determined by the codebook matrix. Hence, the CDF of Z can be expressed by the series expansion in (2.4.23) as

$$F_Z(z) = \sum_{n=0}^{\infty} \sum_{i=1}^{s_n} \hat{c}\left(p_{i,1}^{(n)}, \ldots, p_{i,L}^{(n)}\right) \prod_{j=1}^{L} \Delta_{p_{i,j}^{(n)}}^{N_R}\left(w^2 z\right), \tag{5.2.3}$$

where $\Delta_n^{\alpha}(\cdot)$ are the delta functions defined in (2.4.13), s_n is the number of possible integer partitions of n into L elements, $P_i^{(n)} = \left\{p_{i,1}^{(n)}, \ldots, p_{i,L}^{(n)}\right\}$ is the i-th integer partition of n, $i = 1, ..., s_n$, and the coefficients $\hat{c}\left(p_{i,1}^{(n)}, \ldots, p_{i,L}^{(n)}\right)$ are the ones defined below (2.4.23). These coefficients depend on N_R and the correlation matrix $\mathbf{R}_{bf}$, and are easily computed with the algorithm in Appendix B.2. Then, the previous result allows obtaining the outage probability of the codebook-based transmit beamforming system, which is given by

$$\begin{aligned} P_{out}(x) &\triangleq \Pr\{\gamma \le \gamma_0\} = \Pr\left\{Z \le \frac{\gamma_0}{\bar{\gamma}}\right\} \\ &= F_Z\left(\frac{1}{x}\right) = \sum_{n=0}^{\infty} \sum_{i=1}^{s_n} \hat{c}\left(p_{i,1}^{(n)}, \ldots, p_{i,L}^{(n)}\right) \prod_{j=1}^{L} \Delta_{p_{i,j}^{(n)}}^{N_R}\left(\frac{w^2}{x}\right), \end{aligned} \tag{5.2.4}$$

where γ_0 is the outage threshold and $x \triangleq \frac{\bar{\gamma}}{\gamma_0}$ is the normalized average SNR. The OP is now expressed as an infinite series in terms of the delta functions, defined in (2.4.13), which are basically a scaled version of the generalized Laguerre polynomials multiplied by the exponential function.

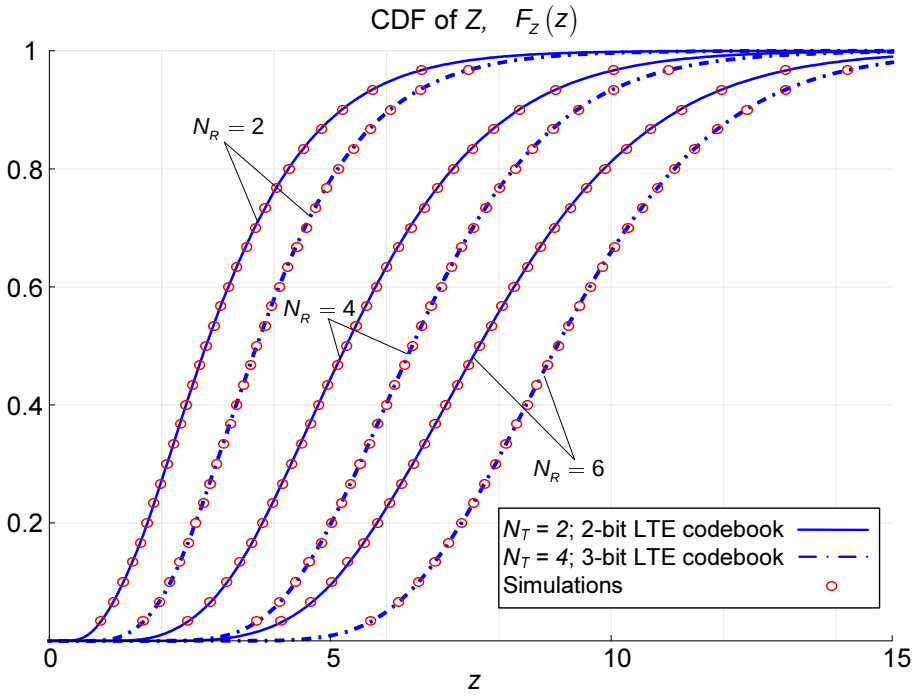

Figure 5.5: CDF of Z, the effective SNR at the output of the MRC processing when the optimal beamforming codeword is employed.

5.2.3 Numerical Results

Figures 5.5 and 5.6 depict the performance results for the codebook-based transmit beamforming system with MRC at the receiver. The system performance has been evaluated for three different values of the receive antennas, $N_R = 2, 4, 6$, and two transmit antenna configurations $N_T = 2, 4$ with 2-bit and 3-bit codebooks ($\mathbf{B}_{2-LTE}$ and $\mathbf{B}_{3-LTE}$) respectively. These codebooks have been chosen according to the Long Term Evolution (LTE) cellular technology specification [79], and can be found in Table 5.3.

Figure 5.5 shows the numerical evaluation of the CDF of Z, given in (5.2.3), for the mentioned cases. The simulated CDF has also been superimposed to the analytical curves in order to check the validity of the derived expression. In this case, the truncation limit has been set to $N_{max} = 10$ yielding a total of 20 and 37 terms for the 2-bit and the 3-bit codebooks, respectively. Again, it is observed that the simulated values fit reasonably well with the analytical ones for the considered series truncation limit. The outage probability of the codebook-based MIMO beamforming system is shown in Figure 5.6 for the same antenna configurations and codebooks.

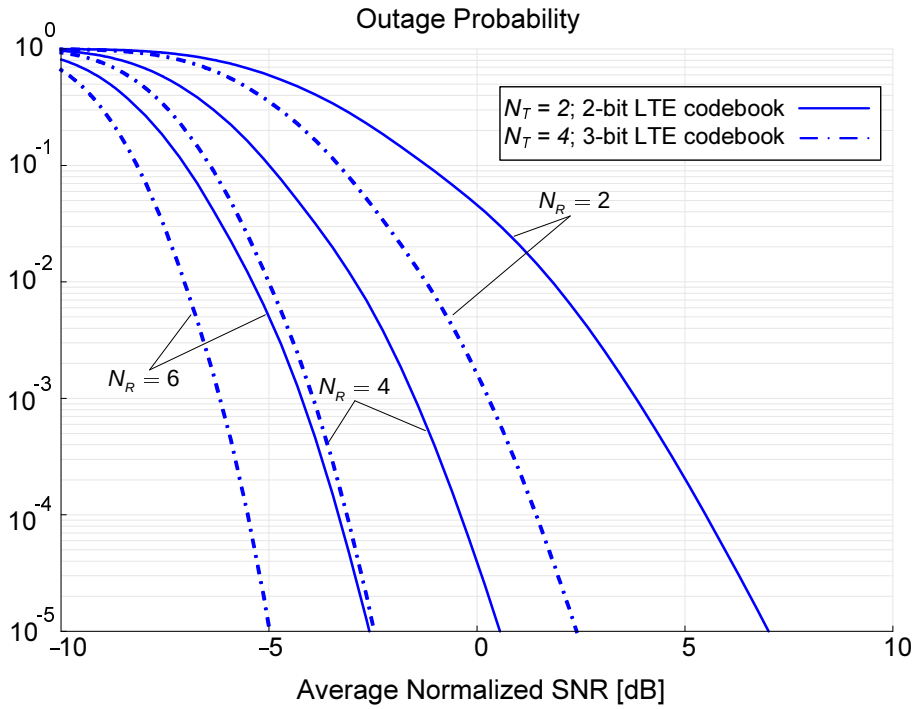

Figure 5.6: Outage probability versus average normalized SNR for a MIMO beamforming system with different antenna configurations and LTE-based codebooks.

Table 5.3: LTE-based codebook matrices considered in the performance analysis of the MIMO beamforming system.

$\mathbf{B}_{2-LTE}$	$\begin{pmatrix} 1/\sqrt{2} & 1/\sqrt{2} & 1/\sqrt{2} & 1/\sqrt{2} \\ 1/\sqrt{2} & j/\sqrt{2} & -1/\sqrt{2} & -j/\sqrt{2} \end{pmatrix}$
$\mathbf{B}_{3-LTE}$	$\begin{pmatrix} 1/2 & 1/2 & 1/2 & 1/2 & 1/2 & 1/2 & 1/2 & 1/2 \\ 1/2 & j/2 & -1/2 & -j/2 & 1/2 & j/2 & -1/2 & -j/2 \\ 1/2 & -1/2 & 1/2 & -1/2 & -1/2 & 1/2 & -1/2 & 1/2 \\ 1/2 & -j/2 & -1/2 & j/2 & -1/2 & j/2 & 1/2 & -j/2 \end{pmatrix}$

5.3 Summary

The diagonal distribution of complex Wishart matrices has been addressed earlier in Chapter 2, where the joint PDF and CDF, as well as the distribution of the maximum of the diagonal elements were derived. In this chapter, these statistical results have been applied to the performance analysis of two different MIMO systems under practical conditions. First, our statistical results have been applied to the OP analysis of MIMO SC systems in arbitrarily correlated Rayleigh fading. Then, the same analytical approach for the OP has been applied to codebook-based transmit beamforming systems with MRC at the receiver. The obtained expressions for the OP are in the form of an infinite series representation in terms of the well-known Laguerre polynomials, and have been shown to be easily computable. At the best of the author's knowledge, the derived expressions and results from both analyses are novel and represent remarkable contributions of this thesis.

Chapter 6

Conclusions and Future Work

In this final chapter, the main conclusions which arise from the contributions of this work are outlined. Besides, some future lines and possible applications regarding the work developed in this thesis are suggested.

6.1 Conclusions

In this thesis, we have addressed the performance analysis of different SIMO and MIMO systems in fading channels under certain non-ideal (practical) conditions. We have aimed to obtain closed-form expressions for the two most commonly extended performance measures, the outage probability (OP) and the bit error probability (BEP). However, the existing mathematical tools in some cases have not been enough to accomplish such analysis. Therefore, the development of new mathematical tools and statistical functions has been an essential part of this work in order to analyze the performance of SIMO and MIMO systems.

In the context of SIMO systems, recent results for the explicit solutions of the incomplete integrals ILHI and IIMQ [20] have been applied to the BEP and OP analysis for the following receive diversity schemes and practical conditions:

- Switch-and-examine combining (SEC) under non-orthogonal signaling has been analyzed in terms of BEP for different non-coherent and differentially coherent modulation formats in Nakagami-m fading channels for a general L-branch receiver. The derived expressions have led to easily computable results which are useful for the analysis and design of switched diversity based systems.

- Maximum ratio combining (MRC) systems under the presence of co-channel interferences have been analyzed in terms of the outage probability in Nakagami-q (Hoyt) fading channels for a general L-branch receiver. This analysis has motivated the derivation of new statistical functions related to the Hoyt fading distribution. Specifically, the incomplete generalized MGF (IG-MGF) of the Hoyt distribution has been obtained in closed-form and applied to the OP analysis. Besides, some simplified expressions and approximations in the high SINR regime have been obtained for the case of a single antenna receiver.

In the context of MIMO, it has been observed that the SNR output statistics of several systems depends on the diagonal distribution of a complex Wishart matrix. Due to the lack of results for this distribution in the literature, we have focused on it as a previous and fundamental step towards further performance analysis of MIMO systems. Specifically, we have derived the joint density of the diagonal elements of a complex Wishart matrix, which follow a particular multivariate chi-square distribution. The density expression is in the form of an infinite series representation which converges rapidly and is easy to compute. This expression has been used to obtain the distribution of the maximum of the diagonal elements, which has been applied to the performance analysis of two different MIMO systems under practical conditions:

- First, our statistical results have been applied to the OP analysis of MIMO selection combining (MIMO SC) systems in arbitrarily correlated Rayleigh fading. The analytical expressions are general and valid for any number of receive antennas with arbitrary correlation. Also, our results are in the form of a single series expansion in terms of the Laguerre polynomials, which facilitates further closed-form performance analysis (e.g. BEP analysis).

- Then, the same analytical approach has been applied to the OP analysis of MIMO beamforming systems under limited-rate feedback, i.e., systems with codebook-based transmit beamforming and MRC at the receiver side.

6.2 Future Work

As stated above, the performance analysis of MIMO systems under non-ideal conditions has motivated the development of new mathematical tools, which may be applied elsewhere. As such, an interesting future line of work can be the application of these tools to extend the analysis of current systems or to investigate upcoming systems. Specifically, the statistical results on the diagonal distribution of complex Wishart matrices could be used in the BEP analysis of MIMO SC or MIMO beamforming systems with adaptive modulation.

Moreover, different scenarios may be considered in the performance analysis, implying different fading conditions or practical limitations. Given the recent relevancy of η-μ fading channels, it could be interesting to consider this fading model in future works. Also, an important practical limitation in systems relying on a feedback channel is the user mobility, which may significantly degrade the performance of beamforming or adaptive modulation strategies.

Finally, the obtained expressions for the outage and bit error probabilities of SIMO and MIMO systems could be applied to the design of these systems under realistic conditions. In this context, other practical limitations such as errors in the channel estimation process could be considered.

Appendix A

Incomplete Lipschitz-Hankel Integrals

A.1 Proof of Lemma 1

As in [53], integration by parts is performed in (2.3.25) with

$$\begin{cases} u = Q_n\left(a\sqrt{t}, b\sqrt{t}\right), \\ du = \dfrac{b}{2}\left(\dfrac{b}{a}\right)^{n-1} e^{-\frac{a^2+b^2}{2}t}\left(a\, I_n(abt) - b\, I_{n-1}(abt)\right) dt, \\ v = \{[41,\ \text{eq. } 2.231\text{-}2]\} = -e^{-\beta t}\left(\dfrac{m!}{\beta^{m+1}}\displaystyle\sum_{r=0}^{m}\dfrac{(\beta t)^r}{r!}\right), \\ dv = t^m e^{-\beta t} dt. \end{cases}$$

Then, after some algebra, (2.3.26) is obtained.

A.2 Proof of Lemma 2

As a previous step to the proof of Lemma 2, we need to introduce the following identity, referred to as the modified Sonine identity [20]:

$$\int t^{\nu+1}\left\{-\frac{d^2 f(t)}{dt^2} - \frac{2\nu+1}{t}\frac{df(t)}{dt} + f(t)\right\} I_\nu(t) dt = t^{\nu+1}\left\{-\frac{df(t)}{dt} I_\nu(t) + f(t) I_{\nu+1}(t)\right\}, \tag{A.2.1}$$

where $I_\nu(t)$ is the ν-th order modified Bessel function of the first kind and $f(t)$ is any twice-differentiable function.

Note that $I_{e_{0,0}}(x;\alpha) = \frac{1}{\alpha} I_e(\frac{1}{\alpha}, \alpha x)$, where I_e is the Rice I_e-function. Then, we obtain (i) by using the connection between the Rice I_e-function and the Marcum Q function [45] and after some algebra. To show (ii) we first apply (A.2.1) with $\nu = 0$ and $f(t) = \exp(-\alpha t)$, followed by the substitution of $I_{e_{0,0}}$ by (i). Expression (iii) is obtained using integration by parts with $u = \exp(-\alpha t), du = -\alpha \exp(-\alpha t)dt$, $v = I_0(t)$, $dv = I_1(t)dt$ and applying (i). Finally, integrating by parts $I_{e_{1,1}}$ with $u = t\exp(-\alpha t), du = (-\alpha t \exp(-\alpha t) + \exp(-\alpha t))dt$, $v = I_0(t), dv = I_1(t)dt$ yields

$$I_{e_{1,1}}(x;a) = xe^{-\alpha x} I_0(x) - I_{e_{0,0}}(x;a) + aI_{e_{1,0}}(x;a). \tag{A.2.2}$$

Substituting (i) and (ii) in (A.2.2) the expression (iv) holds and the proof is complete.

A.3 Proof of Proposition 1

Let us consider the following recursive Luke's formulas for the ILHI of Bessel type [50, pp. 120]

$$\begin{aligned}(\alpha^2 - 1)I_{e_{m,n}}(x;\alpha) = &-e^{-\alpha x}x^m I_{n+1}(x) + (m-n-1)e^{-\alpha x}x^{m-1}I_n(x) - \alpha e^{-\alpha x}x^m I_n(x) \\ &+\alpha(2m-1)I_{e_{m-1,n}}(x;\alpha) + (n^2 - (m-1)^2)I_{e_{m-2,n}}(x;\alpha)\end{aligned} \tag{A.3.1}$$

$$-(n-1)I_{e_{1,n+1}}(x;\alpha) = -2ne^{-\alpha x}xI_n(x) - 2n\alpha I_{e_{1,n}}(x;\alpha) + (n+1)I_{e_{1,n-1}}(x;\alpha) \tag{A.3.2}$$

$$-nI_{e_{0,n+1}}(x;\alpha) = -2ne^{-\alpha x}I_n(x) - 2n\alpha I_{e_{0,n}}(x;\alpha) + (n+1)I_{e_{0,n-1}}(x;\alpha) \tag{A.3.3}$$

First, we show that $I_{e_{0,n}}(x;\alpha)$ is represented by (2.3.27). Such statement for $n = 0$ and $n = 1$ is obviously true by direct inspection of Lemma 2, where the corresponding coefficients are explicitly given. Let us set $m = 0$ and perform strong induction over n for $n \geqslant 2$. Applying Lemma 2 to (A.3.3) and identifying with (2.3.27), the following coefficients are obtained for $I_{e_{0,2}}(x;\alpha)$

$$\begin{cases} \mathcal{A}^l_{0,2}(\alpha) = 2\alpha\mathcal{A}^l_{0,1}(\alpha) - \mathcal{A}^l_{0,0}(\alpha),\ l = 0,1 \\ \mathcal{B}^{0,0}_{0,2}(\alpha) = 2\alpha\mathcal{B}^{0,0}_{0,1}(\alpha) - \mathcal{B}^{0,0}_{0,0}(\alpha) \\ \mathcal{B}^{0,1}_{0,2}(\alpha) = 2 \end{cases} \tag{A.3.4}$$

where unspecified coefficients are assumed to be zero. For $n \geqslant 2$, application of the induction hypothesis to (A.3.3) and identification with (2.3.27) lead to the following coefficients for $I_{e_{0,n}}(x;\alpha)$

$$\begin{cases} \mathcal{A}_{0,n}^{l}(\alpha) = 2\alpha\mathcal{A}_{0,n-1}^{l}(\alpha) - \mathcal{A}_{0,n-2}^{l}(\alpha),\ l = 0,1 \\ \mathcal{B}_{0,n}^{0,j}(\alpha) = 2\alpha\mathcal{B}_{0,n-1}^{0,j}(\alpha) - \mathcal{B}_{0,n-2}^{0,j}(\alpha), 0 \leqslant j \leqslant n-2 \\ \mathcal{B}_{0,n}^{0,n-1}(\alpha) = 2\alpha\mathcal{B}_{0,n-1}^{0,n-1}(\alpha) + 2 \end{cases} \tag{A.3.5}$$

Therefore, $I_{e_{0,n}}(x;\alpha)$ is represented by (2.3.27) for $n \geqslant 0$ and the corresponding coefficients are obtained recursively using Lemma 2, (A.3.4) and (A.3.5).

Second, we prove that $I_{e_{1,n}}(x;\alpha)$ is represented by (2.3.27). Again, such statement for $n = 0$ and $n = 1$ is obviously true by direct inspection of Lemma 2. Applying [41, eq. 8.486-1] to the definition of $I_{e_{1,2}}(x;\alpha)$ we obtain

$$I_{e_{1,2}}(x;\alpha) = I_{e_{1,0}}(x;\alpha) - 2I_{e_{0,1}}(x;\alpha),$$

then, using again Lemma 2, the non-zero coefficients for $m = 1$ and $n = 2$ are

$$\begin{cases} \mathcal{A}_{1,2}^{l}(\alpha) = \mathcal{A}_{1,0}^{l}(\alpha) - 2\mathcal{A}_{0,1}^{l}(\alpha),\ l = 0,1 \\ \mathcal{B}_{1,2}^{0,0}(\alpha) = \mathcal{B}_{1,0}^{0,0} - 2\mathcal{B}_{0,1}^{0,0}(\alpha) \\ \mathcal{B}_{1,2}^{1,0}(\alpha) = \mathcal{B}_{1,0}^{1,0}(\alpha) \\ \mathcal{B}_{1,2}^{1,1}(\alpha) = \mathcal{B}_{1,0}^{1,1}(\alpha) \end{cases} \tag{A.3.6}$$

Let us set $m = 1$ and perform strong induction over n for $n \geqslant 3$. Application of the induction hypothesis to (A.3.2) and identification with (2.3.27) lead to the following non-zero coefficients for $I_{e_{1,n}}(x;\alpha)$

$$\begin{cases} \mathcal{A}_{1,n}^{l}(\alpha) = 2\alpha\dfrac{n-1}{n-2}\mathcal{A}_{1,n-1}^{l}(\alpha) - \dfrac{n}{n-2}\mathcal{A}_{1,n-2}^{l}(\alpha),\ l = 0,1 \\ \mathcal{B}_{1,n}^{i,j}(\alpha) = 2\alpha\dfrac{n-1}{n-2}\mathcal{B}_{1,n-1}^{i,j}(\alpha) - \dfrac{n}{n-2}\mathcal{B}_{1,n-2}^{i,j}(\alpha), \begin{cases} i = 0,1 \\ 0 \leqslant j \leqslant n-2 \end{cases} \\ \mathcal{B}_{1,n}^{0,n-1}(\alpha) = 2\alpha\dfrac{n-1}{n-2}\mathcal{B}_{1,n-1}^{0,n-1}(\alpha) \\ \mathcal{B}_{1,n}^{1,n-1}(\alpha) = 2\alpha\dfrac{n-1}{n-2}\mathcal{B}_{1,n-1}^{1,n-1}(\alpha) + 2\dfrac{n-1}{n-2} \end{cases} \tag{A.3.7}$$

Therefore, $I_{e_{1,n}}(x;\alpha)$ is represented by (2.3.27) for $n \geqslant 0$ and the corresponding coefficients are obtained recursively using Lemma 2, (A.3.6) and (A.3.7).

Finally, we are in position to show that $I_{e_{m,n}}(x;\alpha)$ is represented by (2.3.27), by fixing n and performing strong induction over m for $m \geqslant 2$. We have proven that such statement is true for $I_{e_{0,n}}(x;\alpha)$ and $I_{e_{1,n}}(x;\alpha)$. For $m \geqslant 2$, using [41, eq. 8.486-1] equation (A.3.1) can be rearranged as follows

$$\begin{aligned} I_{e_{m,n}}(x;\alpha) = &-\frac{1}{\alpha^2-1}e^{-\alpha x}x^m I_{n-1}(x) + \frac{m+n-1}{\alpha^2-1}e^{-\alpha x}x^{m-1}I_n(x) - \frac{\alpha}{\alpha^2-1}e^{-\alpha x}x^m I_n(x) \\ &+\frac{\alpha(2m-1)}{\alpha^2-1}I_{e_{m-1,n}}(x;\alpha) + \frac{n^2-(m-1)^2}{\alpha^2-1}I_{e_{m-2,n}}(x;\alpha). \end{aligned} \tag{A.3.8}$$

For $I_{e_{2,n}}(x;\alpha)$, expression (A.3.8) allows to obtain the representation (2.3.27) with coefficients

$$\begin{cases} \mathcal{A}^{l}_{2,n}(\alpha) = \dfrac{3\alpha}{\alpha^2-1}\mathcal{A}^{l}_{1,n}(\alpha) + \dfrac{n^2-1}{\alpha^2-1}\mathcal{A}^{l}_{0,n}(\alpha), \ l=0,1 \\ \mathcal{B}^{0,j}_{2,n}(\alpha) = \dfrac{3\alpha}{\alpha^2-1}\mathcal{B}^{0,j}_{1,n}(\alpha) + \dfrac{n^2-1}{\alpha^2-1}\mathcal{B}^{0,j}_{0,n}(\alpha), \ 0 \leqslant j \leqslant n+1 \\ \mathcal{B}^{1,j}_{2,n}(\alpha) = \dfrac{3\alpha}{\alpha^2-1}\mathcal{B}^{1,j}_{1,n}(\alpha) + \dfrac{n+1}{\alpha^2-1}\delta[j-n], \ 0 \leqslant j \leqslant n+1 \\ \mathcal{B}^{2,j}_{2,n}(\alpha) = \begin{cases} n=0 \Rightarrow -\dfrac{\alpha}{\alpha^2-1}\delta[j] - \dfrac{1}{\alpha^2-1}\delta[j-1], \ 0 \leqslant j \leqslant n+1 \\ n>0 \Rightarrow -\dfrac{\alpha}{\alpha^2-1}\delta[j-n] - \dfrac{1}{\alpha^2-1}\delta[j-(n-1)], \ 0 \leqslant j \leqslant n \end{cases} \end{cases} \tag{A.3.9}$$

where $\delta[\cdot]$ is the Kronecker's delta. For $m \geqslant 2$, application of the induction hypothesis to (A.3.8) and identification with (2.3.27) lead to the following coefficients for $I_{e_{m,n}}(x;\alpha)$

$$\begin{cases} \mathcal{A}^{l}_{m,n}(\alpha) = \dfrac{\alpha(2m-1)}{\alpha^2-1}\mathcal{A}^{l}_{m-1,n}(\alpha) + \dfrac{n^2-(m-1)^2}{\alpha^2-1}\mathcal{A}^{l}_{m-2,n}(\alpha), \ l=0,1 \\ \mathcal{B}^{i,j}_{m,n}(\alpha) = \dfrac{\alpha(2m-1)}{\alpha^2-1}\mathcal{B}^{i,j}_{m-1,n}(\alpha) + \dfrac{n^2-(m-1)^2}{\alpha^2-1}\mathcal{B}^{i,j}_{m-2,n}(\alpha), \ \text{for} \begin{cases} 0 \leqslant i \leqslant m-2 \\ 0 \leqslant j \leqslant n+1 \end{cases} \\ \mathcal{B}^{m-1,j}_{m,n}(\alpha) = \dfrac{\alpha(2m-1)}{\alpha^2-1}\mathcal{B}^{m-1,j}_{m-1,n}(\alpha) + \dfrac{m+n-1}{\alpha^2-1}\delta[j-n], \ 0 \leqslant j \leqslant n+1 \\ \mathcal{B}^{m,j}_{m,n}(\alpha) = \begin{cases} n=0 \Rightarrow -\dfrac{\alpha}{\alpha^2-1}\delta[j] - \dfrac{1}{\alpha^2-1}\delta[j-1], \ 0 \leqslant j \leqslant n+1 \\ n>0 \Rightarrow -\dfrac{\alpha}{\alpha^2-1}\delta[j-n] - \dfrac{1}{\alpha^2-1}\delta[j-(n-1)], \ 0 \leqslant j \leqslant n \end{cases} \end{cases} \tag{A.3.10}$$

Therefore, $I_{e_{m,n}}(x;\alpha)$ is represented by (2.3.27) for $m \geqslant 0$ and $n \geqslant 0$, and the corresponding coefficients are obtained using Lemma 2, (A.3.4)-(A.3.7) and (A.3.9)-(A.3.10).

A.4 MATHEMATICA™ 7.0 program to compute the ILHI coefficients

```
coeffILHI[mm_,nn_,aa_]:=
Module[{m=mm,n=nn,a=aa,\[Delta],b, a0,a1,bb,a0n1,a0n2,
a1n1,a1n2,bbn1,bbn2,i,j,a0m1,a1m1,bbm1,a0m2,a1m2,bbm2},
\[Delta][k_]:=KroneckerDelta[k];
b=1/Sqrt[a^2-1];a0=0;a1=0;
bb=ConstantArray[0,{m+1,n+2}];
Which[
{m,n}=={0,0}, a0=b;a1=-2 b;bb={{b,0}},
{m,n}=={1,0}, a0=a b^3;a1=-2 a b^3;
              bb={{a b^3,0},{-a b^2,-b^2}},
{m,n}=={0,1}, a0=a b-1;a1=-2 a b;
              bb={{1+a b,0,0}},
{m,n}=={1,1}, a0=b^3;a1=-2 b^3;
              bb={{b^3,0,0},{-b^2,-a b^2,0}},
{m,n}=={1,2}, a0=a b^3-2 (a b-1);a1=-2 a b^3-2 (-2 a b);
              bb={{a b^3-2 (1+a b),0,0,0},{-a b^2,-b^2,0,0}},
m==0,
    {a0n1,a1n1,bbn1}=coeffILHI[0,n-1,a];{a0n2,a1n2,bbn2}=coeffILHI[0,n-2,a];
    a0=2 a a0n1-a0n2;a1=2 a a1n1-a1n2;
    Do[bb[[1+0,1+j]]=
    2 a bbn1[[1+0,1+j]]-bbn2[[1+0,1+j]],{j,0,n-2}];
    bb[[1+0,1+n-1]]=2 a bbn1[[1+0,1+n-1]]+2,
m==1,
    {a0n1,a1n1,bbn1}=coeffILHI[1,n-1,a];{a0n2,a1n2,bbn2}=coeffILHI[1,n-2,a];
    a0=2 a (n-1 )/(n-2) a0n1-n/(n-2) a0n2;
    a1=2 a (n-1 )/(n-2) a1n1-n/(n-2) a1n2;
    Do[bb[[1+i,1+j]]=
    2 a (n-1 )/(n-2) bbn1[[1+i,1+j]]-n/(n-2) bbn2[[1+i,1+j]],{i,0,1},{j,0,n-2}];
    bb[[1+0,1+n-1]]=2 a (n-1 )/(n-2) bbn1[[1+0,1+n-1]];
    bb[[1+1,1+n-1]]=2 a (n-1 )/(n-2) bbn1[[1+1,1+n-1]]+2 (n-1 )/(n-2),
m>=2,
    {a0m1,a1m1,bbm1}=coeffILHI[m-1,n,a];{a0m2,a1m2,bbm2}=coeffILHI[m-2,n,a];
    a0=a b^2 (2m-1)a0m1+b^2 (n^2-(m-1)^2)a0m2;
    a1=a b^2 (2m-1)a1m1+b^2 (n^2-(m-1)^2)a1m2;
    Do[bb[[1+i,1+j]]=
    a b^2 (2m-1) bbm1[[1+i,1+j]]+b^2 (n^2-(m-1)^2)bbm2[[1+i,1+j]],{i,0,m-2},{j,0,n+1}];
    Do[bb[[1+m-1,1+j]]=
    a b^2 (2m-1) bbm1[[1+m-1,1+j]]+b^2 (m+n-1)\[Delta][j-n],{j,0,n+1}];
    If[n==0,
    Do[bb[[1+m,1+j]]=
    -a b^2 \[Delta][j-0]-b^2 \[Delta][j-1],{j,0,n+1}],
    Do[bb[[1+m,1+j]]=
    -a b^2 \[Delta][j-n]-b^2 \[Delta][j-(n-1)],{j,0,n}]]];
{a0,a1,bb}];
```

Appendix B

The Diagonal Distribution of Complex Wishart Matrices

B.1 Proof of Proposition 2

The coefficients $c(n_1, \ldots, n_k)$ can be obtained from the expansion of the CF in (2.4.5). Specifically, the expansion

$$|\mathbf{I} - (\mathbf{I} - \mathbf{WRW})\,\mathbf{U}|^{-p} = \sum_{n=0}^{\infty} \underbrace{\sum_{(n=n_1+\cdots+n_k)} c(n_1, \ldots, n_k) \prod_{j=1}^{k} u_j^{n_j}}_{\theta_n(u_1,u_2,\ldots,u_k)} \tag{B.1.1}$$

has been used in the derivation of (2.4.9). The determinant in (B.1.1) can be expressed as [34]

$$|\mathbf{I} - (\mathbf{I} - \mathbf{WRW})\,\mathbf{U}| = 1 + \sum_{j=1}^{k} D_j, \tag{B.1.2}$$

where D_j is the j-order polynomial defined in (2.4.15). Now, considering (B.1.2) and making use of the binomial expansion, it is possible to write

$$|\mathbf{I} - (\mathbf{I} - \mathbf{WRW})\,\mathbf{U}|^{-p} = \sum_{n=0}^{\infty} \binom{p+n-1}{n} (-1)^n \left(\sum_{j=1}^{k} D_j\right)^n. \tag{B.1.3}$$

Then, after applying the multinomial theorem [51, eq. 24.1.2] to (B.1.3) and further simplifications the expansion can be rewritten as

$$|\mathbf{I} - (\mathbf{I} - \mathbf{WRW})\,\mathbf{U}|^{-p} = \sum_{n=0}^{\infty} \frac{\Gamma(p+n)}{\Gamma(p)} \sum_{(n=\ell_1+\ldots+\ell_k)} \prod_{j=1}^{k} \frac{(-D_j)^{\ell_j}}{\ell_j!}. \tag{B.1.4}$$

Finally, the expression (2.4.14) for the polynomial $\theta_n(u_1, u_2, \ldots, u_k)$ with coefficients $c(n_1, \ldots, n_k)$ is obtained by rearranging the terms of the expansion in (B.1.4).

B.2 MATHEMATICA™ 7.0 program for the coefficients computation

```
Needs["Combinatorica`"]
GetCoefs[R_, nDeg_, w_, Nmax_] := Module[{Pcoef, Vcoef},

  (* INITIALIZATION *)
  nVar = Length[R]; Nr = nDeg;
  Pcoef = List[ConstantArray[0, nVar]]; Vcoef = List[1];
  W = w*IdentityMatrix[nVar];
  Rp = IdentityMatrix[nVar] - W.R.W;
  Pos = Table[KSubsets[Range[nVar], j], {j, nVar}];
  Val = Table[A = Pos[[j]]; Table[Re[Det[Rp[[A[[i]], A[[i]]]]]], {i, Length[A]}], {j, nVar}];

  (* AUX. ROUTINE: INTEGER SOLUTIONS OF l1 + 2 l2 +...+ k lk = n *)
  Sol[K_] := Module[{r, l},
    Clear[n];
    cond = Table[If[Apply[And, PossibleZeroQ[Val[[i]]]], n[i] == 0,
                n[i] >= 0], {i, 1, nVar}];
    r = Reduce[Join[{K == Sum[j n[j], {j, nVar}]}, cond], Table[n[i], {i, nVar}], Integers];
    l = List[ToRules[r]];
    Table[n[i], {i, nVar}] /. l];

  (* AUX. ROUTINE: COMPUTATION OF POLYNOMIAL Theta_n *)
  Polynomial[N_] := Module[{poly = 0},
    Y = Table[y[i], {i, nVar}];
    If [w == 1, Dr[1] := 1;, Clear[Dr];];
    Dr[r_] := (-1)^r Sum[Val[[r]][[m]] Product[Y[[Pos[[r]][[m]][[l]]]], {l, r}],
                         {m, Length[Val[[r]]]}];
    intSol = Sol[N];
    If[ArrayDepth[intSol] == 1, ,
      poly = (Gamma[Nr])^-1 Sum[Gamma[Nr + Total[intSol[[m]]]]
             Product[(-Dr[l])^intSol[[m]][[l]]/(intSol[[m]][[l]])!, {l, nVar}],
             {m, Length[intSol]}]]];

  (* GET COEFFICIENTS c^, defined under (2.4.23), FOR n=1:Nmax *)
  For[m = 1, m < Nmax + 1, m++,
    polym = Polynomial[m]; Clear[a, p, t];
    If[Length[polym] == 0, ,
      a = CoefficientRules[polym]; b = List[];
      For[k = 1, k < Length[a] + 1, k++,
        AppendTo[b, Sort[a[[k]][[1]], Greater] -> a[[k]][[2]]];];
      b = Sort[b]; p = b[[1]][[1]]; t = b[[1]][[2]];
      AppendTo[b, ConstantArray[0, nVar] -> 1];
      For[l = 2, l < Length[a] + 2, l++,
        If[b[[l]][[1]] == p, t = t + b[[l]][[2]];,
          AppendTo[Pcoef, p];
          AppendTo[Vcoef, t];
          t = b[[l]][[2]]; p = b[[l]][[1]];];];];]; {Pcoef, Vcoef}]
```

Appendix C

Derivations for the CDF of the $\eta - \mu$ Fading Distribution

C.1 Proof of Proposition 3

After making the change of variable $z = xt^2$ in (3.3.5), we can write

$$Y_{\mu}(x,0) = \frac{2^{\frac{1}{2}-\mu}\sqrt{\pi}\,(1-x^2)^{\mu}}{x^{2\mu}\Gamma(\mu)} \int_0^{\pm\infty} z^{\mu-\frac{1}{2}} e^{-\frac{z}{x}} I_{\mu-\frac{1}{2}}(z)\,dz, \tag{C.1.1}$$

where the sign of the upper integration limit is in accordance with the sign of x. Then, by making use of [18, eq. 5.7] we check that $Y_{\mu}(x,0) = 1$. From this fact, and considering the previous change of variable, we can express (3.3.5) as

$$\begin{aligned} Y_{\mu}(x,y) = 1 - \frac{2^{\frac{1}{2}-\mu}\sqrt{\pi}\,(1-x^2)^{\mu}}{x^{2\mu}\Gamma(\mu)} \\ \times \int_0^{xy^2} z^{\mu-\frac{1}{2}} e^{-\frac{z}{x}} I_{\mu-\frac{1}{2}}(z)\,dz. \end{aligned} \tag{C.1.2}$$

Denoting $p = xy^2$ and $q = 1/x$ and with the help of [51, eq. 29.3.50], we can rearrange the Laplace transform $\mathcal{L}[f(p);p,s] \doteq \int_0^{\infty} f(p)\,e^{-ps}dp$ of the integral in (C.1.2) in the

following form:

$$\begin{aligned}
&\mathcal{L}\left[\int_0^p z^{\mu-\frac{1}{2}}e^{-q\,z}I_{\mu-\frac{1}{2}}\left(z\right)dz;p,s\right]=\\
&\frac{2^{\mu-\frac{1}{2}}\Gamma(\mu)}{\sqrt{\pi}}\frac{1}{s\left(s+q+1\right)^{\mu}\left(s+q-1\right)^{\mu}}=\\
&\frac{2^{\mu-\frac{1}{2}}\Gamma(\mu)}{\sqrt{\pi}}\frac{1}{(q^2-1)^{\mu}}\frac{1}{s\left(1+\frac{s}{q+1}\right)^{\mu}\left(1+\frac{s}{q-1}\right)^{\mu}}=\\
&\frac{2^{\mu-\frac{1}{2}}\Gamma(\mu)}{\sqrt{\pi}}\frac{1}{(q^2-1)^{\mu}}\left\{\frac{(q^2-1)^{\mu}}{\Gamma\left(1+2\mu\right)}\right\}\\
&\times\left\{\frac{\Gamma\left(1+2\mu\right)}{s^{1+2\mu}}\right\}\left(1-\frac{(-(q+1))}{s}\right)^{-\mu}\left(1-\frac{(-(q-1))}{s}\right)^{-\mu}.
\end{aligned}\tag{C.1.3}$$

Identifying [44, eq. 3.43.1.4] with (C.1.3) and substituting in (C.1.2) we obtain the desired result.

C.2 Proof of Proposition 4

The result for an odd 2μ is obtained after identifying the ILHI, introduced in Definition 1 (see Section 2.3.3), with the integral in (C.1.2) and taking into account the sign of x. The result for an even 2μ is again obtained working out the integral in (C.1.2). First, [51, eq. 29.3.50] is used to represent the involved integral by an inverse Laplace transform

$$\begin{aligned}
&\mathcal{L}\left[\int_0^p z^{\mu-\frac{1}{2}}e^{-q\,z}I_{\mu-\frac{1}{2}}\left(z\right)dz;p,s\right]=\\
&\frac{2^{\mu-\frac{1}{2}}\Gamma(\mu)}{\sqrt{\pi}}\frac{1}{2\pi j}\int_{\varepsilon-j\infty}^{\varepsilon+j\infty}\frac{e^{sx}}{s\left(s+q+1\right)^{\mu}\left(s+q-1\right)^{\mu}}ds.
\end{aligned}\tag{C.2.1}$$

Then, since μ is a nonnegative integer in this case, we can use the well-known residue theorem and, after some tedious but straightforward algebra, the desired expression is obtained.

Appendix D

Incomplete Generalized MGF of the Hoyt Fading Distribution

D.1 Incomplete generalized MGF

Let us focus on the following generalization of the MGF.

Definition 3 (Incomplete Generalized MGF). *Let us consider a continuous random variable (RV) X with PDF $f_X(x)$. The Incomplete Generalized MGF (IG-MGF) of X, if it exists, is defined as*

$$\mathcal{G}_X(n, s; \zeta) = \int_{\zeta}^{\infty} x^n \, \mathrm{e}^{sx} \, f_X(x) \, dx,$$

where[1] *$s \in \mathbb{C}$, n is a nonnegative integer and $\zeta \in \mathbb{R}$ with $\zeta \geq 0$.*

Note that Definition 3 includes, as particular cases, several important statistical functions associated to the RV X: $\mathcal{G}_X(0, 0; \zeta)$ is the complementary cumulative distribution function (CDF); $\mathcal{G}_X(0, s; 0)$ is the MGF; $\mathcal{G}_X(0, s; \zeta)$ is the marginal MGF and $\mathcal{G}_X(n, s; 0)$ is the generalized MGF. To facilitate the analysis the following concepts are introduced.

Definition 4 (Complementary IG-MGF). *The complementary IG-MGF $\tilde{\mathcal{G}}_X(n, s; \zeta)$ of a RV X is (if it exists) $\tilde{\mathcal{G}}_X(n, s; \zeta) = \int_0^{\zeta} x^n \, \mathrm{e}^{sx} \, f_X(x) \, dx$.*

[1] *The variable s is only evaluated along the real line, however the complex domain is assumed here, in accordance with the usual definition of the MGF in the context of communications theory [1].*

The IG-MGF of squared Hoyt RVs has been found to be useful in the performance analysis of certain communication systems subject to co-channel interference (see Chapter 4). The next two sections are devoted to present original closed-form expressions for the IG-MGF of either a single squared Hoyt RV (Section D.2) or the sum of squared Hoyt variates (Section D.3).

D.2 Closed-form expression for IG-MGF of a squared Hoyt RV

For convenience, we start by defining a normalized squared Hoyt variate. Then, in order to obtain an expression for the IG-MGF, we will first derive a closed-form expression for the generalized MGF, i.e., $\mathcal{G}_X(n,s;0)$, followed by an expression for the complementary IG-MGF, and arriving at the final IG-MGF, which is obtained as the difference of the two previous expressions.

Definition 5 (Normalized Squared Hoyt RV). *For a given RV $X = Y^2$ with mean $E[X] = \Omega_X$, where Y is Hoyt distributed with parameter q, we define a 'normalized' squared Hoyt RV as $\langle X \rangle \doteq \frac{1-q^4}{4q^2\Omega_X} X$.*

Some useful properties of the distribution of a squared Hoyt RV regarding the existence of its generalized MGF are summarized in the following Lemma.

Lemma 3. *Let us consider a squared Hoyt RV X with mean $E[X] = \Omega_X$ and Hoyt parameter q. Sufficient conditions for the existence of the statistical functions $\mathcal{G}_X(n,s;\zeta)$, $\tilde{\mathcal{G}}_X(n,s;\zeta)$, $\mathcal{G}_{\langle X\rangle}(n,s;\zeta)$ and $\tilde{\mathcal{G}}_{\langle X\rangle}(n,s;\zeta)$ are: $n \geq 0$ and $\Re\{s\} < \frac{2q^2}{1-q^2}$. In such a case, the following equalities hold*

$$\begin{cases} \mathcal{G}_X(n,s;\zeta) = \left(\dfrac{4q^2\Omega_X}{1-q^4}\right)^n \mathcal{G}_{\langle X\rangle}\left(n, \frac{4sq^2\Omega_X}{1-q^4}; \frac{1-q^4}{4q^2\Omega_X}\zeta\right) \\ \tilde{\mathcal{G}}_{\langle X\rangle}(n,s;\zeta) + \mathcal{G}_{\langle X\rangle}(n,s;\zeta) = \dfrac{2q(n!)}{1-q^2}\,\bar{\alpha}(s)^{n+1} P_n\left(\alpha(s)\,\bar{\alpha}(s)\right) \end{cases}, \tag{D.2.1}$$

where $\alpha(s) \doteq \frac{1+q^2}{1-q^2} - s$, $\bar{\alpha}(s) \doteq \frac{1}{\sqrt{\alpha(s)^2-1}}$ and P_n is the Legendre polynomial of degree n.

Proof. Since the integrands involving $\tilde{\mathcal{G}}_X(n,s;\zeta)$ and $\tilde{\mathcal{G}}_{\langle X\rangle}(n,s;\zeta)$ are bounded and continuous for $n \geq 0$, both exist under this assumption. Also, $\mathcal{G}_X(n,s;\zeta)$ exists if $\mathcal{G}_{\langle X\rangle}(n,s;\zeta)$ does and, considering [41, eq. 6.624-5], this occurs when $n \geq 0$ and $\Re\{s\} < \frac{2q^2}{1-q^2}$. The

first equality in (D.2.1) is obtained by the change of variable $\langle X\rangle = \frac{1-q^4}{4q^2\Omega_X}X$ and the second equality is straightforward by [41, eq. 6.624-5] after some simple algebraic manipulations. □

Note that the second equality in (D.2.1) corresponds to the generalized MGF of a squared Hoyt RV, i.e. $\tilde{\mathcal{G}}_{\langle \mathrm{X}\rangle}(n,s;\zeta) + \mathcal{G}_{\langle \mathrm{X}\rangle}(n,s;\zeta) = \mathcal{G}_{\langle \mathrm{X}\rangle}(n,s;0)$. Now, we express $\tilde{\mathcal{G}}_{\langle X\rangle}(n,s;\zeta)$ in closed-form by the following Proposition.

Proposition 5. *Let us consider a squared Hoyt RV X with $E[X] = \Omega_X$ and Hoyt parameter q. Then, if $n \geq 0$ and $\Re\{s\} < \frac{2q^2}{1-q^2}$, the complementary IG-MGF of $\langle X\rangle$ is given by*

$$\begin{aligned}\tilde{\mathcal{G}}_{\langle X\rangle}(n,s;\zeta) = \frac{2q}{1-q^2}\Big\{ & A_n(s) \\ & + B_n(s)\, Q\left(\tfrac{\sqrt{\zeta}}{\sqrt{\alpha(s)+\bar{\alpha}(s)^{-1}}}, \sqrt{\zeta}\sqrt{\alpha(s)+\bar{\alpha}(s)^{-1}}\right) \\ & + \mathrm{e}^{-\alpha(s)\zeta}\sum_{\ell=0}^{n}\left[C_n^{\ell}(s)\, I_0(\zeta) + D_n^{\ell}(s)\, I_1(\zeta)\right]\zeta^{\ell}\Big\},\end{aligned} \tag{D.2.2}$$

where Q is the Marcum Q function, I_1 is the first order modified Bessel function and, $A_n(s)$, $B_n(s)$, $C_n^{\ell}(s)$ and $D_n^{\ell}(s)$ are obtained recursively in a finite number of steps as follows:

$$\underline{n=0}\begin{cases} A_0(s) = \bar{\alpha}, \\ B_0(s) = -2\bar{\alpha}, \\ C_0^0(s) = \bar{\alpha}, \\ D_0^0(s) = 0, \end{cases} \qquad \underline{n=1}\begin{cases} A_1(s) = \alpha\bar{\alpha}^3, \\ B_1(s) = -2\alpha\bar{\alpha}^3, \\ C_1^0(s) = \alpha\bar{\alpha}^3, \\ C_1^1(s) = -\alpha\bar{\alpha}^2, \\ D_1^0(s) = 0, \\ D_1^1(s) = -\bar{\alpha}^2, \end{cases}$$

$$\begin{aligned} &\underline{n \geqslant 2} \\ &A_n(s) = (2n-1)\alpha\bar{\alpha}^2 A_{n-1} - (n-1)^2\bar{\alpha}^2 A_{n-2}, \\ &B_n(s) = (2n-1)\alpha\bar{\alpha}^2 B_{n-1} - (n-1)^2\bar{\alpha}^2 B_{n-2}, \end{aligned} \tag{D.2.3}$$

$$C_n^{\ell}(s) = \begin{cases} (2n-1)\alpha\bar{\alpha}^2 C_{n-1}^{\ell} - (n-1)^2\bar{\alpha}^2 C_{n-2}^{\ell} \\ \qquad \textit{for } 0 \leqslant \ell = n-2, \\ (2n-1)\alpha\bar{\alpha}^2 C_{n-1}^{n-1} + (n-1)\bar{\alpha}^2 \\ \qquad \textit{for } \ell = n-1, \\ -\alpha\bar{\alpha}^2 \quad \textit{for } \ell = n, \end{cases}$$

$$D_n^{\ell}(s) = \begin{cases} (2n-1)\alpha\bar{\alpha}^2 D_{n-1}^{\ell} - (n-1)^2\bar{\alpha}^2 D_{n-2}^{\ell} \\ \qquad \textit{for } 0 \leqslant \ell = n-2, \\ (2n-1)\alpha\bar{\alpha}^2 D_{n-1}^{n-1} \textit{ for } \ell = n-1, \\ -\bar{\alpha}^2 \qquad \textit{for } \ell = n. \end{cases}$$

The functions $\alpha(s)$ and $\bar{\alpha}(s)$ are defined as in Lemma 3.

Proof. The result in this proposition can be obtained by simplifying the general equations derived in [20]. Alternatively, a direct proof is carried out by induction over n whose key steps are as follows. For $n = 1$ the identity [18, eq. 5.7] obtained by Agrest and Maksimov is used. The case $n = 2$ is proved by considering a straightforward modification of the Sonine identity [49, pp. 132] for $I_\nu(t)$, and then particularizing for $\nu = 0$ and $f(t) = \exp(-\alpha t)$. Finally, the general case $n = k \geq 2$ follows from Luke's recursive formulas [50, pp. 120, eq. 5]. □

Finally, by taking Proposition 5 and Lemma 3 into account, we obtain a closed-form expression for $\mathcal{G}_X(n, s; \zeta)$, i.e., the IG-MGF of a squared Hoyt RV.

Corollary 2. *Under the conditions of Lemma 3 and Proposition 5, the IG-MGF of the squared Hoyt RV X is given by*

$$\begin{aligned}\mathcal{G}_X(n,s;\zeta) = \left(\frac{4q^2\Omega_X}{1-q^4}\right)^n \Bigg\{ & \frac{2q(n!)}{1-q^2}\,\bar{\alpha}\left(\tfrac{4sq^2\Omega_X}{1-q^4}\right)^{n+1} \\ & P_n\left(\alpha\left(\tfrac{4sq^2\Omega_X}{1-q^4}\right)\bar{\alpha}\left(\tfrac{4sq^2\Omega_X}{1-q^4}\right)\right) \\ & -\tilde{\mathcal{G}}_{\langle X\rangle}\left(n, \tfrac{4sq^2\Omega_X}{1-q^4}; \tfrac{1-q^4}{4q^2\Omega_X}\zeta\right) \Bigg\},\end{aligned} \tag{D.2.4}$$

where $\tilde{\mathcal{G}}_{\langle X\rangle}(n, s; \zeta)$ is given in (D.2.2).

D.3 Closed-form expression for IG-MGF of the sum of squared Hoyt variates

Let us focus on the following RV $X = \sum_{i=1}^{L} Y_i^2$, where Y_i^2, $i = 1, ..., L$, are independent and identically distributed (i.i.d.) squared Hoyt variates with parameter q and mean $\Omega = \mathtt{E}[Y_i^2]$. The RV X with mean $\Omega_X = L\Omega$ is the sum of L i.i.d. squared Hoyt variates and its PDF is given by

$$f_X(x) = \frac{\sqrt{\pi}}{\Gamma\left(\frac{L}{2}\right) q(1-q^2)^{\frac{L-1}{2}}\Omega L}\left(\frac{L(1+q^2)}{2}\right)^{\frac{L+1}{2}}\left(\frac{x}{\Omega L}\right)^{\frac{L-1}{2}}\exp\left(-\tfrac{(1+q^2)^2}{4q^2}\tfrac{x}{\Omega}\right) I_{\frac{L-1}{2}}\left(\tfrac{(1-q^4)}{4q^2}\tfrac{x}{\Omega}\right), \tag{D.3.1}$$

where $\Gamma(\cdot)$ is the gamma function and $I_\nu(\cdot)$ is the ν-th order modified Bessel function.

Now, in order to obtain the IG-MGF of X in closed-form, we start by deriving an expression for the generalized MGF, i.e., $\mathcal{G}_X(n, s; 0)$, followed by another expression for the complementary IG-MGF, $\tilde{\mathcal{G}}_X(n, s; \zeta)$, and arriving at the final IG-MGF which is written as the difference of the two previous expressions.

Lemma 4. *Let us consider a RV X with mean $E[X] = \Omega_X = L\Omega$, which is the sum of L i.i.d. squared Hoyt variates with mean Ω and Hoyt parameter q. Then, the following expressions for the generalized MGF of X, $\mathcal{G}_X(n,s;0) = \mathcal{G}_X(n,s;\zeta) + \tilde{\mathcal{G}}_X(n,s;\zeta)$, hold for even and odd values of L. On the one hand, for even values of L, the generalized MGF of X is given by*

$$\mathcal{G}_X(n,s;0) = \left(\frac{(1+q^2)}{2\Omega(1-q^2)}\right)^{\frac{L}{2}} \sum_{k=0}^{\frac{L}{2}-1} \binom{\frac{L}{2}-1+k}{k} \frac{\left(\frac{L}{2}-1-k+n\right)!}{\left(\frac{L}{2}-1-k\right)!\left(\frac{(1-q^4)}{2q^2\Omega}\right)^k} \left(\frac{(-1)^k}{(c_2-s)^{-k+\frac{L}{2}+n}} + \frac{(-1)^{\frac{L}{2}}}{(c_1-s)^{-k+\frac{L}{2}+n}}\right), \tag{D.3.2}$$

where $\binom{\cdot}{\cdot}$ is the binomial coefficient, $c_1 = \frac{q^2+1}{2q^2\Omega}$, and $c_2 = \frac{q^2+1}{2\Omega}$.

On the other hand, for odd values of L, the generalized MGF of X is given by

$$\mathcal{G}_X(n,s;0) = \frac{\sqrt{\pi}}{\Gamma\left(\frac{L}{2}\right) 2^{-\left(\frac{L+1}{2}+n\right)} q^{-(L+2n)} (1-q^2)^{L+n}} \left(\frac{(1+q^2)}{2\Omega}\right)^{-n} \frac{\Gamma(L+n)}{(c_3^2-1)^{\frac{-1}{2}\left(\frac{L+1}{2}+n\right)}} P_{n+(L-1)/2}^{-(L-1)/2}(c_3), \tag{D.3.3}$$

where $P_a^b(\cdot)$ is the associated Legendre polynomial [41, (8.7)], and $c_3 = \frac{\left(q^2+1\right)^2 - 4sq^2\Omega}{2q\sqrt{4s^2q^2\Omega^2 - 2s(q^2+1)^2\Omega + (q^2+1)^2}}$.

Proof. The two expressions for $\mathcal{G}_X(n,s;0) = \int_0^\infty x^n \, \mathrm{e}^{sx} \, f_X(x) \, dx$, with $f_X(x)$ given in (D.3.1), are obtained after taking into account [41, eq. 8.467] and [41, eq. 6.624-5] for the cases of even and odd values of L, respectively, and straightforward algebraic manipulations. □

Now, we express $\tilde{\mathcal{G}}_X(n,s;\zeta)$ in closed-form by the following Proposition.

Proposition 6. *Let us consider a RV X with mean $E[X] = \Omega_X = L\Omega$, which is the sum of L i.i.d. squared Hoyt variates with mean Ω and Hoyt parameter q. Then, the complementary IG-MGF of X is given by*

$$\tilde{\mathcal{G}}_X(n,s;\zeta) = \frac{\zeta^{L+n}(-1)^n (c_1c_2)^{\frac{L}{2}}}{\Gamma(L+n+1)} \sum_{k=0}^{n} \binom{n}{k} \left(\frac{-L}{2}-k+1\right)_k \left(\frac{-L}{2}-n+k+1\right)_{n-k} \Phi_2^{(2)}\left[\frac{L}{2}+k, \frac{L}{2}+n-k; L+n+1; (c_1+s)\zeta, (c_2+s)\zeta\right], \tag{D.3.4}$$

where $(\cdot)_a$ is the pochhammer symbol, $\Phi_2^{(2)}$ is the confluent Lauricella function, defined in (2.3.21), $c_1 = -\frac{q^2+1}{2q^2\Omega}$, and $c_2 = -\frac{q^2+1}{2\Omega}$.

Proof. The expression for $\tilde{\mathcal{G}}_X(n,s;\zeta)$ is obtained on the basis of the following rearrangement of its Laplace transform

$$\mathcal{L}\left[\tilde{G}_X(a,b;t);t,s\right] = \frac{1}{s}\mathcal{L}\left[t^a \mathrm{e}^{bt} f_X(t);s\right] = \frac{1}{s}(-1)^a \frac{d^a}{ds^a}\left[\mathcal{L}\left[f_X(t);s-b\right]\right]. \tag{D.3.5}$$

Then, $\mathcal{L}\left[f_X(t);s-b\right]$ is replaced by the MGF of X evaluated at $s-b$, and after some algebraic manipulations, we arrive at the following expression

$$\begin{aligned}\mathcal{L}\left[\tilde{G}_X(a,b;t);t,s\right] = \frac{(c_1c_2)^{\frac{L}{2}}}{s^{L+a+1}}(-1)^a \sum_{k=0}^{a}\binom{a}{k}\left(\frac{-L}{2}-k+1\right)_k \\ \left(\frac{-L}{2}-a+k+1\right)_{a-k}\left(1-\frac{c_1+b}{s}\right)^{\frac{-L}{2}-k}\left(1-\frac{c_2+b}{s}\right)^{\frac{-L}{2}-a+k},\end{aligned} \tag{D.3.6}$$

with c_1 and c_2 as defined in Proposition 6. Finally, the expression for the IG-MGF of X is obtained after identifying (D.3.6) with (2.3.22). □

Finally, by taking Proposition 6 and Lemma 4 into account, we obtain a closed-form expression for $\mathcal{G}_X(n,s;\zeta)$, i.e., the IG-MGF of the sum of L i.i.d. squared Hoyt variates.

Corollary 3. *Under the conditions of Lemma 4 and Proposition 6, the IG-MGF of the sum of L i.i.d. squared Hoyt RVs is given by*

$$\mathcal{G}_X(n,s;\zeta) = \mathcal{G}_X(n,s;0) - \tilde{\mathcal{G}}_X(n,s;\zeta), \tag{D.3.7}$$

where $\tilde{\mathcal{G}}_X(n,s;\zeta)$ is given in (D.3.4) and $\mathcal{G}_X(n,s;0)$ is given in (D.3.2) and (D.3.3) for even and odd values of L, respectively.

Appendix E

Resumen en Castellano

E.1 Introducción y motivación

Los sistemas basados en múltiples antenas han sido utilizados durante mucho tiempo para mitigar los efectos de los desvanecimientos en comunicaciones inalámbricas. Las técnicas de diversidad de recepción suelen aplicarse en sistemas con una sola antena transmisora y múltiples antenas receptoras, también conocidos como sistemas SIMO (*single-input multiple-output*). Estas técnicas realizan una cierta combinación de las señales recibidas, de forma que se obtiene un cierto incremento de la relación señal a ruido (SNR, *signal-to-noise power ratio*) proporcionada por la diversidad espacial. La estrategia de combinación óptima en términos de maximizar la SNR a la salida del combinador es MRC (*maximum ratio combining*), que requiere un conocimiento perfecto del canal en el receptor. Otras estrategias de combinación subóptimas, que dan lugar a receptores menos complejos, han sido propuestas en la bibliografía: *equal gain combining* (EGC), donde las señales recibidas se suman, o *selection combining* (SC), donde se selecciona la señal recibida con máxima SNR. Por otra parte, las estrategias del tipo *Switched Diversity* tales como SSC (*switch-and-stay combining*) o SEC(*switch-and-examine combining*) son más simples de implementar que MRC, EGC, o SC y, por tanto, se utilizan frecuentemente en receptores prácticos limitados en cuanto a complejidad. Una descripción completa de estos sistemas puede encontrarse en [1, ch. 9].

Sin embargo, el rendimiento de los sistemas SIMO se ve a menudo degradado por ciertas limitaciones prácticas o no-idealidades como son las interferencias co-canal o el empleo de señalización no-ortogonal. Así pues, incluir estas limitaciones en el análisis de rendimiento de estos sistemas resulta especialmente interesante, especialmente desde el punto de vista del diseño de sistemas prácticos (reales). Por un lado, es bien conocido que MRC es la técnica de combinación óptima en ausencia de interferencias. Sin embargo, determinar la combinación óptima en presencia de señales interferentes resulta mucho más complicado, ya que requeriría información acerca de las interferencias que normalmente no está disponible. En la práctica se emplea MRC aun en presencia de interferencias co-canal y, por ello, es particularmente interesante analizar el rendimiento bajo esta limitación. Por otro lado, la modulación y detección no-coherente, de complejidad reducida, suele adoptarse en sistemas prácticos de diversidad en recepción (p.ej., SEC o SSC). En estos casos, las señales transmitidas pueden ser no-ortogonales con el fin de reducir el ancho de banda utilizado, produciéndose una cierta degradación del rendimiento [3, ch. 5]. Esta no-ortogonalidad puede verse como una limitación práctica de este tipo de sistemas.

Recientemente, las cada vez más sofisticadas aplicaciones han propiciado la aparición de los sistemas MIMO (*multiple-input multiple-output*), que desempeñan un papel fundamental para satisfacer la demanda de capacidad y cobertura [4–6]. Estos sistemas pueden combinar el uso de técnicas de codificación espacio-tiempo (STBC) en el transmisor y técnicas de diversidad en recepción, tales como SC o MRC [7–9]. Cuando se dispone de información del canal en el transmisor, otros esquemas más sofisticados pueden emplearse para mejorar el rendimiento. El sistema MIMO *beamforming*, también conocido como MIMO MRC, maximiza la relación señal a ruido aplicando los pesos MRC conjuntamente en el transmisor y en el receptor [10–12]. Sin embargo, el rendimiento de estos sistemas se ve a menudo degradado por ciertas limitaciones prácticas como la correlación entre antenas, que reduce la diversidad espacial, o el canal de retorno de capacidad limitada, ante el cual suelen adoptarse esquemas *beamforming* basados en *codebook*.

El principal objetivo de esta tesis es abordar el análisis de rendimiento de diferentes sistemas SIMO y MIMO en canales con desvanecimiento y en presencia de las condiciones prácticas (no-ideales) mencionadas. Las herramientas matemáticas existentes son

en algunos casos insuficientes para llevar acabo dicho análisis. En otros casos, las herramientas matemáticas disponibles dan lugar a un análisis muy limitado o a resultados (expresiones) intratables desde el punto de vista matemático. A menudo, es difícil establecer conclusiones sobre el rendimiento del sistema a partir de estos resultados, cuya evaluación numérica suele ser complicada. Así pues, la motivación de esta tesis es doble: por un lado, encontrar y/o desarrollar nuevas herramientas matemáticas que posibiliten o simplifiquen el análisis de estos sistemas; por otro lado, analizar el rendimiento de estos sistemas en términos de las medidas más utilizadas, la probabilidad de *outage* (OP, *outage probability*) y la probabilidad de error de bit (BEP, *bit error probability*), tratando de llegar a expresiones cerradas y exactas para estas medidas.

E.2 Análisis de rendimiento de sistemas SIMO no-ideales

El análisis de sistemas SIMO bajo las condiciones no-ideales mencionadas conlleva la aparición de ciertas integrales incompletas que recientemente han sido resueltas de forma explícita en [20]. Estas integrales contienen en su integrando a las funciones de Bessel y Marcum Q, y son conocidas como integrales de Lipschitz-Hankel incompletas (ILHIs) e integrales incompletas de funciones Marcum Q (IIMQ), respectivamente.

En particular, este tipo de integrales aparecen en el análisis de la BEP para sistemas *Switched Diversity*, tales como SSC o SEC, cuando se emplea detección no-coherente o diferencialmente coherente de señales no-ortogonales. Por otro lado, el mismo tipo de integrales aparece en el análisis de la OP de sistemas MRC con interferencias co-canal cuando se consideran canales Nakagami-q (Hoyt). Sin embargo, no existen expresiones cerradas resultantes del análisis de estos sistemas debido a la ausencia de soluciones explícitas para este tipo de integrales [21, 22]. Por ello, y con la motivación de los resultados recientemente obtenidos en [20] para estas integrales, nos hemos centrado en la aplicación de estos resultados al análisis de los sistemas mencionados. Las integrales del tipo ILHI e IIMQ han sido presentadas en el Capítulo 2, donde se proporcionan las expresiones explícitas para sus soluciones (véase la Sección 2.3.3). Estas expresiones han posibilitado la obtención de determinadas funciones estadísticas para la caracterización de canales con desvanecimientos Hoyt.

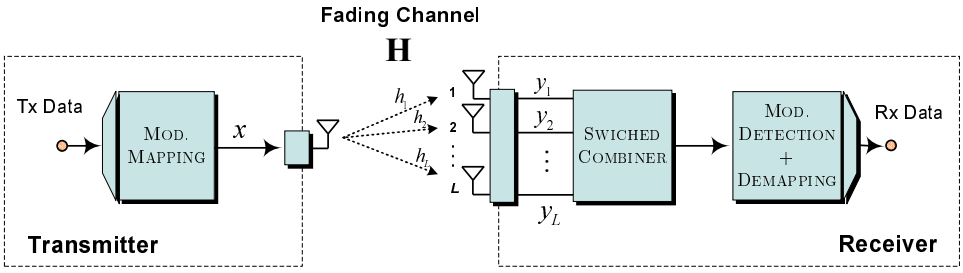

Figure E.1: Modelo de sistema *Switched Diversity*.

En esta sección se presentan brevemente los sistemas considerados y los principales resultados obtenidos en el análisis. En primer lugar se presenta el análisis en términos de BEP de sistemas *Switched Diversity* que emplean señalización no-ortogonal y detección no-coherente en canales Nakagami-m. Posteriormente se analiza la probabilidad de *outage* de sistemas MRC en presencia de interferencias co-canal en canales Hoyt.

E.2.1 Sistemas *Switched Diversity* con señalización no-ortogonal

El análisis de esta sección extiende los resultados obtenidos en [39], proporcionando una generalización en 3 sentidos: primero, un número general de antenas L; segundo, se considera el modelo de canal Nakagami-m, más general que el modelo Rayleigh; y tercero, el análisis incluye otros esquemas de modulación tales como DQPSK (*differential quadrature phase shift keying*).

Modelo de sistema

Asumimos un sistema *Switched Diversity* con L antenas como el que se representa en la Figura E.1. En concreto, nos centramos en un sistema con configuración SEC. En este caso, la función densidad de probabilidad (PDF) de la SNR instantánea a la salida del combinador γ_S viene dada por [1, eq. (9.341)]

$$f_{\gamma_S}(x) = \begin{cases} [F_\gamma(\gamma_T)]^{L-1} f_\gamma(x), & 0 \leqslant x < \gamma_T \\ \sum_{\ell=0}^{L-1} [F_\gamma(\gamma_T)]^\ell f_\gamma(x), & x \geqslant \gamma_T \end{cases}, \tag{E.2.1}$$

donde f_γ y F_γ son la PDF y la CDF (*cumulative distribution function*) de la SNR instantánea γ en cada antena receptora, mientras que γ_T es el umbral de conmutación definido.

Table E.1: Parámetros para distintas modulaciones no-coherentes y diferencialmente coherentes.

	Orthogonal Binary Signals	Nonorthogonal Binary Signals*	DPSK	DQPSK
a	0	$\left(\frac{1-\sqrt{1-\rho^2}}{2}\right)^{1/2}$	0	$\left(1-\frac{1}{\sqrt{2}}\right)^{1/2}$
b	1	$\left(\frac{1+\sqrt{1-\rho^2}}{2}\right)^{1/2}$	$\sqrt{2}$	$\left(1+\frac{1}{\sqrt{2}}\right)^{1/2}$
η	1	1	1	1

* donde $0 \leq \rho \leq 1$ es el módulo de la correlación entre las dos señales transmitidas.

Consideramos el modelo de desvanecimientos Nakagami-m para la señal transmitida. Así, $F_\gamma(\gamma_T)$ y $f_\gamma(x)$ en (E.2.1) vienen dadas por [1, table (9.5)] [41, eq. (8.352-2)]

$$F_\gamma(\gamma_T) = 1 - e^{-\frac{m}{\bar{\gamma}}\gamma_T} \sum_{\ell=0}^{m-1} \frac{\gamma_T^\ell}{(\ell)!} \left(\frac{m}{\bar{\gamma}}\right)^\ell \tag{E.2.2}$$

y

$$f_\gamma(x) = \left(\frac{m}{\bar{\gamma}}\right)^m \frac{x^{m-1}}{(m-1)!} e^{-m\frac{x}{\bar{\gamma}}} \quad , \tag{E.2.3}$$

donde $\bar{\gamma}$ es la SNR media por símbolo en cada antena receptora.

Análisis de la probabilidad de error

Dada la BEP condicional $P_b(x) \triangleq \Pr\{\text{biterror} \,|\gamma_S = x\}$ y la PDF de la SNR a la salida del combinador f_{γ_S}, la BEP media para el sistema SEC considerado se calcula como

$$\bar{P}_b = \int_0^\infty P_b(x) f_{\gamma_S}(x)\, dx. \tag{E.2.4}$$

La BEP condicional cuando se emplean modulaciones no-coherentes y diferencialmente coherentes puede expresarse como [56, eq. (4B.21)]

$$P_b(x) = Q_1\left(a\sqrt{x}, b\sqrt{x}\right) - \frac{\eta}{1+\eta} e^{-\frac{a^2+b^2}{2}x} I_0(abx), \tag{E.2.5}$$

donde Q_1 es la función Marcum Q de primer orden, I_0 es la función de Bessel modificada de orden cero, y a, b and η son parámetros dependientes de la modulación. Algunos casos

de modulaciones de especial importancia y sus correspondientes parámetros se especifican en la Tabla E.1.

Sustituyendo (E.2.5) y (E.2.1) en (E.2.4) y, tras realizar algunas simplificaciones, se obtiene la siguiente expresión genérica para la BEP media

$$\begin{aligned}\bar{P}_b = {} & \alpha_{L,m}\left(\gamma_T;\bar{\gamma}\right)\left[\mathcal{I}_1\left(a,b,\bar{\gamma},m\right)-\frac{\eta}{1+\eta}\mathcal{I}_2\left(a,b,\bar{\gamma},m\right)\right] \\ & -\alpha_{L-1,m}\left(\gamma_T;\bar{\gamma}\right)\left[\mathcal{J}_1\left(\gamma_T;a,b,\bar{\gamma},m\right)-\frac{\eta}{1+\eta}\mathcal{J}_2\left(\gamma_T;a,b,\bar{\gamma},m\right)\right],\end{aligned} \tag{E.2.6}$$

donde $\alpha_{L,m}\left(\gamma_T;\bar{\gamma}\right)$ son coeficientes conocidos, definidos como

$$\alpha_{L,m}\left(\gamma_T;\bar{\gamma}\right) \triangleq \frac{\left(\frac{m}{\bar{\gamma}}\right)^m}{(m-1)!}\left[\frac{1-\left[F_\gamma\left(\gamma_T\right)\right]^L}{1-F_\gamma\left(\gamma_T\right)}\right], \tag{E.2.7}$$

con $F_\gamma\left(\gamma_T\right)$ dada en (E.2.2) y donde $\mathcal{I}_1$, $\mathcal{I}_2$, $\mathcal{J}_1$, $\mathcal{J}_2$ son integrales definidas por

$$\begin{cases}\mathcal{I}_1\left(a,b,\bar{\gamma},m\right) \triangleq \displaystyle\int_0^\infty x^{m-1}e^{-\frac{m}{\bar{\gamma}}x}Q_1\left(a\sqrt{x},b\sqrt{x}\right)dx \\ \mathcal{I}_2\left(a,b,\bar{\gamma},m\right) \triangleq \displaystyle\int_0^\infty x^{m-1}e^{-\left[\frac{m}{\bar{\gamma}}+\frac{a^2+b^2}{2}\right]x}I_0\left(abx\right)dx \\ \mathcal{J}_1\left(\gamma_T;a,b,\bar{\gamma},m\right) \triangleq \displaystyle\int_0^{\gamma_T} x^{m-1}e^{-\frac{m}{\bar{\gamma}}x}Q_1\left(a\sqrt{x},b\sqrt{x}\right)dx \\ \mathcal{J}_2\left(\gamma_T;a,b,\bar{\gamma},m\right) \triangleq \displaystyle\int_0^{\gamma_T} x^{m-1}e^{-\left[\frac{m}{\bar{\gamma}}+\frac{a^2+b^2}{2}\right]x}I_0\left(abx\right)dx\end{cases} \tag{E.2.8}$$

Para completar el análisis, falta obtener expresiones cerradas y exactas para $\mathcal{I}_1$, $\mathcal{I}_2$, $\mathcal{J}_1$ y $\mathcal{J}_2$. Las integrales completas $\mathcal{I}_1$ y $\mathcal{I}_2$ aparecen frecuentemente en el análisis de modulaciones no-coherentes y han sido estudiadas en [53, 54]. En [53] se proporciona una expresión para $\mathcal{I}_1$ en términos de la función hipergeométrica de Gauss. Esta función hipergeométrica puede expresarse a su vez en términos de los polinomios de Legendre, sin más que aplicar [51, eq. 15.4.10], y las relaciones [41, eq. 8.731-4] y [41, eq. 8.914-1]. De este modo, la solución explícita de $\mathcal{I}_1$ puede escribirse como

$$\begin{aligned}\mathcal{I}_1\left(a,b,\bar{\gamma},m\right) = {} & (m-1)!\left(\frac{\bar{\gamma}}{m}\right)^m \\ & \times\left\{1+\frac{b^2}{c_1}\sum_{\ell=0}^{m-1}\frac{\left(\frac{\ell+1}{2\ell+1}\right)\left(\frac{2m}{\bar{\gamma}c_1\sqrt{1-c_2}}\right)^\ell}{\left(\frac{c_1}{2b^2}-1\right)^{-1}}\left[P_{\ell+1}\left(\frac{1}{\sqrt{1-c_2}}\right)-\left(1+\frac{\left(\frac{c_1}{2b^2}-1\right)^{-1}}{\left(\frac{\ell+1}{2\ell+1}\right)}\right)P_{\ell-1}\left(\frac{1}{\sqrt{1-c_2}}\right)\right]\right\}.\end{aligned} \tag{E.2.9}$$

donde $c_1 \triangleq a^2+b^2+2\frac{m}{\bar{\gamma}}$, $c_2 \triangleq \frac{4a^2b^2}{c_1^2}$, y $P_n(\cdot)$ es el polinomio de Legendre de grado n.

Tras un simple re-escalado, $\mathcal{I}_2$ puede expresarse también en términos de los polinomios de Legendre como [41, eq. 6.624-5]

$$\mathcal{I}_2\left(a,b,\bar{\gamma},m\right)=\frac{(m-1)!}{(ab)^m}\left(\frac{c_2}{1-c_2}\right)^{\frac{m}{2}}P_{m-1}\left(\frac{1}{\sqrt{1-c_2}}\right). \tag{E.2.10}$$

Las integrales $\mathcal{J}_1$ and $\mathcal{J}_2$ pertenecen a las familias de integrales IIMQ e ILHI, respectivamente, cuyas definiciones y expresiones cerradas pueden encontrarse en la Sección 2.3.3. En esa misma sección, se muestra el modo de expresar las IIMQ en términos de las ILHI. Así pues, $\mathcal{J}_1$ y $\mathcal{J}_2$ pueden ser expresadas en términos de la ILHI tras un cierto re-escalado y algunas simplificaciones, quedando

$$\begin{aligned}\mathcal{J}_1\left(\gamma_T;a,b,\bar{\gamma},m\right)=(m-1)!\left(\frac{\bar{\gamma}}{m}\right)^m\Bigg\{1-e^{-\frac{m}{\bar{\gamma}}\gamma_T}Q_1\left(a\sqrt{\gamma_T},b\sqrt{\gamma_T}\right)\sum_{\ell=0}^{m-1}\frac{\left(\frac{m}{\bar{\gamma}}\right)^\ell}{\ell!}\gamma_T^\ell\\ +\frac{1}{2}\sum_{\ell=0}^{m-1}\frac{\left(\frac{m}{\bar{\gamma}}\right)^\ell}{\ell!}\frac{1}{(ab)^\ell}\left(I_{e_{\ell,1}}\left(ab\gamma_T;\frac{1}{\sqrt{c_2}}\right)-\frac{b}{a}I_{e_{\ell,0}}\left(ab\gamma_T;\frac{1}{\sqrt{c_2}}\right)\right)\Bigg\},\end{aligned} \tag{E.2.11}$$

y

$$\mathcal{J}_2\left(\gamma_T;a,b,\bar{\gamma},m\right)=\frac{1}{(ab)^m}I_{e_{m-1,0}}\left(ab\gamma_T;\frac{1}{\sqrt{c_2}}\right), \tag{E.2.12}$$

donde $I_{e_{r,k}}$ es la ILHI, cuya expresión explícita en términos de las funciones Marcum Q y Bessel puede encontrarse en la Proposición 1 de la Sección 2.3.3.

Finalmente, la expresión de la BEP media se obtiene sustituyendo las expresiones (E.2.9), (E.2.10), (E.2.11), y (E.2.12) para $\mathcal{I}_1$, $\mathcal{I}_2$, $\mathcal{J}_1$, y $\mathcal{J}_2$, respectivamente, en (E.2.6), resultando:

$$\bar{P}_b = \alpha_{L,m}\left(\gamma_T;\bar{\gamma}\right)\left[(m-1)!\left(\frac{\bar{\gamma}}{m}\right)^m\left\{1+\left(\frac{1}{2}-\frac{b^2}{c_1}\right)\sum_{\ell=0}^{m-1}\left(\frac{\ell+1}{2\ell+1}\right)\left(\frac{2m}{\bar{\gamma}c_1\sqrt{1-c_2}}\right)^{\ell}\right.\right.$$
$$\left.\left.\times\left[P_{\ell+1}\left(\frac{1}{\sqrt{1-c_2}}\right)-\left(1+\frac{1}{\left(\frac{\ell+1}{2\ell+1}\right)\left(\frac{c_1}{2b^2}-1\right)}\right)P_{\ell-1}\left(\frac{1}{\sqrt{1-c_2}}\right)\right]\right\}\right.$$
$$\left.-\frac{\eta}{1+\eta}\frac{(m-1)!}{(ab)^m}\left(\frac{c_2}{1-c_2}\right)^{\frac{m}{2}}P_{m-1}\left(\frac{1}{\sqrt{1-c_2}}\right)\right]$$
$$-\alpha_{L-1,m}\left(\gamma_T;\bar{\gamma}\right)\left[(m-1)!\left(\frac{\bar{\gamma}}{m}\right)^m\left\{1-e^{-\frac{m}{\bar{\gamma}}\gamma_T}Q_1\left(a\sqrt{\gamma_T},b\sqrt{\gamma_T}\right)\sum_{\ell=0}^{m-1}\frac{m^\ell}{\ell!}\left(\frac{\gamma_T}{\bar{\gamma}}\right)^{\ell}\right.\right.$$
$$\left.\left.+\frac{1}{2}\sum_{\ell=0}^{m-1}\frac{m^\ell}{\ell!}\frac{1}{(ab\bar{\gamma})^\ell}\left(I_{e_{\ell,1}}\left(ab\gamma_T;\frac{1}{\sqrt{c_2}}\right)-\frac{b}{a}I_{e_{\ell,0}}\left(ab\gamma_T;\frac{1}{\sqrt{c_2}}\right)\right)\right\}\right.$$
$$\left.-\frac{\eta}{1+\eta}\frac{1}{(ab)^m}I_{e_{m-1,0}}\left(ab\gamma_T;\frac{1}{\sqrt{c_2}}\right)\right], \tag{E.2.13}$$

donde los coeficientes $\alpha_{L,m}$, c_1 y c_2 son los definidos anteriormente. Nótese que (E.2.13) es una expresión exacta y cerrada para la BEP media válida para cualquier esquema de modulación cuya BEP condicional se ajuste a la dada en (E.2.5).

Resultados numéricos

A continuación se presentan algunos resultados numéricos de la evaluación de la expresión obtenida en (E.2.13) para la BEP media. Como caso particular para esta evaluación, se ha escogido el esquema de modulación DQPSK (véase la Tabla E.1). Con el fin de comprobar la validez de nuestros resultados, se han realizado distintas simulaciones Monte-Carlo.

La Figura E.2 representa la BEP media en función de la SNR media por antena receptora $\bar{\gamma}$ para diferentes valores del parámetro Nakagami m y del número de antenas L. Para cada valor de $\bar{\gamma}$ se ha considerado el umbral óptimo de conmutación $\gamma_T^\star$, que minimiza la BEP y ha sido obtenido mediante técnicas numéricas de optimización. Las curvas muestran que el rendimiento del sistema en el rango $10^{-6}-10^{-3}$ está esencialmente determinado por el producto de m y L, que puede interpretarse como una medida del orden de diversidad. Los valores obtenidos de las simulaciones han sido representados en la misma Figura E.2, confirmándose así la validez de nuestra expresión analítica.

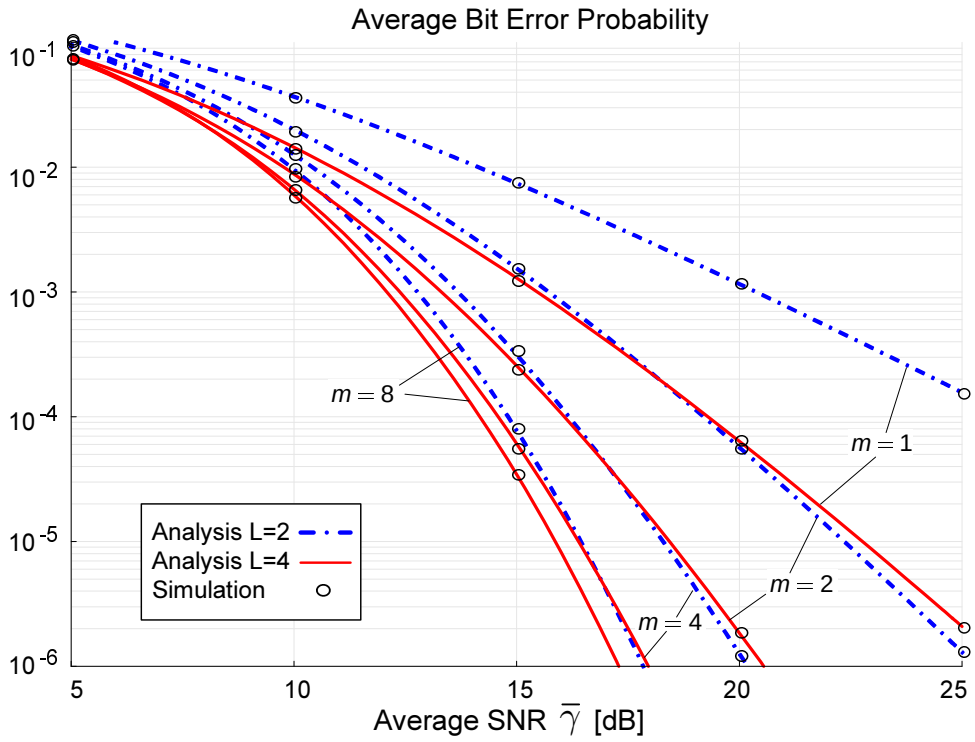

Figure E.2: BEP media versus SNR media por antena para DQPSK empleando umbrales de conmutación óptimos.

E.2.2 Sistemas MRC con interferencias co-canal

La combinación espacial en el receptor es una técnica que se emplea para combatir la degradación del rendimiento asociada a los desvanecimientos y a la presencia de interferencias co-canal (CCI, *co-channel interferences*). Como ya se ha introducido, la técnica de combinación MRC es óptima en cuanto a la SNR efectiva y, por ello, nos hemos centrado en analizar las prestaciones de sistemas MRC en presencia de CCI. La probabilidad de *outage* (OP) es una medida clave en sistemas con señales interferentes. Aunque la OP ha sido analizada en distintos trabajos de la bibliografía, se encuentran pocos resultados para canales Hoyt, que modelan condiciones de desvanecimiento más severas que los canales Rayleigh [63, 66]. Recientemente, se han proporcionado en [67] resultados cerrados y exactos para la OP de un receptor con una única antena en canales Hoyt sin interferencias. Por otro lado, muy pocos trabajos consideran el ruido en el análisis. El análisis en [23] incluye el ruido y asume canales Nakagami-n (Rice) o Nakagami-m para la señal deseada y canal Rayleigh para las señales interferentes.

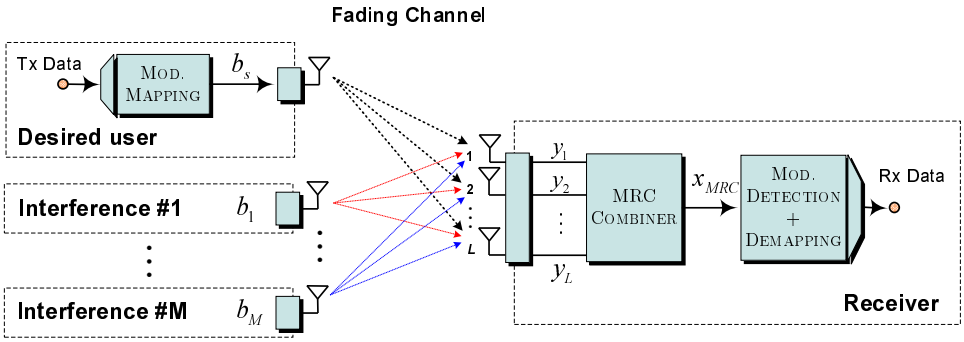

Figure E.3: Modelo de sistema MRC con interferencias co-canal.

En esta sección se presenta brevemente el análisis de la OP llevado a cabo para sistemas MRC en canales Hoyt ante la presencia de CCI. Se ha obtenido una expresión cerrada y exacta en el caso genérico de un receptor con L antenas.

Modelo de sistema

Consideramos un sistema con L antenas receptoras donde se aplica combinación MRC en el receptor. Se asume que la señal deseada en cada antena receptora está contaminada por M señales interferentes, como se muestra en la Figura E.3. Además, consideramos en cada antena receptora la presencia de ruido aditivo blanco Gaussiano de media cero y varianza σ^2. La señal deseada y las interferencias, con potencias arbitrarias, pasan por un canal con desvanecimientos y se emplea un receptor coherente que conoce perfectamente el estado del canal. En cuanto al modelado de los desvanecimientos, adoptamos el modelo de Hoyt para la señal deseada y Rayleigh para las interferencias.

Denotamos con $\mathbf{h}_s = [h_{s1}, \ldots, h_{sL}]^T$ y $\mathbf{h}_i = [h_{i1}, \ldots, h_{iL}]^T$ los vectores de ganancia compleja del canal para la señal deseada y la i-ésima señal interferente. Entonces, el vector de la señal recibida en banda base $\mathbf{y}$ puede escribirse como

$$\mathbf{y} = \mathbf{h}_s b_s + \sum_{i=1}^{M} \sqrt{W_i}\mathbf{h}_i b_i + \mathbf{n}, \tag{E.2.14}$$

donde W_i es la potencia media del i-ésimo interferente en cada antena receptora, $\mathbf{n}$ es el vector de ruido L-dimensional, y b_s y b_i con $|b_s| = |b_i| = 1$ son, respectivamente, los símbolos transmitidos por el usuario deseado y por el i-ésimo usuario interferente.

En un receptor MRC, las señales recibidas en las distintas antenas se multiplican por

las ganancias del canal asociado al usuario deseado, resultando tras la combinación

$$x_{MRC} = \mathbf{h}_s^H \mathbf{y} = |\mathbf{h}_s|^2 b_s + \sum_{i=1}^{M} \sqrt{W_i} \mathbf{h}_s^H \mathbf{h}_i b_i + \mathbf{h}_s^H \mathbf{n}. \tag{E.2.15}$$

En el modelo considerado, la relación señal a ruido más interferencia (SINR) puede escribirse como $\gamma = \frac{X}{Z+\sigma^2}$ [23], donde $X = |\mathbf{h}_s|^2 = \sum_{n=1}^{L} |h_{sn}|^2$ es la potencia efectiva de la señal deseada a la salida del combinador, y Z es la potencia total de las señales interferentes. Nótese que $|h_{sn}|$ es el módulo de la envolvente compleja del canal, que sigue una distribución de Hoyt. Así pues, X está distribuida como la suma de L variables Hoyt al cuadrado i.i.d. y la media de X, denotada por W_s viene dada por $W_s = \mathtt{E}[X] = L\Omega$, donde Ω es la media de la envolvente del canal al cuadrado, es decir, $\Omega = \mathtt{E}\left[|h_{sn}|^2\right]$, $n = 1, ..., L$.

Considerando lo anterior, la PDF de X, f_X, puede obtenerse a partir de la PDF de la distribución $\eta - \mu$ [1] (véase la Sección 3.3) como:

$$f_X(x) = \frac{\sqrt{\pi}}{\Gamma\left(\frac{L}{2}\right) q \left(1-q^2\right)^{\frac{L-1}{2}} \Omega L} \left(\frac{L\left(1+q^2\right)}{2}\right)^{\frac{L+1}{2}} \left(\frac{x}{\Omega L}\right)^{\frac{L-1}{2}} \exp\left(-\frac{(1+q^2)^2}{4q^2}\frac{x}{\Omega}\right) I_{\frac{L-1}{2}}\left(\frac{(1-q^4)}{4q^2}\frac{x}{\Omega}\right), \tag{E.2.16}$$

donde I_ν es la función de Bessel modificada de primera especie y orden ν-ésimo.

Análisis de la probabilidad de *outage*

Consideramos el total de interferentes M dividido en J grupos con n_i interferentes cada uno, donde todos los interferentes de un grupo tienen la misma potencia media W_i. Bajo esta consideración, la OP puede calcularse como [23]

$$P_{out} \doteq \Pr\left\{\frac{X}{Z+\sigma^2} \leq \gamma_o\right\} = \underbrace{\int_0^{\gamma_o\sigma^2} f_X(x)\, dx}_{P_{out}^{\star}} + \sum_{i=1}^{J}\sum_{j=1}^{n_i}\sum_{k=0}^{n_i-j}\sum_{l=0}^{k} E_{i,j} \frac{e^{\sigma^2/W_i}(-\sigma^2)^{k-l}}{l!(k-l)!W_i^k\gamma_o^l} \int_{\gamma_o\sigma^2}^{\infty} x^l \mathrm{e}^{-\frac{x}{\gamma_o W_i}} f_X(x)\, dx, \tag{E.2.17}$$

[1] Como se muestra en la Sección 3.3.2, la PDF de la suma de L variables Nakagami-q (Hoyt) se obtiene directamente a partir de la PDF de la distribución $\eta - \mu$ fijando los valores $\mu = \frac{L}{2}$ y $\eta = q^2$.

donde Z es la potencia total de las señales interferentes, γ_o es un umbral predefinido, σ^2 es la potencia media del ruido, $E_{i,j}$ son ciertas constantes definidas en [23, eq. 6], y f_X es la PDF de la potencia de la señal deseada a la salida del combinador.

La OP en (E.2.17) aparece expresada en términos de ciertas integrales incompletas. Con el fin de obtener una expresión cerrada, procedemos a resolver estas integrales. La primera representa la OP en ausencia de interferencias y viene dada por la CDF de X. Recientemente se ha obtenido una expresión para esta CDF en [37]. Haciendo uso de [37, eq. 7], el primer término de (4.2.5) puede expresarse como

$$\underbrace{\int_0^{\gamma_o\sigma^2} f_X(x)\,dx}_{P_{out}^{\star}} = 1 - Y_{\frac{L}{2}}\left(\frac{1-q^2}{1+q^2}, \frac{(1+q^2)}{2q}\sqrt{\frac{L\gamma_o\sigma^2}{\Omega L}}\right), \tag{E.2.18}$$

donde $Y_{\frac{L}{2}}$ es la integral de Yacoub, definida por (3.3.5) en la Sección 3.3. Las expresiones cerradas para la solución de $Y_{\frac{L}{2}}$ pueden encontrarse en la Sección 3.3, concretamente en (3.3.8) and (3.3.9) para valores impares y pares de L, respectivamente. Para un número par de antenas L, $Y_{\frac{L}{2}}$ viene dada en términos de los polinomios de Jacobi.

El segundo término de (E.2.17) representa el impacto de las interferencias en la probabilidad de *outage*. Este término consiste en una combinación lineal de la función generadora de momentos generalizada incompleta, también llamada IG-MGF (*incomplete generalized moment generating function*), $\mathcal{G}_X(\cdot,\cdot;\cdot)$, definida en (3.1.5). En concreto, las integrales en el segundo término de (E.2.17) pueden identificarse con la IG-MGF como

$$\int_{\gamma_o\sigma^2}^{\infty} x^l \mathrm{e}^{-\frac{x}{\gamma_o W_i}} f_X(x)\,dx = \mathcal{G}_X\left(l, -\frac{1}{\gamma_o W_i}; \gamma_o\sigma^2\right). \tag{E.2.19}$$

Es importante recordar que f_X es la PDF de la suma de variables Hoyt al cuadrado, dada en (E.2.16), donde esencialmente aparece la función de Bessel modificada y la función exponencial. Así pues, la integral incompleta en (E.2.19) pertenece a la familia de integrales ILHI (véase la Sección 2.3.3). Basándonos en las soluciones explícitas para las ILHI [20], que pueden encontrarse en la Sección 2.3.3, se han derivado expresiones para la IG-MGF $\mathcal{G}_X(\cdot,\cdot;\cdot)$. Estas expresiones están incluidas en el Apéndice D.

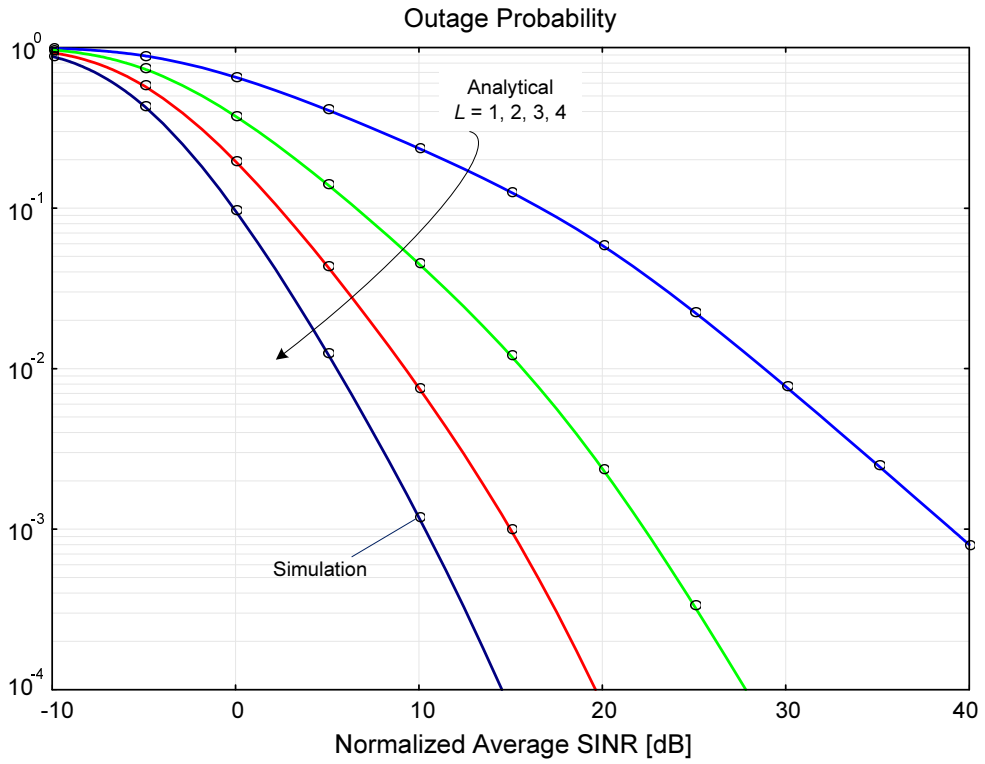

Figure E.4: OP en función de la SINR media para un receptor MRC con L antenas, parámetro Hoyt $q = 1/16$, potencia de ruido $\sigma^2 = 1/10$, y 3 interferentes con $W_1 = 1/4$, $W_2 = W_3 = 1/8$.

Finalmente, la OP para sistemas MRC en canales Hoyt con interferencias se obtiene sustituyendo (E.2.18) y (E.2.19) en (E.2.17), resultando

$$\begin{aligned} P_{out} = 1 - Y_{\frac{L}{2}}\left(\frac{1-q^2}{1+q^2}, \frac{(1+q^2)}{2q}\sqrt{\frac{L\gamma_o\sigma^2}{\Omega L}}\right) \\ + \sum_{i=1}^{J}\sum_{j=1}^{n_i}\sum_{k=0}^{n_i-j}\sum_{l=0}^{k} E_{i,j}\frac{e^{\sigma^2/W_i}(-\sigma^2)^{k-l}}{l!(k-l)!W_i^k\gamma_o^l}\mathcal{G}_X\left(l, \frac{-1}{\gamma_o W_i}; \gamma_o\sigma^2\right), \end{aligned} \tag{E.2.20}$$

donde los coeficientes $E_{i,j}$ vienen dados por [23, eq. 6], y $\mathcal{G}_X(\cdot,\cdot,\cdot)$ es la IG-MGF de la suma de variables Hoyt al cuadrado, que se obtiene directamente del Corolario 3 en el Apéndice D.3. Puede comprobarse que la OP en (E.2.20) está expresada esencialmente en términos de la función Lauricella confluente, definida en (2.3.21), y los polinomios de Jacobi.

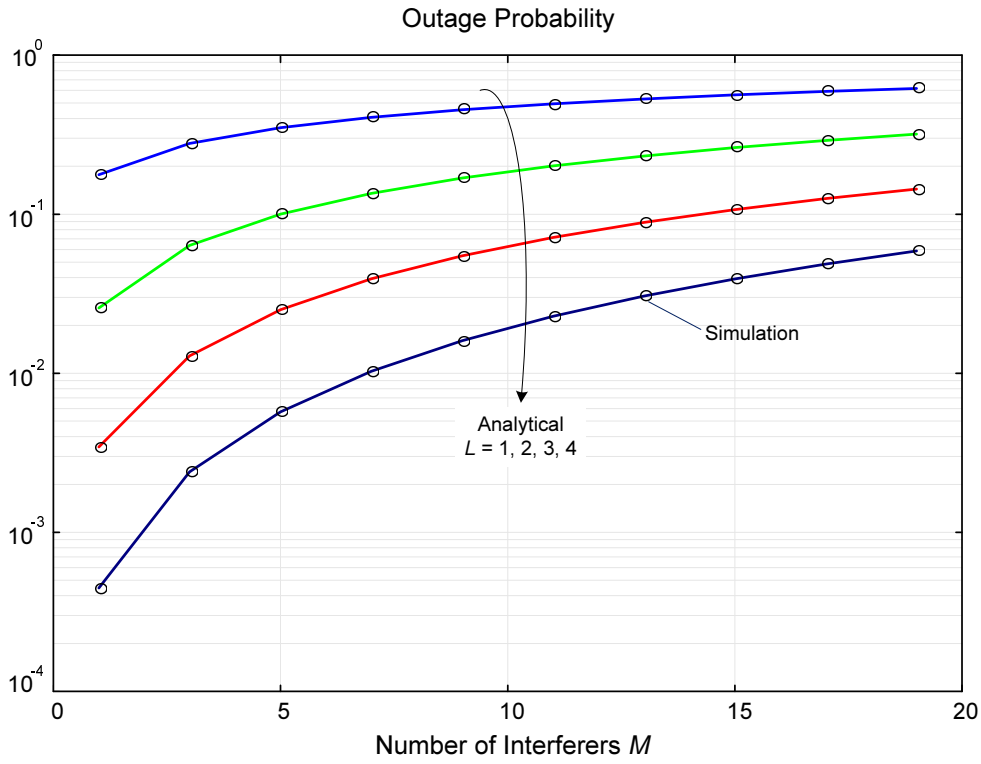

Figure E.5: OP en función del número de interferentes con parámetro Hoyt $q = 1/16$, potencia normalizada de la señal deseada $W_s/\gamma_o = 1/4$, potencia de ruido $\sigma^2 = 1/200$, e igual potencia $W_1 = 1/100$ para todos los interferentes.

Resultados numéricos

A continuación se muestran algunos resultados de la evaluación numérica de la expresión para la OP obtenida en (E.2.20). La Figura E.4 representa la OP en función de la SINR media, normalizada y expresada en decibelios como

$$10\log_{10}\left(\frac{W_s}{\gamma_o\sum W_i + \gamma_o\sigma^2}\right),$$

para distintos valores del número de antenas L y parámetro Hoyt $q = 1/16$. En este ejemplo se han considerado 3 señales interferentes con potencia media $W_1 = 1/4$ y $W_2 = W_3 = 1/8$, y una potencia media de ruido $\sigma^2 = 1/10$. Los resultados de simulación, también representados en la Figura E.4, confirman la validez de la expresión obtenida.

Por otro lado, en la Figura E.5 se representa la OP en función del número de interferentes para el receptor MRC considerado con $q = 1/16$ y distintos valores del número de antenas L . En primer lugar se observa cómo el rendimiento se degrada de forma

significativa a medida que el número de interferentes aumenta. Además, puede verse que la degradación de rendimiento asociada a la presencia de señales interferentes es significativamente mayor cuanto mayor es el número de antenas L.

E.3 Análisis de rendimiento de sistemas MIMO no-ideales

Las propiedades estadísticas de las matrices Wishart han sido utilizadas frecuentemente para analizar el rendimiento de los sistemas MIMO. En concreto, los estadísticos de la SNR efectiva en diferentes sistemas MIMO dependen de la distribución de los elementos de la diagonal de de una matriz Wishart compleja. Esta distribución aparece cuando el análisis de estos sistemas se realiza bajo determinadas condiciones prácticas como la correlación espacial o el canal de retorno de capacidad limitada. Así pues, en el segundo bloque de esta tesis nos hemos centrado en estudiar la distribución de los elementos de la diagonal de las matrices Wishart complejas. En concreto, se han obtenido expresiones originales para la PDF y la CDF conjunta de los elementos de la diagonal. A partir de estas expresiones, se ha obtenido la distribución del máximo de los elementos de la diagonal. La Sección 2.4 incluye los detalles acerca de estas derivaciones y resultados estadísticos.

En esta sección, las expresiones obtenidas para la distribución del máximo de los elementos de la diagonal de una matriz Wishart compleja son aplicadas al análisis de rendimiento de dos sistemas MIMO con diferentes condiciones prácticas. En primer lugar, se analiza la probabilidad de *outage* de sistemas MIMO que emplean *selection combining* en el receptor (MIMO SC) considerando canales con correlación espacial. Posteriormente, se analizan las prestaciones de sistemas MIMO *beamforming* con un canal de retorno de capacidad limitada, es decir, donde la técnica de *beamforming* aplicada en el transmisor se basa en un conjunto predefinido de vectores o *codebook*.

E.3.1 Sistemas MIMO SC con correlación espacial

La técnica *selection combining* (SC) consiste en seleccionar para la recepción la antena que experimenta la mayor SNR en cada instante. De ese modo, solo se necesita una cadena de

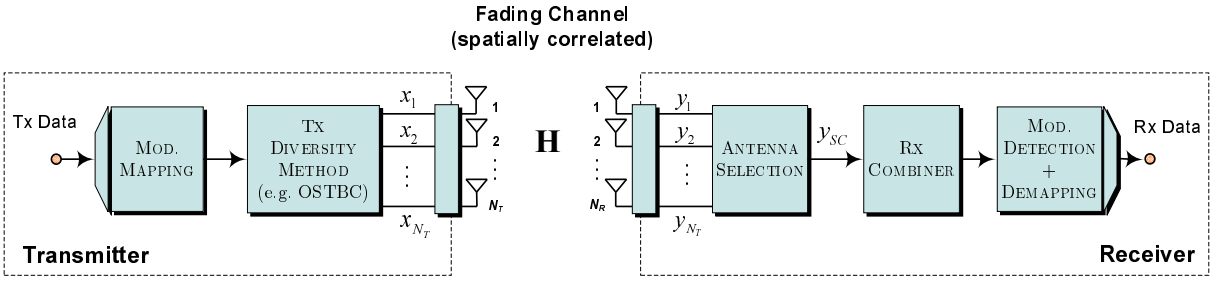

Figure E.6: Modelo de sistema MIMO con *selection combining*.

radio frecuencia (RF), estableciéndose así un compromiso entre el rendimiento del sistema y la complejidad (coste) de los receptores. Los sistemas MIMO SC emplean la técnica SC en el receptor y alguna otra técnica de diversidad, como por ejemplo codificación espacio-tiempo, en el transmisor.

Por otro lado, las señales recibidas en las diferentes antenas están, en la práctica, espacialmente correladas debido a la insuficiente separación física entre antenas o a la geometría del entorno de propagación. Cuando existe correlación espacial se reduce la diversidad espacial y, por tanto, el rendimiento de los sistemas MIMO se degrada de forma significativa [13].

A continuación se presenta el análisis de OP de sistemas MIMO SC en canales Rayleigh con correlación espacial arbitraria.

Modelo de sistema

Consideramos un sistema MIMO con N_T antenas transmisoras y N_R antenas receptoras (véase la Figura E.6), donde todas las antenas se usan para la transmisión y sólo se selecciona una antena receptora, la que maximiza la SNR instantánea. El canal MIMO con desvanecimientos se modela mediante la matriz aleatoria $\mathbf{H}$, de dimensiones $N_R \times N_T$, que se define de acuerdo al conocido modelo de correlación espacial de Kronecker [76]

$$\mathbf{H} = [\mathbf{h}_1, \mathbf{h}_2, \ldots, \mathbf{h}_{N_T}] = \mathbf{R}_R^{\frac{1}{2}} \mathbf{G} \mathbf{R}_T^{\frac{1}{2}}, \tag{E.3.1}$$

donde $\mathbf{R}_T$ y $\mathbf{R}_R$ son las matrices de correlación del transmisor y del receptor, respectivamente, mientras que los elementos de $\mathbf{G}$ son variables aleatorias Gaussianas complejas

i.i.d. con media cero y varianza unidad. Se asume que las antenas transmisoras se encuentran lo suficientemente separadas como para que la correlación en el transmisor sea despreciable, es decir, $\mathbf{R}_T = \mathbf{I}$, de manera que la correlación espacial únicamente se debe al extremo del receptor.

En este caso, los vectores-columna de la matriz del canal $\mathbf{h}_j = [h_{1j}, h_{2j}, \ldots, h_{N_R j}]^T$, para $j = 1, \ldots, N_T$, son procesos Gaussianos i.i.d. con media cero y matriz de covarianza $\mathbf{R}_R$, esto es, $\mathbf{h}_j \sim \mathcal{CN}(\mathbf{0}, \mathbf{R}_R)$. Nótese que la matriz $\mathbf{S}_h = \sum_{j=1}^{N_T} \mathbf{h}_j \mathbf{h}_j^H$ sigue la distribución de Wishart compleja $\mathcal{CW}_{N_R}(N_T, \mathbf{R}_R)$ y que los N_R elementos de su diagonal son las normas al cuadrado de los vectores-fila de $\mathbf{H}$.

La envolvente compleja en basa base de la señal recibida puede escribirse como $\mathbf{y} = \mathbf{H}\mathbf{x} + \mathbf{n}$, donde $\mathbf{n}$ es el vector de dimensión N_R correspondiente al ruido blanco aditivo, cuyos elementos son variables aleatorias Gaussianas complejas con media cero y varianza σ_n^2. La señal transmitida se denota con el vector-columna $\mathbf{x}$ y la potencia media transmitida total está normalizada a la unidad, es decir, $\mathtt{E}\left[\mathbf{x}^H\mathbf{x}\right] = 1$, y distribuida a partes iguales entre todas las antenas. Bajo todas estas consideraciones, la SNR media en cada una de las antenas receptoras viene dada por $\bar{\gamma} = \frac{1}{\sigma_n^2}$.

La técnica *selection combining* selecciona la antena receptora que maximiza la SNR instantánea SNR [8]. En el sistema MIMO que se ha considerado, asumimos que el estado del canal es conocido perfectamente por el receptor pero no está disponible en el transmisor, donde se aplica alguna técnica de diversidad como, por ejemplo, codificación espacio-tiempo ortogonal (OSTBC).

Análisis de la probabilidad de *outage*

La SNR instantánea a la salida del combinador viene dada por $\gamma = \frac{\bar{\gamma}}{N_T} Z$, donde

$$Z = \max_{1 \le i \le N_R} \sum_{j=1}^{N_T} |h_{ij}|^2$$

es el máximo de las normas de los vectores-fila de la matriz del canal, es decir, el máximo de los elementos de la diagonal de la matriz Wishart compleja $\mathbf{S}_h$. Los estadísticos de las matrices Wishart complejas han sido abordados en en el Capítulo 2, donde se ha

obtenido un nuevo desarrollo en serie para la distribución del máximo de los elementos de la diagonal. Así pues, la CDF de Z puede obtenerse a partir de la expresión (2.4.23) como

$$F_Z(z) = \sum_{n=0}^{\infty} \sum_{i=1}^{s_n} \hat{c}\left(p_{i,1}^{(n)}, \ldots, p_{i,N_R}^{(n)}\right) \prod_{j=1}^{N_R} \Delta_{p_{i,j}^{(n)}}^{N_T}\left(w^2 z\right), \tag{E.3.2}$$

donde $\Delta_n^{\alpha}(\cdot)$ son determinadas funciones delta, definidas en (2.4.13), s_n es el número de posibles particiones enteras de n en N_R elementos, $P_i^{(n)} = \left\{p_{i,1}^{(n)}, \ldots, p_{i,N_R}^{(n)}\right\}$ es la i-ésima partición entera de n, $i = 1, ..., s_n$, y los coeficientes $\hat{c}\left(p_{i,1}^{(n)}, \ldots, p_{i,N_R}^{(n)}\right)$ son los correspondientes a la serie (2.4.23). Estos coeficientes dependen de N_T y de la matriz de correlación $\mathbf{R}_R$, y pueden calcularse fácilmente con el algoritmo proporcionado en el Apéndice B.2. Es importante destacar que las funciones delta, definidas en (2.4.13), son básicamente una versión escalada de los polinomios de Laguerre generalizados multiplicados por la función exponencial.

Finalmente, la OP para un sistema MIMO SC con correlación espacial viene dada por

$$\begin{aligned} P_{out}(x) &\triangleq \Pr\{\gamma \leq \gamma_0\} = \Pr\left\{Z \leq N_T \frac{\gamma_0}{\bar{\gamma}}\right\} \\ &= F_Z\left(N_T \frac{1}{x}\right) = \sum_{n=0}^{\infty} \sum_{i=1}^{s_n} \hat{c}\left(p_{i,1}^{(n)}, \ldots, p_{i,N_R}^{(n)}\right) \prod_{j=1}^{N_R} \Delta_{p_{i,j}^{(n)}}^{N_T}\left(\frac{w^2 N_T}{x}\right), \end{aligned} \tag{E.3.3}$$

donde γ_0 es el umbral de *outage* y $x \triangleq \frac{\bar{\gamma}}{\gamma_0}$ es la SNR media normalizada. Esta expresión original y general para la OP es válida para cualquier matriz de correlación compleja y cualquier número de antenas receptoras. Recientemente, el mismo sistema considerado aquí ha sido analizado en [8], pero asumiendo en este caso un modelo de correlación real exponencial para $N_R > 3$. Este es un modelo válido sólo cuando las antenas están situadas en un *array* lineal uniforme [77] y, por tanto, nuestro análisis extiende los resultados en [8] al caso general de correlación arbitraria.

Resultados numéricos

Las expresiones analíticas obtenidas para sistemas MIMO SC con correlación espacial han sido evaluadas numéricamente. A continuación se muestran algunos de los resultados obtenidos de esta evaluación.

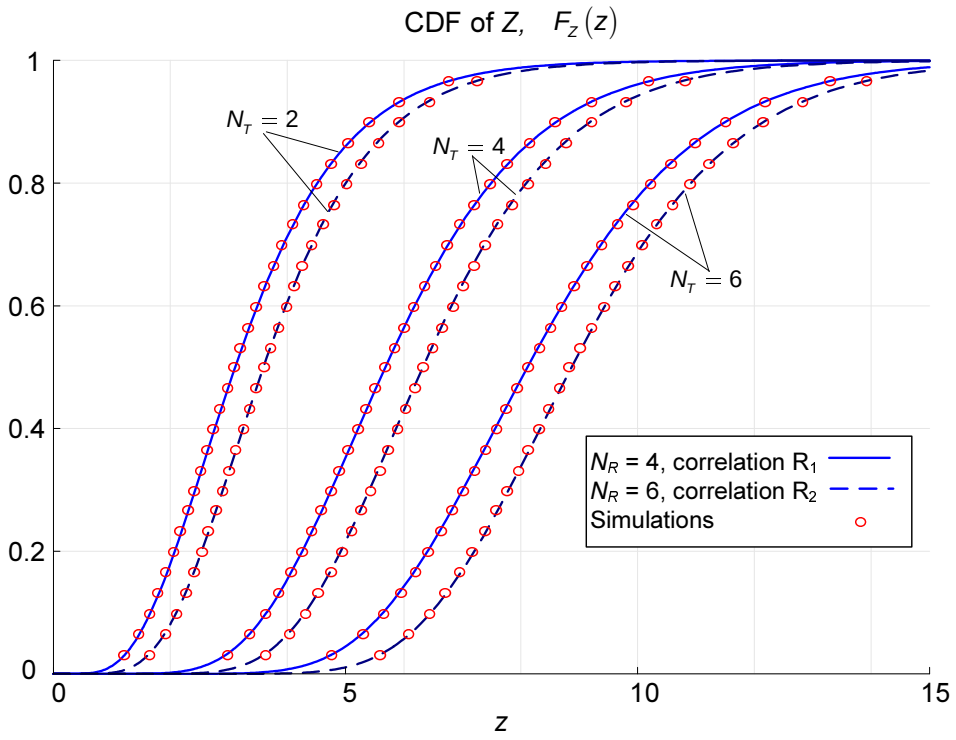

Figure E.7: CDF de Z, el máximo de las normas de los vectores-fila de la matriz del canal $\mathbf{H}$.

En primer lugar, la Figura E.7 muestra la CDF de Z, que es una versión escalada de la SNR a la salida del combinador. La expresión analítica (E.3.2) ha sido evaluada para dos matrices de correlación arbitrarias, $\mathbf{R}_1$ y $\mathbf{R}_2$ (véase la Tabla 5.1 en la Sección 5.1), que corresponden a $N_R = 4$ y $N_R = 6$ antenas receptoras, respectivamente, $w = 1$, y distintos valores de N_T. El límite de truncamiento de la serie (E.3.2) se ha fijado a $N_{max} = 8$, dando lugar a un total de 25 términos para $N_R = 4$ y 36 términos para $N_R = 6$. Los valores de simulación Monte-Carlo de la CDF se han superpuesto a las curvas analíticas en la Figura E.7, mostrando que ambos resultados coinciden casi perfectamente con pocos términos de la serie.

Por otro lado, la OP del sistema MIMO SC con $N_R = 4$ se representa en la Figura E.8 para distintos valores de N_T y dos matrices de correlación. En este caso, se compara el escenario de correlación alta propuesto en [78] ($\mathbf{R}_3$) con el escenario de correlación baja definido por la matriz arbitraria $\mathbf{R}_1$. Se puede ver que el escenario de correlación alta determinado por $\mathbf{R}_3$ conlleva un rendimiento significativamente peor que el correspondiente al escenario $\mathbf{R}_1$. Sin embargo, esta pérdida de prestaciones asociada a una mayor correlación espacial podría combatirse aumentando el número de antenas transmisoras.

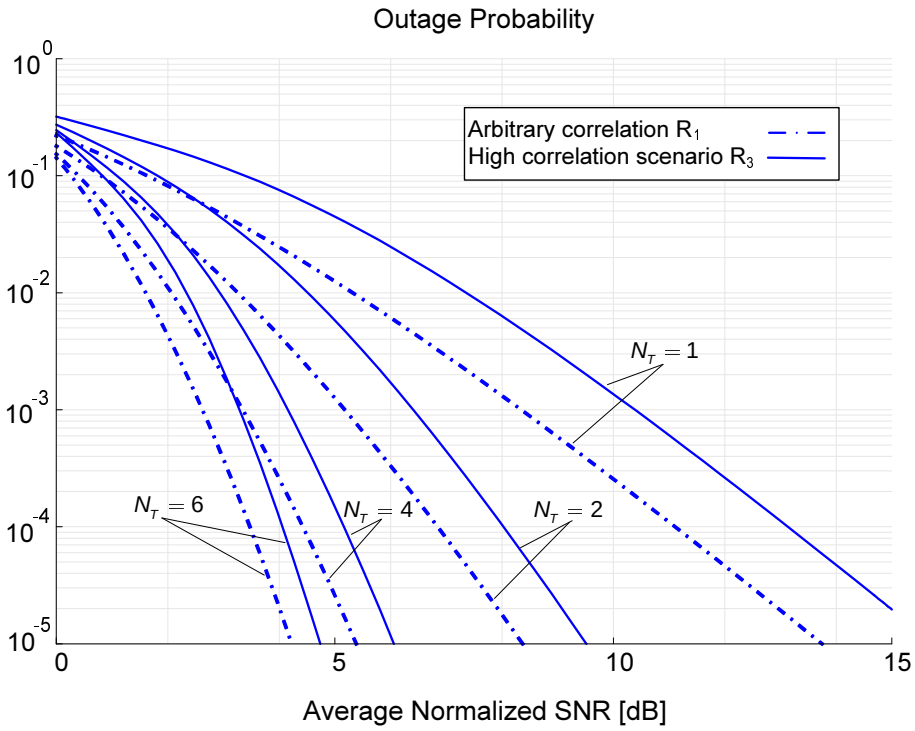

Figure E.8: OP en función de la SNR media normalizada para un sistema MIMO SC con distintas configuraciones de antenas y correlación espacial arbitraria.

E.3.2 Sistemas MIMO *beamforming* con canal de retorno de capacidad limitada

El sistema MIMO *beamforming*, también conocido como MIMO MRC, se basa en la aplicación de los pesos MRC de forma conjunta en el transmisor y en el receptor [10–12]. Sin embargo, el conocimiento total del estado del canal en el transmisor es algo a menudo inviable debido a la limitación de capacidad del canal de retorno. Como solución práctica, se suele considerar un conjunto de vectores de precodificación llamado *codebook* que está disponible en el transmisor y en el receptor. Así, el receptor únicamente informa al transmisor, mediante un índice, del vector del *codebook* que optimiza la SNR.

A continuación se presentan brevemente el sistema *MIMO beamforming* con canal de retorno de capacidad limitada y los resultados del análisis de prestaciones del mismo.

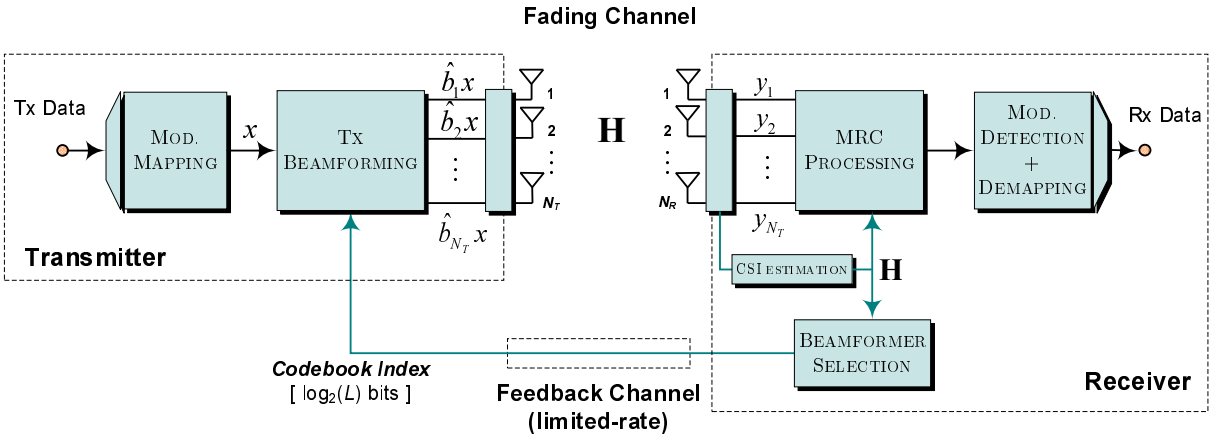

Figure E.9: Modelo de sistema MIMO *beamforming* con canal de retorno de capacidad limitada.

Modelo de sistema

Consideramos un sistema MIMO *beamforming* con N_T antenas transmisoras y N_R antenas receptoras, donde se aplica *beamforming* basado en *codebook* en el transmisor y combinación MRC en el receptor (véase la Figura E.9). El canal MIMO se modela mediante la matriz $\mathbf{H}$ de dimensión $N_R \times N_T$, cuyos elementos son variables aleatorias Gaussianas i.i.d. con media cero y varianza unidad. La técnica de *beamforming* aplicada en el transmisor se basa en el *codebook* definido por la matriz $\mathbf{B} = [\mathbf{b}_1, \mathbf{b}_2, \ldots, \mathbf{b}_L]$, de donde se extraen los L vectores-columna $\mathbf{b}_i$, $i = 1, \ldots, L$, de dimensión $N_T \times 1$ que se emplearán para precodificar los símbolos transmitidos. Para cada realización del canal, el receptor selecciona el vector de precodificación del *codebook* que maximiza la SNR instantánea y lo reporta al transmisor a través de un canal de retorno de capacidad limitada empleando para ello $\log_2(L)$ bits.

En este caso, la envolvente compleja de la señal recibida antes del procesado MRC puede expresarse como $\mathbf{y} = \mathbf{H}\hat{\mathbf{b}}x + \mathbf{n}$, donde x es el símbolo transmitido, $\hat{\mathbf{b}}$ es el vector de precodificación seleccionado tal que

$$\hat{\mathbf{b}} = \arg\max_{\mathbf{b}\in\mathbf{B}} \|\mathbf{H}\mathbf{b}\|^2, \tag{E.3.4}$$

y $\mathbf{n}$ es el vector de ruido blanco, de dimensión N_R, cuyos elementos son variables aleatorias Gaussianas complejas con media cero y varianza σ_n^2. La potencia media transmitida total se asume normalizada a la unidad, y consecuentemente, $\mathtt{E}[|x|^2] = 1$ y $\|\mathbf{b}_i\|^2 = 1$, para $i = 1, \ldots, L$. Así, la SNR media en cada antena receptora viene dada por $\bar{\gamma} = \frac{1}{\sigma_n^2}$.

Análisis de la probabilidad de *outage*

Asumiendo la matriz del canal $\mathbf{H}$ perfectamente conocida en el receptor, la SNR instantánea tras el procesado MRC puede expresarse como $\gamma = \bar{\gamma} Z$, con

$$Z = \max_{1 \leq i \leq L} \|\mathbf{H}\mathbf{b}_i\|^2 = \max_{1 \leq i \leq L} \sum_{j=1}^{N_R} |\mathbf{h}_j \mathbf{b}_i|^2,$$

donde $\{\mathbf{h}_j\}$ son los vectores-fila de la matriz $\mathbf{H}$. Se observa que Z es el máximo de las normas $v_i = \|\mathbf{H}\mathbf{b}_i\|^2$, para $i = 1, \ldots, L$, las cuales pueden ser identificadas como los elementos de la diagonal de cierta matriz Wishart compleja. En concreto, v_i son los elementos de la diagonal de la matriz $\mathbf{S}_{bf} = \sum_{j=1}^{N_R} \mathbf{k}_j \mathbf{k}_j^H$, con $\mathbf{k}_j = \mathbf{B}^H \mathbf{h}_j^H$. Esta matriz sigue la distribución Wishart compleja $\mathcal{CW}_L(N_R, \mathbf{B}^H\mathbf{B})$. De forma equivalente, Z es el máximo de L variables chi-square centrales correladas con matriz de correlación subyacente dada por $\mathbf{R}_{bf} = \mathbf{B}^H\mathbf{B}$, es decir, con correlación determinada por la matriz del *codebook*. Así, la CDF de Z puede expresarse mediante el desarrollo en serie (2.4.23) como

$$F_Z(z) = \sum_{n=0}^{\infty} \sum_{i=1}^{s_n} \hat{c}\left(p_{i,1}^{(n)}, \ldots, p_{i,L}^{(n)}\right) \prod_{j=1}^{L} \Delta_{p_{i,j}^{(n)}}^{N_R}\left(w^2 z\right), \tag{E.3.5}$$

donde $\Delta_n^{\alpha}(\cdot)$ son determinadas funciones delta, definidas en (2.4.13), s_n es el número de posibles particiones enteras de n en L elementos, $P_i^{(n)} = \left\{p_{i,1}^{(n)}, \ldots, p_{i,L}^{(n)}\right\}$ es la i-ésima partición entera de n, $i = 1, ..., s_n$, y los coeficientes $\hat{c}\left(p_{i,1}^{(n)}, \ldots, p_{i,L}^{(n)}\right)$ son los correspondientes a la serie (2.4.23). Estos coeficientes dependen de N_R y de la matriz $\mathbf{R}_{bf}$, y pueden calcularse fácilmente con el algoritmo proporcionado en el Apéndice B.2.

Finalmente, el resultado anterior permite obtener una expresión exacta para la OP de un sistema MIMO *beamforming* basado en *codebook*,

$$\begin{aligned} P_{out}(x) &\triangleq \Pr\{\gamma \leq \gamma_0\} = \Pr\left\{Z \leq \frac{\gamma_0}{\bar{\gamma}}\right\} \\ &= F_Z\left(\frac{1}{x}\right) = \sum_{n=0}^{\infty} \sum_{i=1}^{s_n} \hat{c}\left(p_{i,1}^{(n)}, \ldots, p_{i,L}^{(n)}\right) \prod_{j=1}^{L} \Delta_{p_{i,j}^{(n)}}^{N_R}\left(\frac{w^2}{x}\right), \end{aligned} \tag{E.3.6}$$

donde γ_0 es el umbral de *outage* y $x \triangleq \frac{\bar{\gamma}}{\gamma_0}$ es la SNR media normalizada.

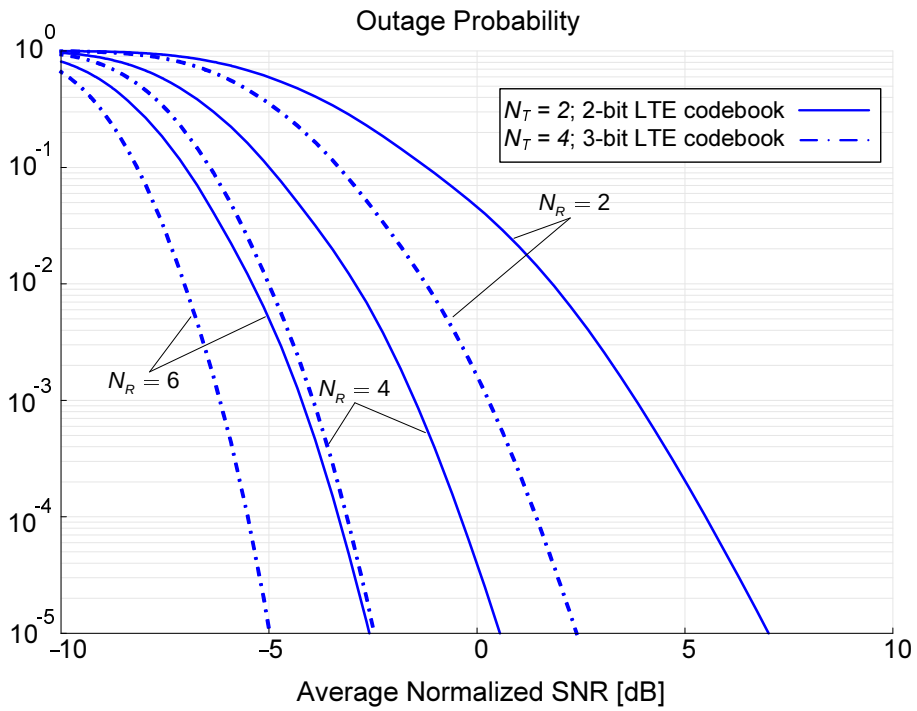

Figure E.10: OP en función de la SNR media normalizada para un sistema MIMO *beamforming* basado en *codebook* con diferentes configuraciones de antenas.

Resultados numéricos

La Figura E.10 muestra los resultados de rendimiento en términos de la OP para un sistema MIMO *beamforming* basado en *codebook*. La OP ha sido evaluada para tres casos con distinto número de antenas receptoras, $N_R = 2, 4, 6$, y dos configuraciones de antenas transmisoras $N_T = 2, 4$ con *codebooks* de 2 bits y 3 bits ($\mathbf{B}_{2-LTE}$ y $\mathbf{B}_{3-LTE}$) respectivamente. Estos *codebooks* han sido escogidos de acuerdo a la especificación de la tecnología LTE (*long term evolution*) [79], y pueden encontrarse en la Tabla 5.3 de la Sección 5.2.

E.4 Conclusiones y líneas futuras

En esta tesis se ha abordado el análisis del rendimiento de diferentes sistemas SIMO y MIMO en canales con desvanecimientos bajo ciertas condiciones no ideales (prácticas). Se ha planteado como objetivo obtener expresiones cerradas y exactas para las dos medidas de rendimiento más extendidas, la probabilidad de *outage* (OP) y la probabilidad de error

de bit (BEP). Sin embargo, las herramientas matemáticas existentes han sido en algunos casos insuficientes para llevar a cabo dicho análisis. Por lo tanto, el desarrollo de nuevas herramientas matemáticas y/o funciones estadísticas ha sido una parte esencial de este trabajo con el fin de analizar el rendimiento de los sistemas SIMO y MIMO.

En el contexto de los sistemas SIMO, la BEP y la OP han sido analizadas para los siguientes esquemas de diversidad en recepción y las condiciones prácticas que se especifican:

- Los sistemas *Switched Diversity* con señalización no ortogonal han sido analizados en términos de BEP para diferentes formatos de modulación no coherente en canales Nakagami-m para un receptor genérico con L antenas.
- Los sistemas MRC han sido analizados en presencia de interferencias co-canal en términos de OP para un receptor con L antenas en canales Nakagami-q (Hoyt). Además, se han obtenido algunas expresiones simplificadas y aproximaciones en el régimen de alta SINR para el caso de un receptor con una única antena. Este análisis ha motivado la derivación de nuevas funciones estadísticas relacionadas con la distribución Hoyt. En concreto, la MGF generalizada incompleta (IG-MGF) de la distribución Hoyt ha sido obtenida en forma cerrada y aplicada al análisis de la OP.

En el contexto de los sistemas MIMO, se ha observado que la SNR efectiva puede caracterizarse de acuerdo a la distribución de los elementos de la diagonal de una matriz Wishart compleja. Dada la ausencia de resultados para esta distribución en la bibliografía, nos hemos centrado en su caracterización estadística como paso previo y fundamental para el análisis de rendimiento de sistemas MIMO. En concreto, se ha obtenido la PDF conjunta de los elementos de la diagonal de una matriz Wishart compleja, que siguen una determinada distribución chi-cuadrado multivariable. La expresión de la PDF se presenta en forma de una serie infinita que converge rápidamente y es fácil de evaluar numéricamente. Esta expresión se ha utilizado para obtener la distribución del máximo de los elementos de la diagonal, la cual permite analizar el rendimiento de dos sistemas MIMO bajo diferentes condiciones prácticas:

- En primer lugar, los resultados estadísticos obtenidos han sido aplicados al análisis de la OP de sistemas MIMO que emplean *selection combining* en canales Rayleigh con correlación espacial arbitraria.

- En segundo lugar, el mismo procedimiento y resultados estadísticos han sido aplicados al análisis de la OP de sistemas MIMO *beamforming* en presencia de un canal de retorno de capacidad limitada.

Líneas futuras

Como se indicó anteriormente, el análisis del rendimiento de los sistemas MIMO en condiciones no ideales ha motivado el desarrollo de nuevas herramientas matemáticas, que pueden aplicarse a otros problemas. Por lo tanto, una futura línea de trabajo interesante puede ser la aplicación de estas herramientas al análisis y posterior diseño de nuevos sistemas de comunicaciones.

Asimismo, las expresiones obtenidas en el análisis de la OP y la BEP de los distintos sistemas SIMO y MIMO podrían aplicarse al diseño de este tipo de sistemas en las mencionadas condiciones prácticas.

Bibliography

[1] M. K. Simon and M.-S. Alouini, *Digital Communications over Fading Channels*, 2nd ed. John Wiley, 2005.

[2] C. Chayawan and V. Aalo, "On the outage probability of optimum combining and maximal ratio combining schemes in an interference-limited Rice fading channel," *IEEE Trans. Commun.*, vol. 50, no. 4, pp. 532–535, Apr 2002.

[3] M. K. Simon, S. H. Hinedi, and W. C. Lindsey, *Digital Communication Techniques: Signal Design and Detection.* Prentice Hall, 1995.

[4] J. Winters, J. Salz, and R. Gitlin, "The impact of antenna diversity on the capacity of wireless communication systems," *IEEE Trans. Commun.*, vol. 42, pp. 1740–1751, 1994.

[5] G. J. Foschini and M. J. Gans, "On limits of wireless communications in a fading environment when using multiple antennas," *Wirel. Pers. Commun.*, vol. 6, no. 3, pp. 311–335, 1998.

[6] I. E. Telatar, "Capacity of multi-antenna Gaussian channels," *Eur. Trans. Telecom.*, vol. 10, pp. 585–595, 1999.

[7] V. Tarokh, H. Jafarkhani, and A. Calderbank, "Space-time block coding for wireless communications: performance results," *IEEE J. Select. Areas Commun.*, vol. 17, no. 3, pp. 451–460, Mar 1999.

[8] Z. Xu, S. Sfar, and R. S. Blum, "Analysis of MIMO systems with receive antenna selection in spatially correlated Rayleigh fading channels," *IEEE Trans. Veh. Technol.*, vol. 58, no. 1, pp. 251–262, 2009.

[9] K. S. Ahn and R. Heath, "Performance analysis of maximum ratio combining with imperfect channel estimation in the presence of cochannel interferences," *IEEE Trans. Wireless Commun.*, vol. 8, no. 3, pp. 1080–1085, Mar 2009.

[10] T. Lo, "Maximum ratio transmission," *IEEE Trans. Commun.*, vol. 47, no. 10, pp. 1458–1461, Oct 1999.

[11] M. Kang and M.-S. Alouini, "Largest eigenvalue of complex Wishart matrices and performance analysis of MIMO MRC systems," *IEEE J. Select. Areas Commun.*, vol. 21, no. 3, pp. 418–426, Apr 2003.

[12] P. Dighe, R. Mallik, and S. Jamuar, "Analysis of transmit-receive diversity in Rayleigh fading," *IEEE Trans. Commun.*, vol. 51, no. 4, pp. 694–703, Apr 2003.

[13] D.-S. Shiu, G. J. Foschini, M. J. Gans, and J. M. Kahn, "Fading correlation and its effect on the capacity of multielement antenna systems," *IEEE Trans. Commun.*, vol. 48, no. 3, pp. 502–513, Mar 2000.

[14] K. K. Mukkavilli, A. Sabharwal, E. Erkip, and B. Aazhang, "On beamforming with finite rate feedback in multiple-antenna systems," *IEEE Trans. Inf. Theory*, vol. 49, no. 10, pp. 2562–2579, 2003.

[15] D. J. Love, J. Heath, R. W., and T. Strohmer, "Grassmannian beamforming for multiple-input multiple-output wireless systems," *IEEE Trans. Inf. Theory*, vol. 49, no. 10, pp. 2735–2747, 2003.

[16] S. Zhou, Z. Wang, and G. B. Giannakis, "Quantifying the power loss when transmit beamforming relies on finite-rate feedback," *IEEE Trans. Wireless Commun.*, vol. 4, no. 4, pp. 1948–1957, Jul 2005.

[17] P. Xia and G. B. Giannakis, "Design and analysis of transmit-beamforming based on limited-rate feedback," *IEEE Trans. Signal Process.*, vol. 54, no. 5, pp. 1853–1863, 2006.

[18] M. M. Agrest and M. Z. Maksimov, *Theory of Incomplete Cylindrical Functions and their Applications*. New York: Springer-Verlag, 1971.

[19] S. Dvorak, "Applications for incomplete Lipschitz-Hankel integrals in electromagnetics," *IEEE Antennas and Propagation Magazine*, vol. 36, no. 6, pp. 26–32, Dec 1994.

[20] J. Paris, E. Martos-Naya, U. Fernandez-Plazaola, and J. Lopez-Fernandez, "Analysis of adaptive MIMO transmit beamforming under channel prediction errors based on incomplete Lipschitz-Hankel integrals," *IEEE Trans. Veh. Technol.*, vol. 58, no. 6, pp. 2815–2824, Jul 2009.

[21] Y.-C. Ko, M.-S. Alouini, and M. Simon, "Analysis and optimization of switched diversity systems," *IEEE Trans. Veh. Technol.*, vol. 49, no. 5, pp. 1813–1831, Sep 2000.

[22] H.-C. Yang and M.-S. Alouini, "Performance analysis of multibranch switched diversity systems," *IEEE Trans. Commun.*, vol. 51, no. 5, pp. 782–794, May 2003.

[23] J. Romero-Jerez and A. Goldsmith, "Receive antenna array strategies in fading and interference: An outage probability comparison," *IEEE Trans. Wireless Commun.*, vol. 7, no. 3, pp. 920–932, Mar 2008.

[24] R. Mallik, "The pseudo-Wishart distribution and its application to MIMO systems," *IEEE Trans. Inform. Theory*, vol. 49, no. 10, pp. 2761–2769, Oct 2003.

[25] A. Maaref and S. Aissa, "Eigenvalue distributions of Wishart-type random matrices with application to the performance analysis of MIMO MRC systems," *IEEE Trans. Wireless Commun.*, vol. 6, no. 7, pp. 2678–2689, Jul 2007.

[26] A. Zanella, M. Chiani, and M. Win, "On the marginal distribution of the eigenvalues of Wishart matrices," *IEEE Trans. Commun.*, vol. 57, no. 4, pp. 1050–1060, Apr 2009.

[27] M. Matthaiou, M. Mckay, P. Smith, and J. Nossek, "On the condition number distribution of complex Wishart matrices," *IEEE Trans. Commun.*, vol. 58, no. 6, pp. 1705–1717, Jun 2010.

[28] O. C. Ugweje and V. A. Aalo, "Performance of selection diversity system in correlated Nakagami fading," in *Proc. IEEE 47th Vehicular Technology Conference*, vol. 3, 1997, pp. 1488–1492.

[29] Q. T. Zhang and H. G. Lu, "A general analytical approach to multi-branch selection combining over various spatially correlated fading channels," *IEEE Trans. Commun.*, vol. 50, no. 7, pp. 1066–1073, 2002.

[30] C. K. Au-Yeung and D. J. Love, "A performance analysis framework for limited feedback beamforming in correlated fading," *IEEE Commun. Lett.*, vol. 10, no. 5, pp. 344–346, May 2006.

[31] D. R. Jensen, "The joint distribution of traces of Wishart matrices and some applications," *The Annals of Mathematical Statistics*, vol. 41, no. 1, pp. 133–145, 1970.

[32] P. R. Krishnaiah, P. Hagis Jr., and L. Steinberg, "A note on the bivariate chi distribution," *SIAM Review*, vol. 5, no. 2, pp. 140–144, 1963.

[33] A. S. Krishnamoorthy and M. Parthasarathy, "A multivariate gamma-type distribution," *The Annals of Mathematical Statistics*, vol. 22, no. 4, pp. 549–557, 1951.

[34] T. Royen, "Expansions for the multivariate chi-square distribution," *J. Multivar. Anal.*, vol. 38, no. 2, pp. 213–232, 1991.

[35] K. S. Miller, R. I. Bernstein, and L. E. Blumenson, "Generalized Rayleigh processes," *Quart. Appl. Math.*, vol. 16, pp. 137–145, 1958.

[36] M. Hagedorn, P. J. Smith, P. J. Bones, R. P. Millane, and D. Pairman, "A trivariate chi-squared distribution derived from the complex Wishart distribution," *Journal of Multivariate Analysis*, vol. 97, no. 3, pp. 655–674, 2006.

[37] D. Morales-Jimenez and J. Paris, "Outage probability analysis for $\eta - \mu$ fading channels," *IEEE Communications Letters*, vol. 14, no. 6, pp. 521–523, 2010.

[38] M. Yacoub, "The κ-μ distribution and the η-μ distribution," *IEEE Antennas and Propagation Magazine*, vol. 49, no. 1, pp. 68–81, Feb 2007.

[39] D. Morales-Jimenez and J. Paris, "Closed-form analysis of dual-branch switched diversity with binary nonorthogonal signalling," *Electronics Letters*, vol. 45, no. 23, pp. 1179–1180, Nov 2009.

[40] J. F. Paris and D. Morales-Jimenez, "Outage probability analysis for Nakagami-q (Hoyt) fading channels under Rayleigh interference," *IEEE Trans. Wireless Commun.*, vol. 9, no. 4, pp. 1272–1276, Apr 2010.

[41] I. S. Gradshteyn and I. M. Ryzhik, *Table of Integrals, Series, and Products*, 6th ed. San Diego: Academic Press, 2000.

[42] A. Erdelyi, *High Order Transcendental Functions*. McGraw-Hill, 1953, vol. 1.

[43] H. Exton, *Multiple Hypergeometric Functions and Applications*. New York: John Wiley & Sons, 1976.

[44] A. P. Prudnikov and Y. A. Brychkov, *Integrals and Series*. Gordon and Breach Science Publishers, 1992, vol. 4.

[45] R. Pawula, "Relations between the Rice Ie-function and the Marcum Q-function with applications to error rate calculations," *Electronics Letters*, vol. 31, no. 24, pp. 2078–2080, Nov 1995.

[46] J. Marcum, "Table of Q functions," Rand Corporation, Santa Monica, CA, U.S. Air Force Project RAND Research Memorandum M-339, ASTIA Document AD 1165451, Jan 1950.

[47] A. H. Nuttall, "Some integrals involving the Q function," Naval Under-water Systems Center, New London, CT, Tech. Rep. 4297, Apr 1972.

[48] ——, "Some integrals involving the Q_M-function," Naval Under-water Systems Center, New London, CT, Tech. Rep. 4755, May 1974.

[49] G. N. Watson, *A treatise on the Theory of Bessel Functions*, 2nd ed. London: Cambridge University Press, 1944.

[50] Y. L. Luke, *Integrals of Bessel Functions*. New York: McGraw-Hill Book Co, 1962.

[51] M. Abramowitz and I. Stegun, *Handbook of mathematical functions*, 9th ed. New York: Dover Publications Inc., 1970.

[52] A. R. Miller, "Incomplete Lipschitz-Hankel integrals of Bessel functions," *Journal of Mathematical Analysis and Applications*, vol. 140, pp. 476–484, 1989.

[53] M. Simon and M.-S. Alouini, "Some new results for integrals involving the generalized Marcum Q function and their application to performance evaluation over fading channels," *IEEE Trans. Wireless Commun.*, vol. 2, no. 4, pp. 611–615, Jul 2003.

[54] S. Gaur and A. Annamalai, "Some integrals involving the $Q_m\left(a\sqrt{x}, b\sqrt{x}\right)$ with application to error probability analysis of diversity receivers," *IEEE Trans. Veh. Technol.*, vol. 52, no. 6, pp. 1568–1575, Nov 2003.

[55] H. Shen and A. Ghrayeb, "Analysis of the outage probability for MIMO systems with receive antenna selection," *IEEE Trans. Veh. Technol.*, vol. 55, no. 4, pp. 1435–1440, Jul 2006.

[56] J. G. Proakis, *Digital Communications*, 2nd ed. New York: McGraw-Hill, 1989.

[57] T. S. Rappaport, *Wireless Communications: Principles and Practice*. Upper Saddle River, NJ: PTR Prentice-Hall, 1996.

[58] G. L. Stüber, *Principles of Mobile Communications*. Norwell, MA: Kluwer Academic Publishers, 1996.

[59] H. Janes and P. Wells, "Some tropospheric scatter propagation measurements near the radio horizon," *Proceedings of the IRE*, vol. 43, no. 10, pp. 1336–1340, Oct 1955.

[60] G. Sugar, "Some fading characteristics of regular VHF ionospheric propagation," *Proceedings of the IRE*, vol. 43, no. 10, pp. 1432–1436, Oct 1955.

[61] S. Basu, E. MacKenzie, E. Costa, P. Fougere, J. Carlson, H., and H. Whitney, "250 MHz/GHz scintillation parameters in the equatorial, polar, and auroral environments," *IEEE J. Select. Areas Commun.*, vol. 5, no. 2, pp. 102–115, Feb 1987.

[62] R. S. Hoyt, "Probability functions for the modulus and angle of the normal complex variate," *Bell Syst. Tech. J.*, vol. 26, pp. 318–359, Apr 1947.

[63] N. Youssef, W. Elbahri, M. Patzold, and S. Elasmi, "On the crossing statistics of phase processes and random FM noise in Nakagami-q mobile fading channels," *IEEE Trans. Wireless Commun.*, vol. 4, no. 1, pp. 24–29, Jan 2005.

[64] B. Chytil, "The distribution of amplitude scintillation and the conversion of scintillation indices," *Journal of Atmospheric and Terrestrial Physics*, vol. 29, pp. 1175–1177, Sep 1967.

[65] K. Bischoff and B. Chytil, "A note on scintillation indices," *Planet. Space Sci.*, vol. 17, pp. 1059–1066, May 1969.

[66] R. Radaydeh, "Performance of cellular mobile systems employing SNR-based GSC in the presence of Rayleigh and Nakagami-q cochannel interferers," *IEEE Trans. Veh. Technol.*, vol. 58, no. 6, pp. 3081–3088, Jul 2009.

[67] J. Paris, "Nakagami-q (Hoyt) distribution function with applications," *Electronics Letters*, vol. 45, no. 4, pp. 210–211, Feb 2009.

[68] M. Nakagami, *Statistical Methods in Radio Wave Propagation.* Oxford, UK: Permagon Press, 1960, ch. "The m-distribution, a general formula of intensity of rapid fading", pp. 3–36.

[69] H. Asplund, A. Molisch, M. Steinbauer, and N. Mehta, "Clustering of scatterers in mobile radio channels-evaluation and modeling in the COST 259 directional channel model," in *IEEE International Conference on Communications (ICC) 2002*, vol. 2, New York, Apr 2002, pp. 901–905.

[70] N. Ermolova, "Moment generating functions of the generalized κ-μ and η-μ distributions and their applications to performance evaluations of communication systems," *IEEE Commun. Lett.*, vol. 12, no. 7, pp. 502–504, 2008.

[71] L. Xiao and X. Dong, "New results on the BER of switched diversity combining over Nakagami fading channels," *IEEE Commun. Lett.*, vol. 9, no. 2, pp. 136–138, Feb 2005.

[72] S. Stein, "Unified analysis of certain coherent and noncoherent binary communications systems," *IEEE Trans. Inform. Theory*, vol. 10, no. 1, pp. 43–51, Jan 1964.

[73] A. J. Goldsmith, *Wireless Communications.* Cambridge University Press, 2005.

[74] M. K. Simon and M.-S. Alouini, *Digital Communications over Generalized Fading Channels: A Unified Approach to Performance Analysis*. New York: Wiley, 2000.

[75] S. Sanayei and A. Nosratinia, "Antenna selection in MIMO systems," *IEEE Commun. Mag.*, vol. 42, no. 10, pp. 68–73, Oct 2004.

[76] C. N. Chuah, D. N. C. Tse, J. M. Kahn, and R. A. Valenzuela, "Capacity scaling in MIMO wireless systems under correlated fading," *IEEE Trans. Inform. Theory*, vol. 48, pp. 637–650, 2002.

[77] V. Aalo, "Performance of maximal-ratio diversity systems in a correlated Nakagami fading environment," *IEEE Trans. Commun.*, vol. 43, no. 8, pp. 2360–2369, Aug 1995.

[78] F. Kohandani, S. Ali, S. Qu, and J. Womack, "MIMO correlation matrices in a microcell scenario for link-layer simulations," in *Proc. IEEE Antennas and Propagation Society International Symposium*, Jul 2008, pp. 1–4.

[79] "Physical channels and modulation," 3GPP, Specification TS 36.211, Release 8, v8.1.0, 2007.